

MSC

2.º
CICLO

FCUP
ICBAS
2021

U. PORTO



U. PORTO



U. PORTO

Evaluation of the anticancer activity of cinnamic acid derivatives targeting COX-2

Ana Luísa de Sousa e Castro Dias



Evaluation of the anticancer activity of cinnamic acid derivatives targeting COX-2

Ana Luísa de Sousa e Castro Dias

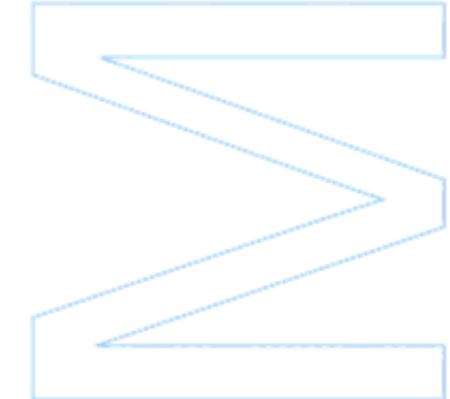
Master's thesis in Biochemistry presented to
Faculty of Sciences and
Abel Salazar's Institute of Biomedical Sciences
University of Porto

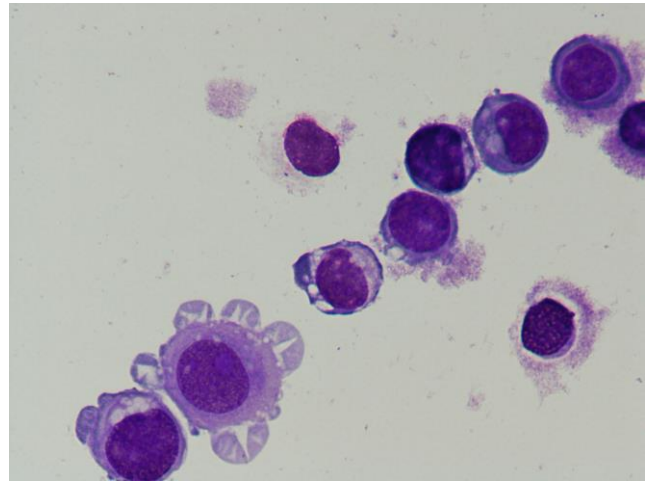
2021

U. PORTO



U. PORTO





Evaluation of the anticancer activity of cinnamic acid derivatives targeting COX-2

Ana Luísa de Sousa e Castro Dias

Master's degree in Biochemistry

Faculty of Sciences and Abel Salazar's Institute of Biomedical Sciences

University of Porto

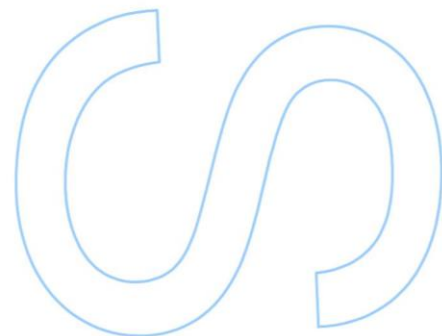
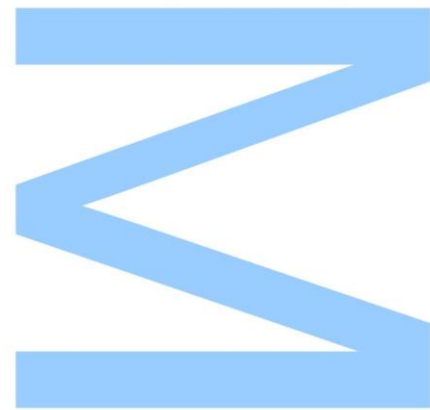
2021

Supervisor

Ana Salomé Pires Lourenço, Assistant Professor,
Faculty of Medicine of University of Coimbra (FMUC)

Co-supervisor

Carmen Jerónimo, Invited Full Professor,
Abel Salazar's Institute of Biomedical Sciences (ICBAS)

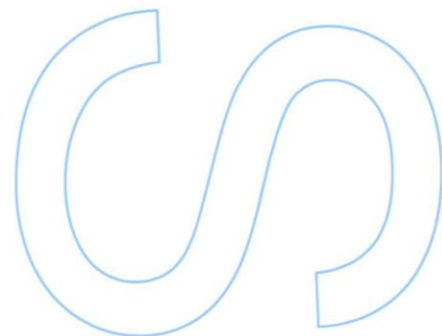
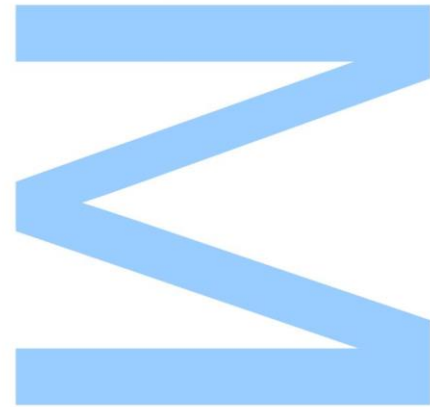




Todas as correções determinadas pelo júri, e só essas, foram efetuadas.

O Presidente do Júri,

Porto, ____ / ____ / ____



Agradecimentos

Este projeto representa o final de mais uma fase na minha vida, que teria sido impossível de terminar sem todo o apoio e ajuda de toda a equipa do Instituto de Biofísica da Faculdade de Medicina da Universidade de Coimbra. A todos, agradeço toda a paciência, ajuda e apoio dados e todo o conhecimento que me foi transmitido durante a minha jornada convosco.

À Professora Doutora Maria Filomena Botelho, Professora Catedrática da Faculdade de Medicina da Universidade de Coimbra, por me ter dado a oportunidade de fazer a minha dissertação no Instituto de Biofísica e por me ter alargado horizontes.

À Professora Doutora Ana Salomé Pires, Professora Auxiliar da Faculdade de Medicina da Universidade de Coimbra, que me orientou durante a dissertação de Mestrado, por toda a disponibilidade, ajuda e conhecimento que me transmitiu, sempre com simpatia e paciência. Agradeço, também, por me acalmar quando tudo parecia correr mal. Um especial agradecimento por tudo o que me transmitiu, dos conhecimentos científicos aos pessoais.

À Professora Doutora Cármen Jerónimo, Professora Catedrática do Instituto de Ciências Biomédicas Abel Salazar, por me ter dado oportunidade de aprender mais e ter orientado durante a dissertação de Mestrado, por toda a disponibilidade, conhecimento e questões pertinentes que enriqueceram o projeto e, também, o meu percurso académico.

À Mestre Inês Marques por me ter acolhido no grupo, ensinado tudo o que sei sobre cultura celular, por toda a ajuda indispensável que me foi dada ao longo destes meses, por todas as oportunidades e, acima de tudo, por toda a paciência.

À Professora Doutora Ana Margarida Abrantes, Professora Auxiliar com Agregação da Faculdade de Medicina da Universidade de Coimbra, por me acolher no Instituto de Biofísica, por todas as oportunidades e toda a ajuda e paciência.

À Doutora Mafalda Laranjo por toda a paciência e ajuda durante todo este percurso, por toda a disponibilidade e por me acolher sempre com simpatia.

À Professora Doutora Fernanda Roleira, Professora Auxiliar da Faculdade de Farmácia da Universidade de Coimbra, e ao Professor Doutor Elisiário Tavares da Silva, Professor Auxiliar da Faculdade de Farmácia da Universidade de Coimbra, pela oportunidade de trabalhar neste projeto, toda a ajuda e conhecimento transmitido.

Ao Mestre Ricardo Teixo, à Mestre Beatriz Serambeque e ao Mestre Miguel Marto, que direta ou indiretamente me ajudaram neste projeto.

À Mestre Catarina Guilherme por toda a disponibilidade e paciência para me ouvir, mas especialmente por toda a amizade duradoura e por nunca me deixar desistir de nada, um obrigado especial por acreditar sempre nas minhas capacidades e me demonstrar que posso sempre fazer mais.

Às minhas colegas de mestrado Beatriz, Lúcia e Gabriela que me acompanharam durante todo este percurso, me ouviram sempre que precisei e me ajudaram em tudo o que podiam, obrigada pela vossa amizade.

A todos os alunos que me acompanharam durante o projeto, Ana Catarina Matos, Maria Combo, Santiago, Inês Graça e Catarina Wright, por toda a paciência, ajuda e disponibilidade. Obrigada pela oportunidade de aprender convosco e transmitir todo o conhecimento que tenho. Um especial agradecimento, à Ana Catarina Matos por toda a amizade e tempo para me ouvir quando mais precisei.

Agradeço também a todos os que me acompanharam durante o meu percurso académico e que me ajudaram durante todos estes anos.

À Bárbara Nunes por toda a amizade, apoio e por me ouvir sempre. Por me acolher quando eu me sentia completamente à margem, por todas as correções e horas de conversa sobre a dissertação.

À Joana Marques por todo o apoio durante este processo, por me ter ajudado quando eu achava que não havia mais nada a fazer, por me ouvir e por me aceitar tal como sou, por todas as correções que me fez durante todo o projeto e, especialmente pela paciência e amizade! Obrigada por estares sempre lá.

À Ana Madeira por todo o tempo despendido para me ajudar e corrigir, pela amizade e todas as conversas infundáveis acerca dos mais variados assuntos, obrigada por toda a paciência para me ouvir e todos os conselhos que me deu.

À Eva Gonçalves por todo o companheirismo, amizade, paciência e confiança. Um especial obrigado pela amizade, por nunca desistir de mim mesmo quando as coisas parecem correr mal e, especialmente, por ser a minha confidente nas piores alturas.

À Maria Inês Oliveira por toda a amizade e apoio sempre que necessitei durante todo o meu percurso académico.

Ao Rafael Marques por todo o amor, carinho e paciência durante todos estes anos, por nunca me deixar desistir e acreditar sempre que posso tudo e que sou a pessoa mais capaz que conhece. Obrigada por estares lá todos os dias e por toda a compreensão durante este percurso.

Aos meus irmãos, João Dias e José Dias por terem a maior paciência comigo e me acompanharem em todos os passeios que necessitei fazer.

O real e mais importante obrigada, aos meus pais, Alice de Sousa e Castro e Humberto Dias, por sempre me darem apoio em todas as minhas escolhas e me permitirem estudar o que realmente gosto.

E, por fim, agradeço a mim mesma, por sempre lutar contra todos os impulsos negativos e por evoluir pessoalmente, academicamente e profissionalmente durante todo este projeto.

A todos estes e aos restantes não mencionados, mas que fazem parte da minha vida, o meu mais sincero bem-haja.

Resumo

A ciclooxigenase-2 (COX-2) está sobreexpressa em vários tipos de cancro, como o cancro da mama (BC) ou o carcinoma hepatocelular (HCC), e está relacionada com diversos *hallmarks* do cancro como a inflamação, a angiogénese e a resistência às terapias. Por esta razão, têm sido procurados novos inibidores de COX-2 para tratamentos antitumorais. Os derivados de ácido cinâmico revelaram ser inibidores seletivos de COX-2 e consideráveis agentes anti-proliferativos contra vários tipos de cancro. Neste projeto foi avaliada a atividade anti-proliferativa de um ácido cinâmico e de cinco amidas de ácido cinâmico com o objetivo de descobrir novos inibidores de COX-2 que possam colmatar as falhas existentes na clínica.

A citotoxicidade dos compostos foi avaliada nas linhas celulares de BC (MCF-7) e de HCC (HuH7 e HepG2) por ensaio de MTT, após 48h de incubação. A seletividade da atividade anti-proliferativa dos compostos **E4**, **F13** e **F19** foi avaliada em células normais da mama (MCF-12A) pelo mesmo método. Alterações do ciclo celular e viabilidade celulares e dados sobre os mecanismos de morte celular foram avaliados por citometria de fluxo, após 48h. Para complementar estes dados, a morfologia celular foi avaliada pela coloração com *May-Grünwald-Giemsa*. A expressão basal COX-2 e a expressão de COX-2 após tratamento com **E4** também foram avaliadas por *western blot*.

Todos os compostos demonstraram atividade anti-proliferativa, sendo o **E4** o composto mais promissor. Além disso, os compostos **E4** e **F13** demonstraram seletividade para as células tumorais da mama em comparação com as células normais. A avaliação da morfologia celular demonstrou que o composto **E4** induziu apoptose em todas as linhas celulares e necrose numa das linhas de células HCC. Este tratamento também induziu a paragem do ciclo celular na fase S nas células HepG2 e HuH7, e uma disrupção do potencial de membrana mitocondrial em todas as linhas celulares. Os resultados da expressão de COX-2 mostraram que o tratamento com **E4** diminuiu a expressão de COX-2 em todas as linhas celulares.

Conclui-se, assim, que os derivados de ácido cinâmico são compostos promissores para colmatar as limitações dos inibidores seletivos da COX-2 atualmente utilizados na prática clínica, e que poderão vir a ser utilizados como agentes anti-inflamatórios e anticancerígenos.

Palavras-chave: Ciclooxigenase-2, inibidores de ciclooxigenase-2, carcinoma hepatocelular, cancro da mama, derivados do ácido cinâmico, atividade anticancerígena.

Abstract

Cyclooxygenase-2 (COX-2) is overexpressed in several types of cancer, such as breast cancer (BC) and hepatocellular carcinoma (HCC), and is related to several hallmarks of cancer, such as inflammation, angiogenesis, and resistance to therapies. For this reason, new COX-2 inhibitors have been sought for anticancer purposes. Cinnamic acid derivatives have been shown to be selective COX-2 inhibitors and considerable antiproliferative agents against various types of cancer. In this project, the antiproliferative activity of one cinnamic acid and five cinnamic acid amides was evaluated with the aim of discovering new COX-2 inhibitors that can fill existing gaps in the clinics.

The cytotoxicity of the compounds was evaluated in BC (MCF-7) and HCC (HuH7 and HepG2) cell lines by MTT assay after 48h of incubation. The selectivity of the antiproliferative activity of compounds **E4**, **F13** and **F19** was evaluated in MCF-12A by the same method. Cell cycle alterations, cell viability and data on cell death mechanisms were evaluated by flow cytometry, 48h after treatment. To complement these data, cell morphology was assessed by *May-Grünwald-Giemsa* staining. Basal COX-2 expression and COX-2 expression after treatment with **E4** for 48h were also evaluated by western blot.

All compounds demonstrated antiproliferative activity, with **E4** being the most promising compound. Furthermore, compounds **E4** and **F13** demonstrated selectivity for breast cancer cells compared to normal cells. Evaluation of cell morphology demonstrated that compound **E4** induced apoptosis in all cell lines and necrosis in one of the HCC cell lines. This treatment also caused cell cycle arrest in S phase in HepG2 and HuH7 cells, and a disruption of mitochondrial membrane potential in all cancer cell lines. The results of COX-2 expression showed that **E4** treatment decreased COX-2 expression in all cell lines.

Thus, it is concluded that cinnamic acid derivatives are promising compounds to exceed the limitations of COX-2 selective inhibitors currently used in clinical practice and could be used in the future as anti-inflammatory and anticancer agents.

Keywords: Cyclooxygenase-2, cyclooxygenase-2 inhibitors, hepatocellular carcinoma, breast cancer, cinnamic acid derivatives, anticancer activity.

Thesis Organization

The development of this master's Thesis was a collaborative process between three academic institutions: ICBR, Faculty of Medicine of the University of Coimbra: Institute of Biophysics, Laboratory Pharmaceutical Chemistry of Faculty of Pharmacy of University of Coimbra, and IPO-Porto: Cancer Biology & Epigenetics Group.

This Thesis is organized in four chapters: Introduction (Chapter 1), Materials and Methods (Chapter 2), Results and Discussion (Chapter 3), Conclusions and Future Perspectives (Chapter 4).

A succinct introduction to each chapter is described below:

Chapter 1. Introduction

- Review of important concepts, recent studies, findings, and Thesis' objectives.

Chapter 2. Materials and Methods

- Description of the materials and methodologies applied in this work.

Chapter 3. Results and Discussion

- Description and discussion of all the results obtained.

Chapter 4. Conclusions and Future Perspectives

- Identification of the major conclusions and proposals for future work.

List of Contents

AGRADECIMENTOS	I
RESUMO	IV
ABSTRACT	V
THESIS ORGANIZATION	VI
LIST OF CONTENTS	VII
LIST OF FIGURES	IX
LIST OF TABLES	XII
LIST OF ABBREVIATIONS AND SYMBOLS	XIII
CHAPTER 1. INTRODUCTION	1
1.1 BACKGROUND	2
1.2 CANCER	3
1.3 EPIDEMIOLOGY	4
1.4 BREAST CANCER	8
1.5 LIVER CANCER	12
1.6 COX-2 AND CANCER	16
1.7 COX-2 INHIBITORS: PHARMACEUTICAL APPLICATIONS	21
1.8 CINNAMIC ACID DERIVATIVES	23
<i>1.8.1 Biomedical applications</i>	23
1.9 CINNAMIC ACID AMIDES: STRUCTURE AND GENERAL PROPERTIES	24
<i>1.9.1 Cinnamic acid amides as COX-2 inhibitors</i>	25
<i>1.9.2 Antitumour activity of cinnamic acid amides</i>	25
1.10 THESIS OBJECTIVES	27
CHAPTER 2. MATERIALS AND METHODS	28
2.1 EVALUATION OF COMPOUNDS <i>IN VITRO</i>	29
<i>2.1.1 Cell culture</i>	29
<i>2.1.2 Treatment with the compounds</i>	31
2.2 ANALYSIS OF BASAL COX-2 EXPRESSION	33
2.3 ANTIPROLIFERATIVE EFFECT	36
<i>2.3.1 Evaluation of metabolic activity by the MTT assay</i>	36
<i>2.3.2 Evaluation of cell proliferation by the SRB assay</i>	36
2.4 CELL CYCLE ANALYSIS	37
2.5 ANALYSIS OF CELL VIABILITY AND CELL DEATH MECHANISMS	38
<i>2.5.1 Analysis of cell viability and death by flow cytometry</i>	38
<i>2.5.2 Evaluation of the mitochondrial membrane potential</i>	39
2.6 ANALYSIS OF CELL MORPHOLOGY	39
2.7 ANALYSIS OF COX-2 EXPRESSION	40
2.8 STATISTICAL ANALYSIS	40
CHAPTER 3. RESULTS AND DISCUSSION	42

3.1 BASAL COX-2 EXPRESSION	43
3.2 ANTIPROLIFERATIVE EFFECT ASSESSMENT	44
3.2.1 <i>Metabolic activity</i>	44
3.2.2 <i>Protein content</i>	52
3.2.3 <i>Selectivity</i>	56
3.3 CELL CYCLE	61
3.4 CELL VIABILITY AND CELL DEATH MECHANISMS.....	64
3.4.1 <i>Viability and cell death</i>	65
3.4.2 <i>Mitochondrial membrane potential ($\Delta\Psi_m$)</i>	72
3.5 COX-2 EXPRESSION.....	74
CHAPTER 4. CONCLUSIONS AND FUTURE PERSPECTIVES	80
4.1 CONCLUSIONS	81
4.2 FUTURE PERSPECTIVES	82
REFERENCES	84
APPENDIX 1 – MTT ASSAY WITH CELECOXIB TREATMENT	102

List of Figures

Figure 1 – Normal cells develop a succession of capabilities known as hallmarks of cancer. Consequently, normal cells change gradually to a neoplastic state. Thus, these hallmarks are transversal to all neoplastic cells. Initially, these hallmarks were only six (sustaining proliferative signalling, evading growth suppressors, activating invasion and metastasis, enabling replicative immortality, inducing angiogenesis, and resisting cell death). However, posterior studies added two new emerging hallmarks: avoiding immune destruction and deregulation of cellular energetics; and two consequential enabling characteristics of neoplasia that facilitate acquisition of hallmarks: genome instability and mutation and tumour-promoting inflammation. Adapted from (16).	4
Figure 2 -Estimated incidence and mortality of the 10 Most Common Cancers in 2020, for both sexes. From (14).	5
Figure 3 - Estimated most common type of cancer incidence in 2020 in Portugal among males and females. From (17)	6
Figure 4 – Estimated most common type of cancer mortality in 2020 in Portugal among males and females. From (18).	7
Figure 5 - Breast Cancer Subtypes. Boxes are associated with the characteristics (proliferation, grade, ER and HER2 expression) and below of these is the percentage of incidence of each subtype. ER – Oestrogen Receptor; PR – Progesterone Receptor; HER2 – Human Epidermal Growth Factor Receptor; Ki67 – Proliferation Marker; GES – gene expression signature; -, negative; +, positive.	8
Figure 6 - Risk Factors of Breast Cancer. The most predominate risk factors are found at the bottom of the pyramid, while the top refers to the least predominate risk factor.	10
Figure 7 – Hepatocarcinogenesis in cirrhotic and noncirrhotic livers. Most hepatocellular carcinomas (>90%) arise on the background of chronic liver inflammation, cirrhosis, and fibrosis (dysplasia-carcinoma sequence). NASH – non-alcoholic steatohepatitis, a type of non-alcoholic fatty liver disease. From (37).	13
Figure 8 – Intrinsic and Extrinsic factors that drive tumour progress. MDSC – Myeloid-derived suppressor cell; BCR – B cell receptor; TGFβ – transforming growth factor-β; Treg – regulatory T cell; IL-10 – Interleukin 10. From (37)	14
Figure 9 – Strategy for HCC treatment in countries with different resource levels. TACE – trans-arterial chemoembolization; TAE – trans-arterial embolization; TARE – trans-arterial radioembolization. From (32).	15
Figure 10 – Multitasking roles of COX-2 in promotion of cancer. From (4).	21
Figure 11 – (A) Some examples of COX-1/COX-2 inhibitors (NSAIDs); (B) Some examples of COX-2 inhibitors (coxibs). From (10).	22
Figure 12 – Cinnamic acid structure.	23
Figure 13 – Example of chemical synthesis of cinnamic acid amide: synthesis of n-hexylamides (secondary amides) of hydroxycinnamic acids. Adapted from (10).	24
Figure 14 – Principal structural features for COX-2 inhibition. From (10).	25
Figure 15 - One cinnamic acid (F11) and five cinnamic acid amides used in this research.	29
Figure 16 - COX-2 basal expression in three cell lines (HuH7, HepG2 and MCF-7). Results are presented as arbitrary units (AU) (without normalization) of COX-2 expression as a function of different cell lines and express the mean±SEM of, at least, three independent experiments, in triplicate. Significant differences are denoted by *p<0.05. Below the bar graph there are western blot diagrams of COX-2 and β-actin expression.	44
Figure 17 - Dose response curves of MCF-7 cell line after treatment with compounds E4, E5, F13, F19 and F20 for 48h. Results are presented as the percentage (%) of metabolic activity as a function of compounds' concentration {log ₁₀ [concentration (μM)]} and express the mean±SEM of, at least, four independent experiments, in triplicate.	46
Figure 18 - Dose response curves of HuH7 cell line after treatment with compounds E4, E5, F13, F19 and F20 for 48h. Results are presented as the percentage (%) of metabolic activity as a function of compounds' concentration {log ₁₀ [concentration (μM)]} and express the mean±SEM of, at least, three independent experiments, in triplicate.	46

- Figure 19 - Dose response curves of HepG2 cell line after treatment with compounds E4, E5, F13, F19 and F20 for 48h. Results are presented as the percentage (%) of metabolic activity as a function of compounds' concentration $\{\log_{10}[\text{concentration } (\mu\text{M})]\}$ and express the mean and standard error of, at least, three independent experiments, in triplicate. 47
- Figure 20 – Results of MTT and SRB assays (MCF-7 cell line) 48 hours after treatment with **E4** and **F19** compounds. Results are presented as the percentage (%) of metabolic activity (MTT) and protein content (SRB) as a function of compounds' concentration (μM) and express the mean \pm SEM of, at least, three independent experiments, in triplicate. Significant differences are denoted by * $p < 0.05$, ** $p < 0.01$. 54
- Figure 21 - Results of MTT and SRB assays (HuH7 cell line) 48 hours after treatment with **E4** and **F19** compounds. Results are presented as the percentage (%) of metabolic activity (MTT) and protein content (SRB) as a function of compounds' concentration (μM) and express the mean \pm SEM of, at least, three independent experiments, in triplicate. Significant differences are denoted by * $p < 0.05$. 55
- Figure 22 – Results of MTT and SRB assays (HepG2 cell line) 48 hours after treatment with **E4** and **F19** compounds. Results are presented as the percentage (%) of metabolic activity (MTT) and protein content (SRB) as a function of compounds' concentration (μM) and express the mean \pm SEM of, at least, three independent experiments, in triplicate. Significant differences are denoted by * $p < 0.05$, ** $p < 0.01$, *** $p < 0.0001$. 56
- Figure 23 – Results of MTT assay (MCF-12A and MCF-7 cell line) 48 hours after treatment with celecoxib and E4 compound. Results are presented as the percentage of metabolic activity (%) as a function of compounds' concentration (μM) and express the mean \pm SEM of, at least, three independent experiments, in triplicate. Significant differences are denoted by *** $p < 0.001$, **** $p < 0.0001$. 58
- Figure 24 - Results of MTT assay (MCF-12A and MCF-7 cell line) 48 hours after treatment with celecoxib and F19 compound. Results are presented as the percentage of metabolic activity (%) as a function of compounds' concentration (μM) and express the mean \pm SEM of, at least, three independent experiments, in triplicate. Significant differences are denoted by * $p < 0.05$, ** $p < 0.01$, *** $p < 0.001$, **** $p < 0.0001$. 58
- Figure 25 - Results of MTT assay (MCF-12A and MCF-7 cell line) 48 hours after treatment with celecoxib and F13 compound. Results are presented as the percentage of metabolic activity (%) as a function of compounds' concentration (μM) and express the mean \pm SEM of, at least, three independent experiments, in triplicate. Significant differences are denoted by ** $p < 0.01$, *** $p < 0.0001$. 59
- Figure 26 – Cell cycle analysis of MCF-7 cell line, 48 hours after treatment with **E4**. Results are presented as the percentage of cells in phases G_0/G_1 , S or G_2/M and express the mean \pm SEM of, at least, three independent experiments, in duplicate. 62
- Figure 27 - Cell cycle analysis of HuH7 cell line, 48 hours after treatment with **E4**. Results are presented as the percentage of cells in phases G_0/G_1 , S or G_2/M and express the mean \pm SEM of, at least, three independent experiments, in duplicate. Significant differences are denoted by * $p < 0.05$, ** $p < 0.01$, *** $p < 0.001$, **** $p < 0.0001$. 63
- Figure 28 - Cell cycle analysis of HepG2 cell line, 48 hours after treatment with **E4**. Results are presented as the percentage of cells in phases G_0/G_1 , S or G_2/M and express the mean \pm SEM of, at least, three independent experiments, in duplicate. Significant differences are denoted by * $p < 0.05$. 64
- Figure 29 – Cell viability and types of cell death induced in MCF-7 cell line 48 hours after treatment with **E4**. Results are presented as a percentage (%) of viable cells, in early apoptosis, in late apoptosis and necrosis and express the mean \pm SEM of, at least, three independent experiments, in duplicate. Significant differences are denoted by *** $p < 0.001$. 66
- Figure 30 – Representative images (50x) of morphologic features in MCF-7 cell line after treatment with **E4** compound for 48 hours, after cells staining by May-Grünwald-Giemsa staining. Red arrows correspond to blebbings (apoptosis marker), and green arrows to cytoplasm leakage (necrotic marker). 67
- Figure 31 - Cell viability and types of cell death induced in HuH7 cell line 48 hours after treatment with **E4**. Results are presented as a percentage (%) of viable cells, in early

apoptosis, in late apoptosis and necrosis and express the mean±SEM of, at least, two independent experiments, in duplicate. Significant differences are denoted by ***p<0.001.

- _____ 68
- Figure 32 - Representative images (50x) of morphologic features in HuH7 cell line after treatment with **E4** compound for 48 hours, after cells staining by May-Grünwald-Giemsa staining. Red arrows correspond to blebbings (apoptosis marker) and green arrows to cytoplasm leakage (necrotic marker). _____ 69
- Figure 33 - Cell viability and types of cell death induced in HepG2 cell line 48 hours after treatment with **E4**. Results are presented as a percentage (%) of viable cells, in early apoptosis, in late apoptosis and necrosis and express the mean±SEM of, at least, two independent experiments. _____ 71
- Figure 34 - Representative images (50x) of morphologic features in HepG2 cell line after treatment with **E4** compound for 48 hours, after cells staining by May-Grünwald-Giemsa staining. Red arrows correspond to blebbings (apoptosis marker), green arrows to cytoplasm leakage (necrotic marker) and orange arrow to binucleated cells (failure in mitosis). _____ 71
- Figure 35 – Mitochondrial membrane potential ($\Delta\Psi_m$) of MCF-7 cell line 48 hours after treatment with **E4**. Results are presented as ratio of M/A for each condition relatively to control expressed by mean±SEM of, at least, three independent experiments, in duplicate. The increase of ratio is directly correlated with mitochondrial dysfunction. _____ 73
- Figure 36 - Mitochondrial membrane potential ($\Delta\Psi_m$) of HuH7 cell line 48 hours after treatment with **E4**. Results are presented as ratio of M/A for each condition relatively to control expressed by mean±SEM of, at least, three independent experiments, in duplicate. The increase of ratio is directly correlated with mitochondrial dysfunction. _____ 73
- Figure 37 - Mitochondrial membrane potential ($\Delta\Psi_m$) of HepG2 cell line 48 hours after treatment with **E4**. Results are presented as ratio of M/A for each condition relatively to control expressed by mean±SEM of, at least, three independent experiments, in duplicate. The increase of ratio is directly correlated with mitochondrial dysfunction. _____ 74
- Figure 38 - COX-2 expression in three used cell lines (HuH7, HepG2 and MCF-7) 48 hours after following treatments: untreated cells (control), IC₅₀, >IC₅₀ and celecoxib. Results are presented as arbitrary units (AU) with normalization to control (untreated cells) of COX-2 expression as a function of different treatments and express the mean±SEM of, at least, three independent experiments, in triplicate. Significant differences are denoted by *p<0.05, **p<0.01. Below the bar graph there are western blot diagram of COX-2 and β -actin expression. _____ 76
- Figure 39 - Results of MTT in MCF-7 cell line 48 hours after treatment with compounds E4 and F19. Results are presented as the percentage of metabolic activity (%) as a function of compounds' concentration (μ M) and express the mean±SEM of, at least, three independent experiments, in triplicate. _____ 102

List of Tables

Table 1 – Different concentrations of compounds used in MCF-7, HuH7 and HepG2 cell lines to MTT assay.	31
Table 2 – Different concentrations of E4, F13, F19 and celecoxib used in MCF-12A cell line to MTT assay.	32
Table 3 - Concentrations of E4 compound tested in MCF-7, HuH7 and HepG2 for Flow Cytometry and <i>May-Grünwald-Giemsa</i> technique.	33
Table 4 - Concentrations of E4 and celecoxib tested in MCF-7, HuH7 and HepG2 cell lines for Protein Extract.	33
Table 5 - IC ₅₀ values obtained after incubation of MCF-7, HuH7 and HepG2 cell lines compounds E4, E5, F13, F19 and F20 for 48h. R ² values and the 95% confidence intervals (95%) are also presented.	47

List of Abbreviations and Symbols

AA	<i>Arachidonic acid</i>
Akt	<i>Protein kinase B</i>
ANOVA	<i>Analysis of variance</i>
ARE	<i>AU-rich elements</i>
ATCC	<i>American Type Collection Culture</i>
AV	<i>Annexin V</i>
BAX	<i>BCL-2-associated X protein</i>
BC	<i>Breast cancer</i>
BCA	<i>Bicinchochonic acid</i>
BCLC	<i>Barcelona Clinic Liver Cancer</i>
BCL-2	<i>B cell lymphoma 2 protein</i>
BCR	<i>B cell receptor</i>
BOP	<i>(benzotriazole-1- yloxy)tris(dimethylamino)phosphodiu m hexafluorophosphate</i>
BRCA1	<i>Breast cancer type 1 gene</i>
BRCA2	<i>Breast cancer type 2 gene</i>
BSA	<i>Bovine serum albumin</i>
CaCl₂	<i>Calcium chloride</i>
CAFs	<i>Cancer associated fibroblasts</i>
cAMP	<i>Cyclic adenosine monophosphate</i>
CAPS	<i>3-(cyclohexylamino)-1-propanesulfonic acid</i>
CD1	<i>Cyclin D1</i>
CDK4	<i>Cyclin-dependent kinase 4</i>
Coxibs	<i>Selective COX-2 inhibitors</i>
COX-1	<i>Cyclooxygenase-1</i>
COX-2	<i>Cyclooxygenase-2</i>
CRE	<i>cAMP response elements</i>
CSCs	<i>Cancer stem cells</i>
CTNNB1	<i>Beta-catenin gene</i>
DMEM	<i>Dulbecco's Modified Eagle Medium</i>
DMF	<i>Dimethylformamide</i>
DMSO	<i>Dimethylsulfoxide</i>

DNA	<i>Deoxyribonucleic acid</i>
DTT	<i>1,4-Dithiothreitol</i>
E4	<i>N-Hexyl-3-(3,4-di-hydroxyphenyl)-2-propenamide</i>
E5	<i>N-Hexyl-3-(4-hydroxy-3-methoxyphenyl)-2-propenamide</i>
EDTA	<i>Ethylenediamine tetraacetic acid</i>
e.g.	Exempli gratia from Latin, which means “for example”
EMT	<i>Epithelial-mesenchymal transition</i>
ER	<i>Oestrogen receptor</i>
ERBB2	<i>Human epidermal growth factor receptor 2 gene</i>
ERK	<i>Extracellular-signal-regulated kinase</i>
F11	<i>3,5-di-tert-butyl-4-hydroxycinnamic acid</i>
F13	<i>N-Hexyl-3-(3,5-di-tert-butyl-4-hydroxyphenyl)-2-propenamide</i>
F19	<i>3N-Hexyl-3-(3-hydroxy-4-methoxyphenyl)-2-propenamide</i>
F20	<i>N,N-Diethyl-3-(3,5-di-tert-butyl-4-hydroxyphenyl)-2-propenamide</i>
FAK	<i>Focal adhesion kinase</i>
FBS	<i>Fetal bovine serum</i>
FITC	<i>Fluorescein isothiocyanate fluorochrome</i>
GI	<i>Gastrointestinal</i>
HBV	<i>Hepatitis B virus</i>
HCV	<i>Hepatitis C virus</i>
HCC	<i>Hepatocellular carcinoma</i>
hEGF	<i>Human epidermal growth factor</i>
HER2	<i>Human epidermal growth factor receptor 2</i>
HEPES	<i>4-(2-hydroxyethyl)-1-piperazineethanesulfonic acid</i>
HepG2	<i>Human liver cancer cell line</i>
HIF-1	<i>Hypoxia-inducible factor 1</i>
HIF-1α	<i>Hypoxia-inducible factor 1 alpha</i>
HIF-2α	<i>Hypoxia-inducible factor 2 alpha</i>
HRT	<i>Hormone replacement therapy</i>
HuH7	<i>Human liver cancer cell line</i>
KCl	<i>Potassium chloride</i>

KH₂PO₄	<i>Monopotassium phosphate</i>
IC₅₀	<i>Half maximal inhibitory concentration</i>
i.e.	<i>Id est from Latin, which means “in other words”</i>
IgG	<i>Immunoglobulin G</i>
IL-1	<i>Interleukin 1</i>
IL-1 β	<i>Interleukin 1 type beta</i>
IL-6	<i>Interleukin 6</i>
IL-10	<i>Interleukin 10</i>
JC-1	<i>5,5',6,6'-Tetrachloro-1,1',3,3'- tetraethylbenzimidazolocarboyanine iodide</i>
JCRB	<i>Japanese Collection of Research Bioresources Cell Bank</i>
iPLA₂	<i>Calcium independent phospholipase A2</i>
M/A	<i>Monomers/Aggregates ratio</i>
mAb	<i>Monoclonal antibody</i>
MAPK	<i>Mitogen-activated protein kinase</i>
MCF-7	<i>Oestrogen-dependent breast cancer cell line</i>
MCF-12A	<i>Normal breast cell line</i>
MDSC	<i>Myeloid-derived suppressor cell</i>
MiR-125b	<i>MicroRNA 125 b</i>
MMP 2	<i>Metalloproteinase 2</i>
MMP 9	<i>Metalloproteinase 9</i>
mRNA	<i>Messenger ribonucleic acid</i>
MTT	<i>3-(4,5-Dimethylthiazol-2-yl)-2,5-diphenyltetrazolium bromide</i>
NaCl	<i>Sodium chloride</i>
Na₂HPO₄.2H₂O	<i>Sodium phosphate dibasic dihydrate</i>
NASH	<i>Non-alcoholic steatohepatitis</i>
NFAT	<i>Nuclear factor of activated T cells</i>
NF-κB	<i>Nuclear factor kappa B</i>
NSAIDs	<i>Non-steroidal anti-inflammatory drugs</i>
P21	<i>Cyclin-dependent kinase inhibitor 1</i>
P53	<i>Tumor suppressor protein 53</i>
PBS	<i>Phosphate buffer saline</i>
PD-1	<i>Programmed cell death protein 1</i>
PDK-1	<i>3-Phosphoinositide-Dependent Protein Kinase-1</i>

PG	<i>Prostaglandin</i>
PGE₂	<i>Prostaglandin E2</i>
PI	<i>Propidium iodide</i>
PI3K	<i>Phosphoinositide 3-kinase</i>
PK	<i>Protein kinase</i>
PKM2	<i>Pyruvate kinase M2</i>
PR	<i>Progesterone receptor</i>
PTEN	<i>Phosphatase and tensin homologue</i>
PTGS2	<i>Prostaglandin-endoperoxide synthase 2</i>
PVDF	<i>Polyvinylidene difluoride</i>
RIPA buffer	<i>Radioimmunoprecipitation assay buffer</i>
RNA	<i>Ribonucleic acid</i>
RNAse	<i>Ribonuclease</i>
RPMI	<i>Roswell Park Memorial Institute Medium</i>
ROS	<i>Reactive oxygen species</i>
SDS	<i>Sodium dodecyl sulphate</i>
SEM	<i>Standard error of mean</i>
SIM2s	<i>Single-minded-2s</i>
Smad 2	<i>SMAD family member 2</i>
Smad 3	<i>SMAD family member 3</i>
SRB	<i>Sulforhodamine B</i>
STAT3	<i>Signal transducer and activator of transcription 3</i>
TACE	<i>Trans-arterial chemoembolization</i>
TAE	<i>Trans-arterial embolization</i>
TARE	<i>Trans-arterial radioembolization</i>
TBS-T	<i>Tris-Buffered Saline Tween 20</i>
TEA	<i>Triethylamine</i>
TERT	<i>Telomerase reverse transcriptase</i>
TET-1	<i>Ten-eleven translocation methylcytosine dioxygenase 1</i>
TGF-β	<i>Transforming growth factor beta</i>
TNBC	<i>Triple-negative breast cancer</i>
TNF-α	<i>Tumour necrosis factor alpha</i>
TP53	<i>Tumour suppressor gene 53</i>
Treg	<i>Regulatory T cell</i>

Tris-NaOH	<i>Tris(hydroxymethyl)aminomethane with sodium hydroxide</i>
Triton X-100	<i>2-[4-(2,4,4-trimethylpentan-2-yl)phenoxy]ethanol</i>
Trizma base	<i>Tris(hydroxymethyl)aminomethane</i>
UTR	<i>3'-untranslated region</i>
VEGF	<i>Vascular endothelial growth factor</i>
VEGFR2	<i>Vascular endothelial growth factor receptor 2</i>
WHO	<i>World Health Organization</i>
WB	<i>Western Blot</i>
YAP	<i>Yes associated protein</i>

Chapter 1. Introduction

This Chapter provides a review of relevant topics for this Thesis project. Firstly, the background of the cyclooxygenase-2 and its presence in some cancers, the use of inhibitors of cyclooxygenase-2 on clinical practice and the discovery of cinnamic acids amides as cyclooxygenase-2 inhibitors are analysed. Further, basic molecular mechanisms and epidemiology of cancer worldwide, including in Portugal, are described followed by literature review of breast and liver cancer. Lastly, the role of cyclooxygenase-2 in cancer and literature review about both the pharmaceutical applications of inhibitors of cyclooxygenase-2 and the cinnamic acids derivatives are also presented. A special emphasis will be given to the cinnamic acids amides, since they are the research focus of this project. Thesis' objectives to be achieved are also outlined.

1.1 Background

Cyclooxygenase-1 (COX-1) and cyclooxygenase-2 (COX-2) are two isoenzymes involved in the prostaglandin (PG) and thromboxane biosynthesis. COX-1 is constitutively expressed, while COX-2 results from an inducible early response gene, which is activated by various extracellular or intracellular physiological stimuli (1–3).

COX-2 is frequently expressed in many types of cancers including cholangiocarcinoma (3–6), hepatocellular carcinoma (3,4,6,7), lung cancer (6–8) and breast cancer (1,8,9) and plays a pleiotropic and multifaceted role in carcinogenesis and cancer cell resistance to chemotherapy and radiotherapy (4). Therefore, COX-2 inhibitors offer a therapeutic approach for the reduction of inflammation and related diseases such as cancer.

Nowadays, there are no anti-inflammatory drugs which are truly safe and can also be used as a suitable therapy with minimal gastrointestinal damage and cardiovascular toxicity (10). As such, it is mandatory to discover new drugs to exceed the limitations of COX-2 inhibitors currently used in clinical practice. Recently, one cinnamic acid and five cinnamic acid amides turned out to be potent and selective COX-2 inhibitors and considerable antiproliferative agents against breast and colon cancers (11,12).

In this project, the anticancer activity and selectivity of one cinnamic acid and five cinnamic acid amides were evaluated, in several cancer cell lines, in order to discover new compounds to exceed the limitations of the COX-2 selective inhibitors currently used in the clinical practice.

To enrich this work, a theoretical introduction is presented below involving all the important subjects for this project: cancer - its molecular mechanisms, worldwide epidemiology, and literature review on breast and liver cancer - and COX-2 - its role in cancer, pharmacological applications of COX-2 inhibitors and cinnamic acid derivatives, with cinnamic acid amides having a great emphasis since they are the focus of this project.

1.2 Cancer

Cancer is one of the most devastating diseases, being a leading cause of death worldwide, as well as a major public health concern. Cancer is one of the main causes of death in economically developed countries. It is a consequence of the growth and ageing of the world population and the adoption of habits that are known to increase cancer risk, such as smoking, poor diet and physical inactivity (13,14).

The development of cancer is explained as a normal cell gradual change to a neoplastic state, obtaining a succession of capabilities known as hallmarks of cancer. These hallmarks include sustaining proliferative signalling, evading growth suppressors, activating invasion and metastasis, enabling replicative immortality, inducing angiogenesis, and resisting cell death (15).

Normal cells have mechanisms that control the production and release of growth-promoting signals, which are responsible for communicating to the cells if they should undergo division or not. Additionally, cancer cells can defeat these mechanisms by deregulating these signals, becoming masters of their own destinies (16). It is also known that cancer cells may induce normal cells to form tumour-associated stroma, being part of the tumour microenvironment. Therefore, these normal cells are active participants in tumourigenesis, contributing for the development and expression of certain hallmark capabilities (16).

Posterior studies added two new emerging hallmarks: avoiding immune destruction and deregulation of cellular energetics; and two consequential enabling characteristics of neoplasia that facilitate acquisition of hallmarks: genome instability and mutation and tumour-promoting inflammation (16). Altogether, they account for the ten hallmarks of cancer (Figure 1).



Figure 1 – Normal cells develop a succession of capabilities known as hallmarks of cancer. Consequently, normal cells change gradually to a neoplastic state. Thus, these hallmarks are transversal to all neoplastic cells. Initially, these hallmarks were only six (sustaining proliferative signalling, evading growth suppressors, activating invasion and metastasis, enabling replicative immortality, inducing angiogenesis, and resisting cell death). However, posterior studies added two new emerging hallmarks: avoiding immune destruction and deregulation of cellular energetics; and two consequential enabling characteristics of neoplasia that facilitate acquisition of hallmarks: genome instability and mutation and tumour-promoting inflammation. Adapted from (16).

1.3 Epidemiology

The World Health Organization (WHO) estimated the occurrence of 19.3 million new cases and 9.9 million cancer deaths worldwide in 2020 (14).

Moreover, these epidemiologic studies estimated that, for both sexes, female breast cancer (BC) was the most diagnosed cancer (11.7% of the total cases), closely followed by lung cancer (11.4%) and colorectal cancer (10%). Furthermore, the one with a higher mortality rate, for both sexes, was lung cancer (18%), followed by colorectal cancer (9.4%) and liver cancer (8.3%) (Figure 2).

In Portugal, BC was the most incident type of cancer (26.4%) and the deadliest (15.5%) among females. Among males, the one with more incidence was prostate cancer (15.2%) and the most mortal (19.9%) was lung cancer (Figure 3 and Figure 4).

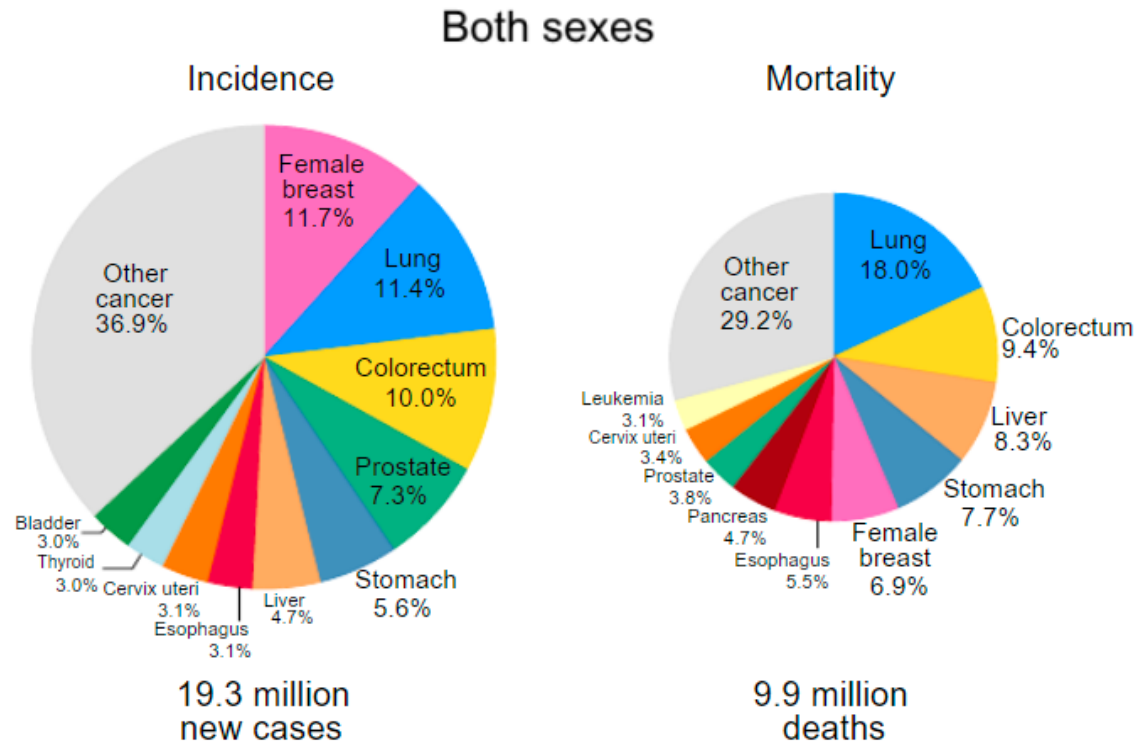


Figure 2 -Estimated incidence and mortality of the 10 Most Common Cancers in 2020, for both sexes. From (14).

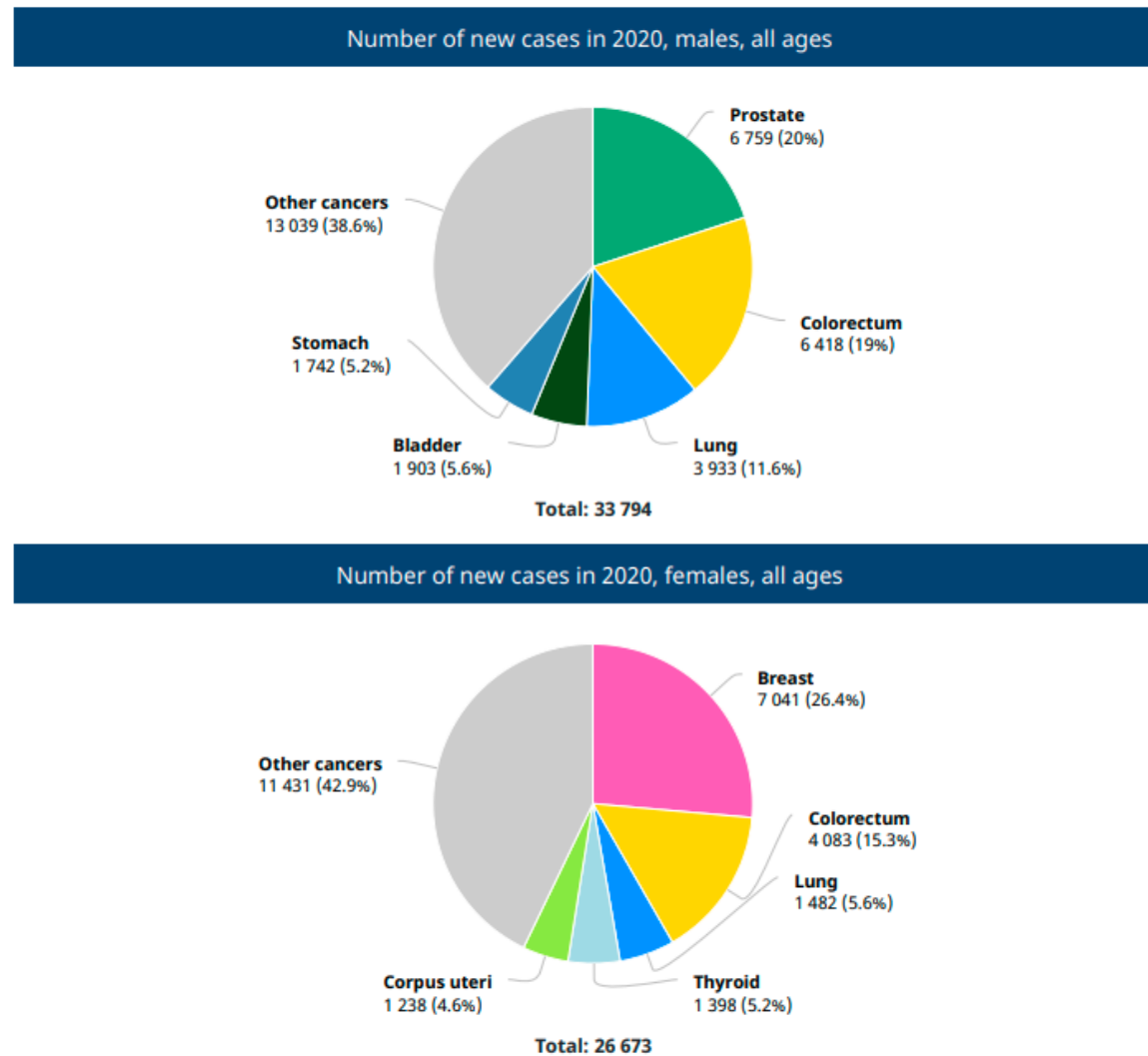
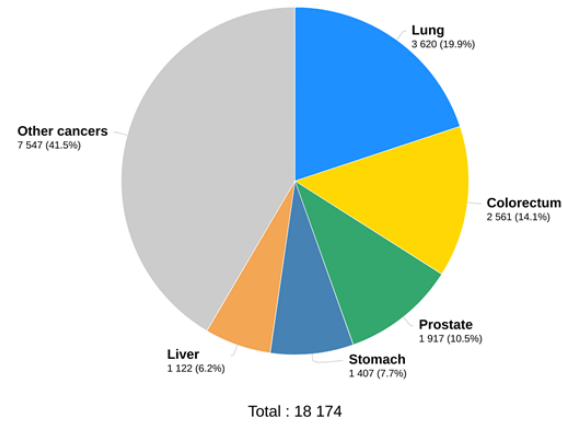


Figure 3 - Estimated most common type of cancer incidence in 2020 in Portugal among males and females. From (17)

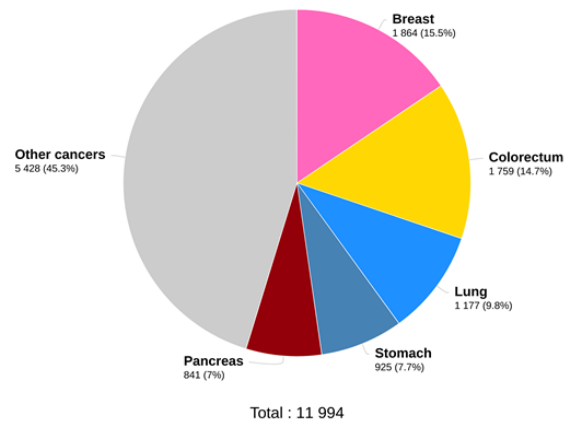
Estimated number of deaths in 2020, Portugal, males, all ages



Data source: Globocan 2020
Graph production: Global Cancer Observatory (<http://gco.iarc.fr>)

International Agency for Research on Cancer
World Health Organization

Estimated number of deaths in 2020, Portugal, females, all ages



Data source: Globocan 2020
Graph production: Global Cancer Observatory (<http://gco.iarc.fr>)

International Agency for Research on Cancer
World Health Organization

Figure 4 – Estimated most common type of cancer mortality in 2020 in Portugal among males and females. From (18).

1.4 Breast cancer

Female BC is, as mentioned above, one of the most frequent and deadliest cancers worldwide. In Portugal, BC has become the number one among females in both: incidence and mortality (14). In early-stage (non-metastatic disease) it is considered a curable disease, whereas in the advanced stage (distant organ metastases) is considered incurable with currently available therapies (19).

This disease is classified as invasive or non-invasive. Non-invasive cancer does not extend away from the lobule or ducts where it is established. An example is ductal carcinoma *in situ* that appears when atypical cells develop within the milk ducts. Even though the atypical cells have not expanded to tissues outer the lobules or ducts, they can progress and grow into invasive BC. This last one may occur early when the tumour is small or later when the tumour is huge. Invasive BC is the most diagnosed carcinoma among females (20).

BC may also be categorized based on histological and molecular characteristics: luminal A-like (expressing the oestrogen receptor (ER)), luminal B-like HER2- (without human epidermal growth factor receptor 2 (HER2) expression), luminal B-like HER2+, HER2-enriched (non-luminal) and Triple-negative (Figure 5) (19,20).

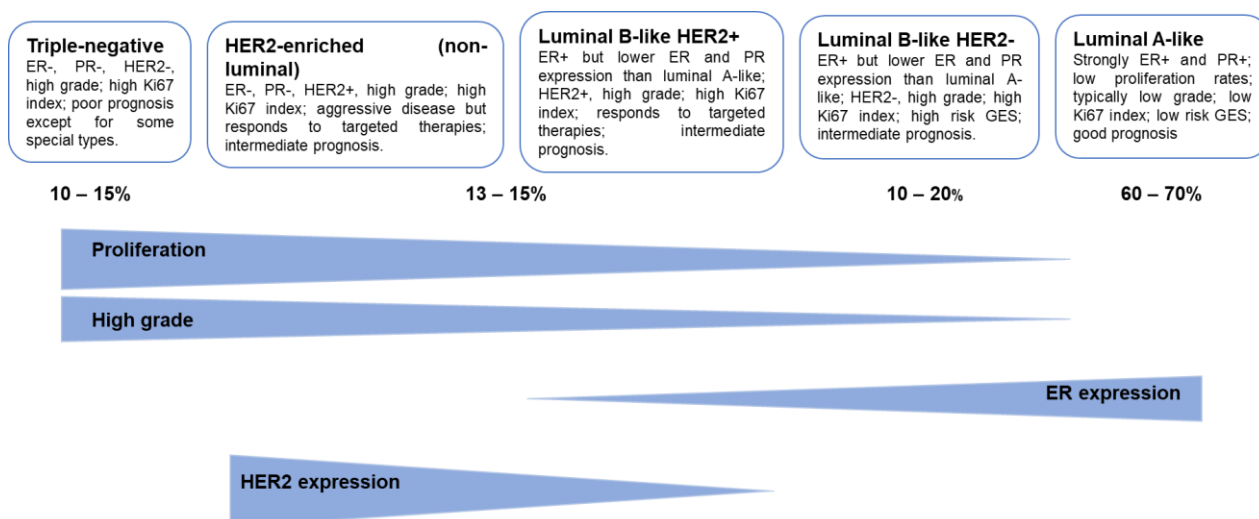


Figure 5 - Breast Cancer Subtypes. Boxes are associated with the characteristics (proliferation, grade, ER and HER2 expression) and below of these is the percentage of incidence of each subtype. ER – Oestrogen Receptor; PR – Progesterone Receptor; HER2 – Human Epidermal Growth Factor Receptor; Ki67 – Proliferation Marker; GES – gene expression signature; -, negative; +, positive.

Tumours that express ER and/or progesterone receptor (PR) are designated as hormone receptor-positive BCs (luminal A-like and luminal B-like), while tumours without

ER, PR or HER2 expression are triple-negative breast cancer (TNBC). This last subtype is a heterogeneous disorder with special sub-forms and is generally associated to the worst prognosis (19,20).

Oestrogen is plainly a promoter of BC, being both endogenous and exogenous oestrogens supplementation (oral contraceptives and the hormone replacement therapy – HRT) associated with the risk of this cancer. Oestrogen binds to the ER located in the nucleus, which is a ligand-activated transcription factor. This receptor can alter gene expression by interacting with oestrogen response elements located in the promoter region of specific genes and interact directly with proteins, such as growth factor receptors, to improve gene expression associated with cell proliferation and survival. Extracellular signals can also promote the expression and activation of the ER in absence of oestrogen. Behaviours associated with the modern lifestyle, such as excessive alcohol consumption and high fat diet can also speed this process, elevating the level of oestrogen-related hormones in the blood (the body fat is involved in synthesis of oestrone, a type of oestrogen) and trigger the ER pathways. Consequently, obesity is one of the risk factors for this disease (19,21).

Hormones stimulate breast development during puberty, menstrual cycles, and pregnancy. The differences between oestrogen and progesterone production during the menstrual cycles enhance cell proliferation and may cause DNA damage. Due to the repetition of this process, a faulty repair process can occur, leading to mutations in pre-malignant, and then in malignant cells. At this stage, oestrogen promotes the growth of these cells and the proliferation of stromal cells that support cancer development (19,20).

Another common molecular alteration observed in BC is the amplification of *ERBB2* gene, which causes activation of the HER2 pathway. HER2 is a transmembrane protein, a member of the human epidermal growth factor family. Its activation happens through dimerization after ligand binding, even though no ligand specific for HER2 has been found. HER2 signalling stimulates proliferation, cell survival, metastasis and adhesion via different pathways, such as Ras pathway and the phosphoinositide 3-kinase (PI3K)-protein kinase B (Akt)-mitogen-activated protein kinase (MAPK) pathway (19).

Breast cancer associated gene 1 and 2 (*BRCA 1* and *BRCA 2*) are two tumour suppressors genes. *BRCA 1* deficiency conducts to the dysregulation of cell cycle checkpoint, abnormal centrosome duplication, genetic instability and eventually apoptosis. *BRCA 2* protein regulates DNA repair by homologous recombination and its faulty function is correlated with high-grade BCs. Mutations on these two genes are

related to a cumulative risk of developing BC. It is mandatory to determine the family's risk, reason why some models have already been developed (e.g. family history score) (19,21).

The risk of BC increases considerably if there is deleterious mutations in either *BRCA 1* or *BRCA 2* genes. About 20-25% of hereditary BCs and 5-10% of all BCs are a consequence of mutations on these genes. It is also known that approximately 10% of BCs are inherited and associated with a family history, although this varies often by ethnicity and the context of early-onset, bilateral and/or TNBC (19,21).

In addition to the risk factors above mentioned (modern lifestyles, external oestrogen intake and family history), sex, ageing and reproductive factors are also related to this disease (Figure 6). Reproductive factors such as early menarche, late menopause, late age at first pregnancy and few pregnancies also rise up the BC risk (21).

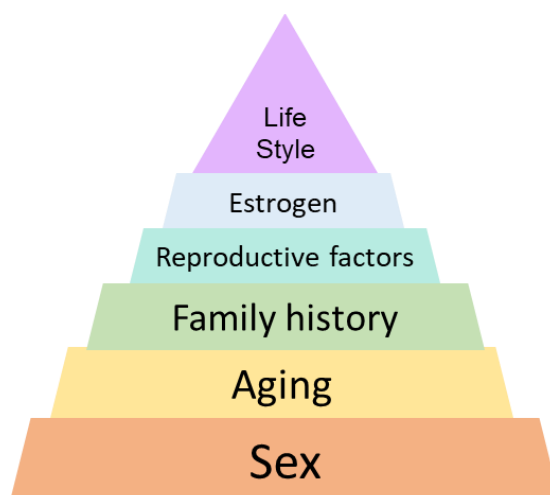


Figure 6 - Risk Factors of Breast Cancer. The most predominate risk factors are found at the bottom of the pyramid, while the top refers to the least predominate risk factor.

The WHO has described two distinct strategies to encourage the early detection of cancer: early diagnosis and screening. Early diagnosis is the detection of symptomatic cancer at an early stage and screening is the identification of asymptomatic disease in a target population of apparently healthy individuals (22).

The diagnosis of BC is centred on a triple test involving clinical examination, imaging (usually mammography and/or ultrasonography) and needle biopsy (19). The

symptoms are palpable breast mass, palpable axillary mass, nipple discharge, nipple inversion, breast asymmetry, breast skin erythema and breast skin thickening (22,23).

Population-based screening with mammography has been related to significant reductions in BC mortality, approximately 20%, however this only concerns high-income countries, when these data are available (22). Therefore, women aged from 40 to 75 years should do mammograms frequently (24).

After a positive result two main molecular targets are assessed: ER alpha and *ERBB2/HER2*. PR is also a marker of ER alpha signalling. This step is to identify the cancer subtype and thus choose the appropriate therapy for the patient (23).

For non-metastatic BC, therapeutic objectives are to eradicate the tumour from the breast and regional lymph nodes and, also, to prevent the metastatic recurrence. Local therapy for this type of BC consists of surgical resection and sampling or removal of axillary lymph nodes, with consideration of postoperative irradiation. Systemic therapy may be preoperative (neoadjuvant), postoperative (adjuvant) or both, depending on the subtype of BC: endocrine therapy for all ER-positive tumours (and chemotherapy in some patients); trastuzumab-based HER2-directed therapy and chemotherapy for all HER2-positive tumours; and chemotherapy alone for patients with TNBC.

Moreover, for metastatic BC, the central objectives of therapy are prolonging life and symptom mitigation. The same basic categories of systemic therapy are applied in metastatic BC as in neoadjuvant/adjuvant tactics; local therapy modalities (surgery and radiation therapy) are often used in metastatic disease for palliation only (23).

Considering all the efforts that have been done to fight this disease, there are still some gaps to overcome, mainly related with secondary effects and resistance of the available therapies.

Chemoradiotherapy is associated with cardiac damage through oxidative stress and consequently, cardiac inflammation (25–27). Furthermore, trastuzumab lead to cardiotoxic effects such a decrease of left ventricular ejection fraction (26). Endocrine therapy has also been associated with development of cardiovascular disease through hormonal and metabolic changes (26). All these therapies are associated with a high heart failure risk in BC survivors.

The major challenge when treating cancer, in general, is the acquired resistance to the treatments. Although there are a lot of studies on the past few years about multidimensional aspects of endocrine therapy and target therapy resistance, the majority of molecular mechanisms are still unknown (28,29). This complex problem can

also be explained by the existence of cancer stem cells (CSCs). These cells present stem-like characteristics and are amplified by the most conventional therapies. Their capacity of quiescence allows tumours late relapse due to the presence of dormant cells that escape therapies and immune surveillance (30). In the context of BC, TNBC is a subtype that is enriched by CSCs, which urgently needs advances in therapeutic options targeting these cells. On the other hand, some studies suggest that endocrine therapy can induce the dedifferentiation of bulk cancer cells into breast CSCs, which can be associated to relapse up to twenty years from treatment in patients with ER+ tumours (30).

Hence, it is important to discover new therapies efficient in the treatment of this disease, not only to solve the gaps of therapies used in current clinical practice but also to give better quality of life to patients.

1.5 Liver cancer

Primary liver cancer is an exceptionally heterogenous malignant disease related to a high ratio of death worldwide. Liver cancers represent the third leading cause of cancer deaths worldwide, being hepatocellular carcinoma (HCC) the dominant type (70-90% of total primary liver tumours) (14,31–35). Beyond HCC, other forms less predominant include intrahepatic cholangiocarcinoma (also known as bile duct carcinoma) originated from the intrahepatic biliary ducts, angiosarcoma from the intrahepatic blood vessels and childhood hepatoblastoma. There is also a mixed or combined hepatocellular-cholangiocarcinoma, an heterogenous tumour with both hepatocytic and cholangiocytic differentiation, often associated with a poor prognosis (36,37).

Chronic liver inflammation and fibrosis (steatosis and cirrhosis), metabolic injuries (diabetes mellitus, non-alcoholic fatty liver disease), toxic insults (aflatoxin, alcohol intake and tobacco use), viral infections (chronic hepatitis B virus and hepatitis C virus) and autoimmune reactions (autoimmune hepatitis) are risk factors for HCC development (31–33,35–38). Further, there is evidence that hepatocarcinogenesis is affected by stress physiology (33). Chronic Hepatitis B virus (HBV) and Hepatitis C virus (HCV) infections are the major recognized risk factors for HCC. However, due to modern lifestyles, there are already evidences that non-alcoholic fatty liver disease will become the dominant risk factor soon (31,35,38).

Hepatocarcinogenesis is a complex multistep process in which different signalling cascades can be altered leading, ultimately, to the heterogeneity of liver cancer disease (Figure 7). Risk factors described above are intimately associated with the environmental and genetic susceptibilities to HCC (32,33,36,37).

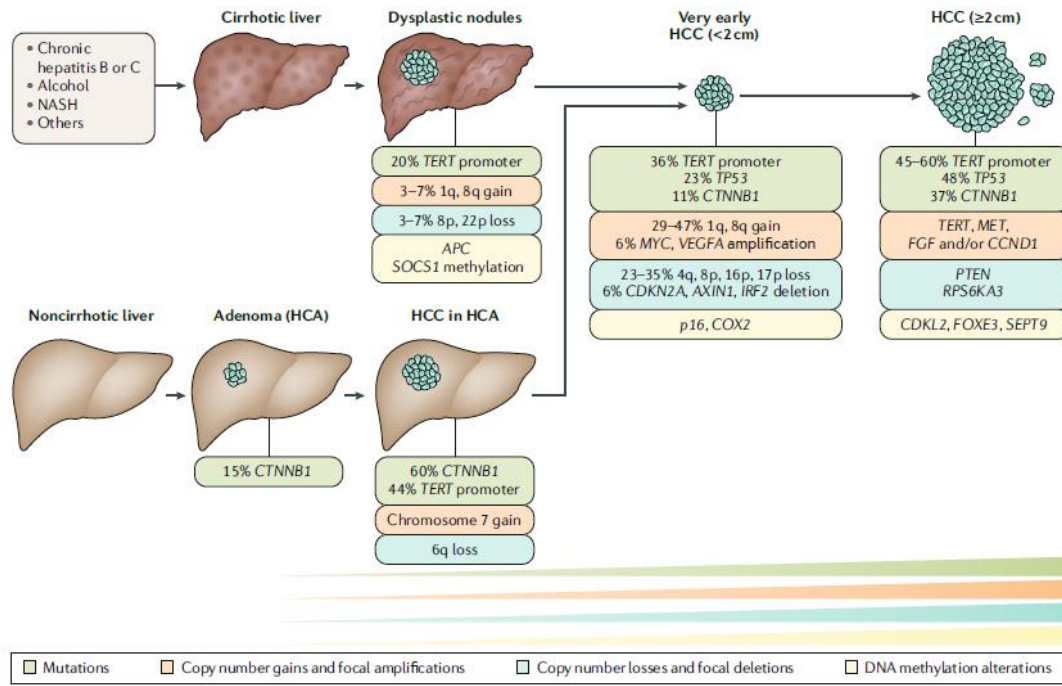


Figure 7 – Hepatocarcinogenesis in cirrhotic and noncirrhotic livers. Most hepatocellular carcinomas (>90%) arise on the background of chronic liver inflammation, cirrhosis, and fibrosis (dysplasia-carcinoma sequence). NASH – non-alcoholic steatohepatitis, a type of non-alcoholic fatty liver disease. From (37).

Several genetic events have been correlated with the progress of HCC (Figure 7) 1) activation of TERT (telomerase reverse transcriptase) promotor, - present in 25-65% of cancers, depending on tumour stage, being the earliest on dysplasia-carcinoma sequence and most frequent somatic event in HCC; 2) mutations in *CTNNB1* (catenin beta-1) gene (27-40%), earliest on adenoma-carcinoma sequence; 3) overexpression of COX-2 and 4) inactivation of suppressor tumour gene *TP53* (21-31%). Furthermore, epigenetic alterations (methylation) are also found on many cancer-related genes. Genomic instability is common in HCC, in which several mechanisms might play a role, such as telomere erosion, chromosome segregation defects and alterations in the DNA-damage response pathways (32,33,36,37).

Immunoediting also helps on tumour progression. Immunoediting explains the interaction between cancer and immune cells during tumour initiation and is divided in three steps: elimination, equilibrium, and escape (Figure 8). Cancer cells have mutations that produce powerful immunogenic neoantigens which are initially identified and

eliminated by the immune system. As cancer cells proliferate and acquire genetic instability, they advance through a stage of equilibrium between elimination and escape from this system. Once most cancer cells with powerfully immunogenic neoantigens have been eliminated, less immunogenic tumour clones can proliferate unrestricted and become the dominant cell population during tumour progression (Figure 8).

Other interaction that facilitates HCC development is tumour-stroma interaction in microenvironment originated from cancer-associated fibroblasts (CAFs). These cells release cytokines and growth factors that benefit tumour growth and invasion, suppressing apoptosis and creating an immunosuppressive microenvironment by recruiting tumour-associated macrophages (37).

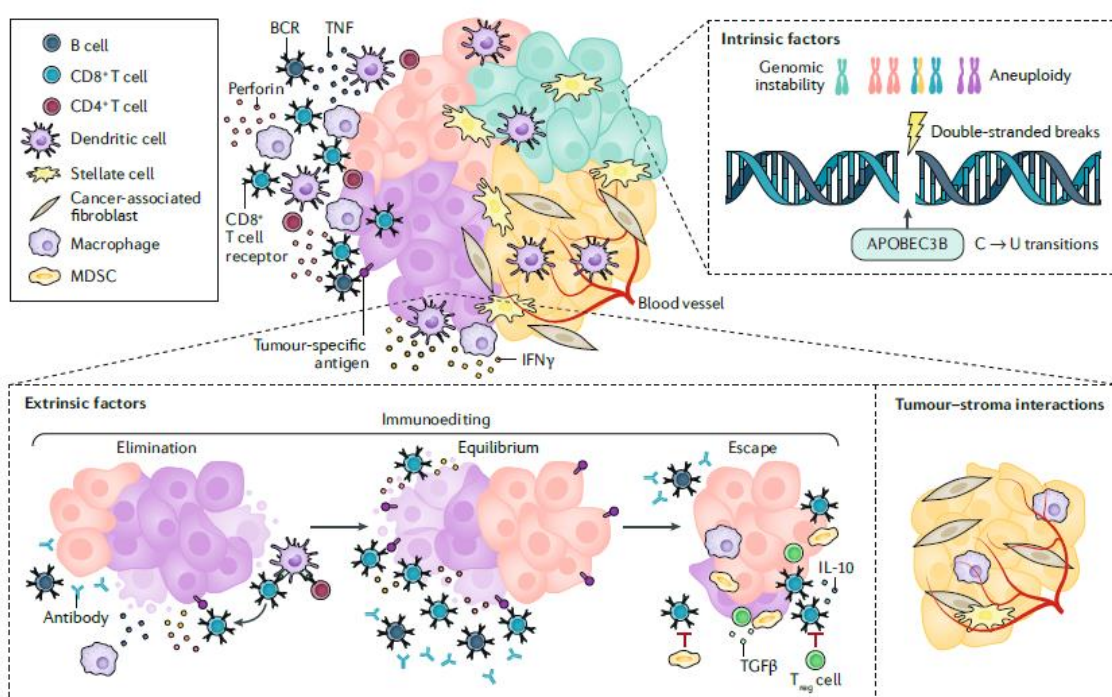


Figure 8 – Intrinsic and Extrinsic factors that drive tumour progress. MDSC – Myeloid-derived suppressor cell; BCR – B cell receptor; TGFβ – transforming growth factor-β-; Treg – regulatory T cell; IL-10 – Interleukin 10. From (37)

Treatment of HCC depends on the assessment of tumour stage using the Barcelona Clinic Liver Cancer (BCLC) stratification, an algorithm that classifies HCC into five stages: 0, A, B, C and D (32). Patients with early-stage HCC (0, A and B) are treated by partial liver resection (removal of a portion of the liver) or liver transplantation or ablation which induces tumour necrosis by injection of chemicals (e.g., ethanol, acetic acid) or temperature modification (microwave, laser or cryoablation) (32). For more advanced stages (C and D), radiation therapy and systemic chemotherapy are the most common treatments (Figure 9).

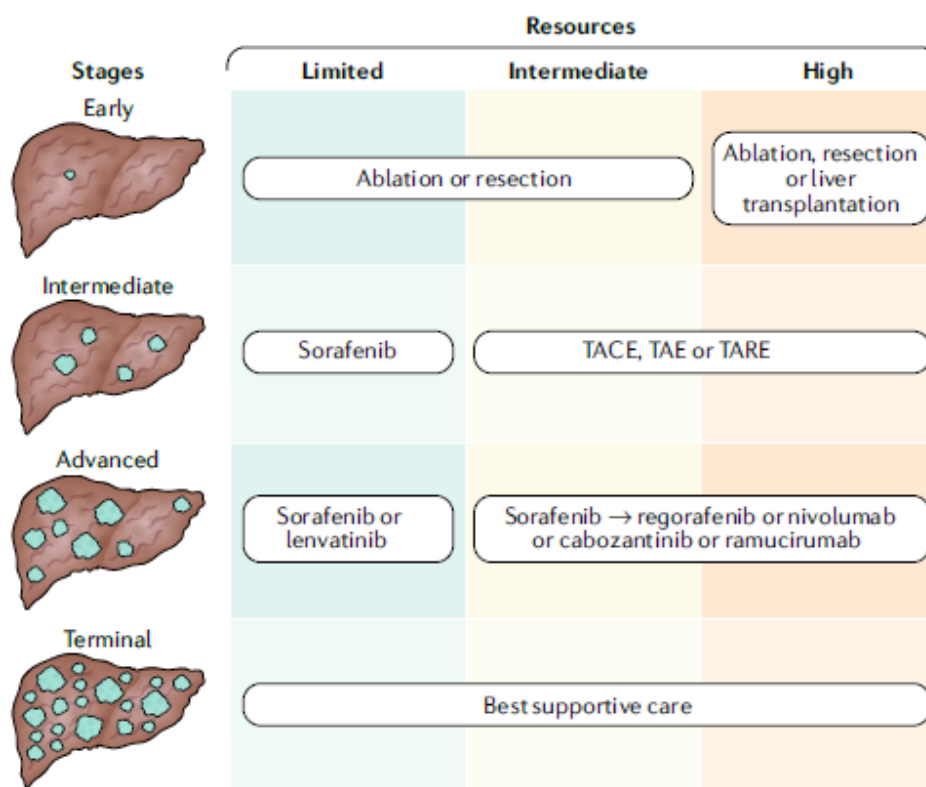


Figure 9 – Strategy for HCC treatment in countries with different resource levels. TACE – trans-arterial chemoembolization; TAE – trans-arterial embolization; TARE – trans-arterial radioembolization. From (32).

Systemic therapy includes the use of multikinase inhibitors as first-line treatment options, such as sorafenib and lenvatinib. Other drugs have been discovered and can be considered a second-line treatment option, such as regorafenib (multikinase inhibitor chemically related to sorafenib), nivolumab [human anti-PD-1 (programmed cell death protein 1) monoclonal antibody], cabozantinib (multikinase inhibitor) and ramucirumab [antiangiogenic VEGFR2 (vascular endothelial growth factor receptor 2) antagonist] (Figure 9) (32).

Despite all the efforts that have been done to combat this disease, acquired resistance to the treatments lead to high mortality of liver cancer.

Sorafenib is an oral multikinase inhibitor that supresses tumour cell proliferation, reduces angiogenesis, stimulates cell apoptosis, and can significantly extend the median survival time of patients. However, these benefits are limited, showing rare objective responses and disease control rate approaching 50-60% with most patients experiencing disease progression at six months (39). Some processes involved in this drug resistance are autophagy, increase of HIF-2 α (hypoxia-inducible factor 2 alpha) synthesis and

CSCs activity (39–43). Autophagy is associated with therapy resistance through support tumour cell survival and anoikis resistance (42), HIF-2 α synthesis can control tumour progression and therapy sensitivity (40,41) and CSCs are involved in tumours late relapse as described above (39,43).

The trans-arterial therapies also present constrains. Some biomarkers were identified after TACE treatment in surgical specimens by immunohistochemical expression, such as VEGF, HIF-2 α and HIF-1 α (hypoxia-inducible factor 1 alpha). These molecules are associated with neoangiogenesis, stemness and, consequently, therapy resistance (44). Furthermore, low levels of miR-125b (microRNA 125 b) are related to cell resistance to doxorubicin under hypoxic conditions, and increase of CSC populations, regulating, thus, cell resistance to TACE (45).

Targeted therapy has some immune-related adverse events that occur frequently during treatment and clinical consequences can be significant. Activation of the immune system leads to damage of normal healthy tissues. Some of clinical consequences are hepatitis, dermatitis, pneumonitis, and inflammatory arthritis (46). In addition, *Wnt/CTNNB1* mutations are associated to resistance to immune checkpoint inhibitors (47).

Because of these constrains of the available therapies, it is important to discover new therapies capable to combat this disease, decreasing mortality associated with liver cancer.

1.6 COX-2 and Cancer

COX-2 is a membrane-bound, short-living and rate-limiting enzyme that results from an inducible early response gene, which is activated by various extracellular or intracellular physiological stimuli, such as cytokines, growth factors and tumour promoters (4,8,48).

As an inducible gene, *COX-2* gene [*PTGS2* (prostaglandin-endoperoxide synthase 2)] contains several key regulatory sites. Its transcription is driven by a number of pathways, with binding sites in the promoter region for specific proteins, such as NF- κ B (nuclear factor kappa B), IL-6 (interleukin 6), CRE (cAMP response elements), YAP (yes associated protein), β -catenin and NFAT (nuclear factor of activated T cells) (3,48). In addition, the 3'-untranslated region (UTR) of *COX-2* mRNA also contains a series of AU-rich elements (ARE) that affect both mRNA decay and protein translation. These 3'-

UTR form complexes with transacting ARE binding factors and modulate both COX-2 mRNA stability and translation (3).

This protein is responsible for the generation of prostanoids such as prostaglandin E₂ (PGE₂), which are molecules that mediate the inflammatory process. PGs are synthesized in a wide range of tissue types and serve as autocrine or paracrine mediators to signal changes within the immediate environment (2,4,10). COX-2 is mainly found in endoplasmic reticulum lumen but also in cytoplasm, mitochondria and caveolar structures (49).

Recent articles refer to COX-2 as constitutively expressed in many important organs of the body, being responsible for very important functions, specifically in the cardiovascular system (10). However, COX-2 is widely upregulated in many human cancers, including breast (1,8,9), lung (3,6–8), hepatocellular carcinoma (4–6) and cholangiocarcinoma (3–5). The activation of COX-2 also increases the generation of others proinflammatory molecules such as IL-1 β (interleukin 1 beta), TNF- α (tumour necrosis factor alpha) and IL-6, whose production can be induced in tumour cells (5,50). Thus, due to the occurrence of many polymorphisms in the *PTGS2* gene, susceptibility between individuals to develop cancer is different (5).

COX-2 stimulates CSC-like activity and promotes apoptotic resistance, proliferation, angiogenesis, inflammation, invasion, and metastasis, playing a pleiotropic and multifaceted role in the promotion of carcinogenesis and cancer cell resistance to chemotherapy and radiotherapy (Figure 10) (4). It is accepted that most of COX-2 functions in tumour-related processes are mediated through overproduction of PGs and it is known that the prolonged increase of PGE₂ is usually a sign of inflammation, cancer genesis and/or spread (4,5).

As mentioned above, COX-2 is a pro-inflammatory protein and is overexpressed in all stages of carcinogenesis, including premalignant lesions (dysplasia and atypia), because of deregulated transcriptional and post-transcriptional control (3,9). Consequently, COX-2 can promote pro-tumour inflammation.

Inflammation occurs at different stages of tumour development and is interrelated with other processes such as angiogenesis, invasion, metastasis, apoptosis resistance and cell resistance to available therapies (51). First, tumours recruit inflammatory cells to infiltrate malignant areas and lead them to produce tumour-promoting molecules such as cytokines, chemokines, reactive oxygen species (ROS), and growth factors. Some examples of these molecules are IL-6, interleukin 10 (IL-10), and TNF- α . These pro-inflammatory molecules contribute to a microenvironment favourable for tumour cell

survival and proliferation along with an extracellular matrix. Furthermore, they also can act as immunosuppressive mediators, hindering the adaptive immune response to evade the host's antitumour defence. In the later stage, tumour cells mostly regulate inflammatory mediators, modify extracellular matrix to stimulate epithelial-mesenchymal transition (EMT), increase tumour-dependent blood vessels and lymphatic vessels, thereby promoting tumour cell survival, mobility, and invasion. Inflammatory mediators promote these physiological activities through activations of tumour-promoting signalling pathways, such as STAT3 (signal transducer and activator of transcription 3), NF- κ B, PI3K/Akt and P38 MAPK (51). COX-2 is involved in all these pathways (6,51,52).

The activation of NF- κ B is mostly driven by inflammatory mediators in the tumour microenvironment. In response to the inflammatory microenvironment NF- κ B efficiently stimulates the expression of tumour-promoting cytokines such as, TNF- α , IL-1 and IL-6 and gives a positive effect on tumour blood vessels development. NF- κ B is crucial for the high expression of pro-inflammatory and pro-tumour genes, including *VEGFR2*, *MMP-9* (metalloproteinase 9) and *COX-2*. COX-2 expression promotes tumour growth by upregulating the production of various angiogenic proteins, such as VEGF (vascular endothelial growth factor), facilitating the angiogenesis through inflammatory environment (4,51,52). Some studies also demonstrated that COX-2 is involved in metastasis and invasion processes through upregulation of MMP2/9 (metalloproteinases 2 and 9) (4).

The role of pro-tumour inflammation through the PI3K/Akt signalling pathway is multifaceted, being tumour angiogenesis the major process. Akt is stimulated by various inflammatory factors and takes part in the synthesis and secretion of inflammatory mediators. COX-2, induced by NF- κ B, performs a role for activation of this molecular pathway by suppressing PTEN (phosphatase and tensin homologue, an essential tumour-suppressing factor) or indirectly through suppression of ten-eleven translocation methylcytosine dioxygenase 1 (TET-1)-induced PTEN activation (4,8,51).

In cancer cells, STAT3 induces gene expression of many pro-inflammatory mediators such as IL-6, IL-10 and TNF- α , which connect to stromal cell receptors and activate the signalling pathway. This pathway is a crucial endogenous and exogenous inflammatory signalling pathway in tumours, being VEGF and HIF-1 (hypoxia-inducible factor-1) the major transcriptional targets and having a role in upregulation of the synthesis of MMP2/9 (51). Furthermore, STAT3/COX-2 signalling contributes to an immunosuppressive microenvironment and proliferation (4). Thus, acting in angiogenesis, invasion, proliferation, and immune system evading.

P38 MAPK is involved in the crosstalk between inflammation and tumour. This interaction is partially linked with tumour blood vessels. This pathway is stimulated through pro-inflammatory factors, such as IL-6. Curiously, IL-6 simultaneously activates NF- κ B, STAT3 and P38 MAPK pathways to upregulate the production of angiogenesis agents such as VEGF (51). P38 MAPK also take a role in the regulation of stability of COX-2 mRNA and, indirectly, in transcriptional expression of COX-2. Furthermore, P38 can also be a downstream target of COX-2 (4). P38/COX-2 pathway play an important role in angiogenesis in cancer cells (4,51).

COX-2 promotes apoptotic resistance via the HIF-1 α /PKM2 (pyruvate kinase M2) pathway. However, this process is suppressed through cross-talk between SIM2s (single-minded-2s) and NF- κ B (52,53). To maintain a survival advantage, cancer cells generate energy mainly via aerobic glycolysis even under aerobic conditions, avoiding the apoptosis. This process is known as 'Warburg effect'. HIF-1 α is known for regulating aerobic glycolysis in cancer and regulate PKM2 expression, a tumour-specific isoform of PK and a critical mediator of this process. *Wang* et al. demonstrated that COX-2 promotes the activation of HIF-1 α /PKM2 pathway in HCC cells, leading to COX-2-induced apoptosis resistance (53). NF- κ B pathway is known for contributing to cancer progression by preventing apoptosis. As mentioned above, the gene that encodes COX-2 is a target of this transcriptional factor, playing a key role in inflammation pro-tumour. SIM2s is a transcriptional tumour suppressor that is implicated in regulation of NF- κ B signalling and, consequently, COX-2. *Wyatt* et al. demonstrated the role of SIM2s as a negative regulator of NF- κ B pathway, inhibiting the activation and expression of COX-2. Thus, inflammation decreased as well as apoptosis resistance promoted by NF- κ B-COX-2 pathway (52). Some studies also showed that COX-2 induce apoptosis resistance through upregulation of BCL-2 (B cell lymphoma 2) and that P38/COX-2 pathway is also involved in this molecular process (4).

Tumour cells can use the apoptotic process to produce potent growth-stimulating signals for their repopulation, after radiotherapy and chemotherapy, as a therapy resistance mechanism. This process is stimulated by caspase-3, a key executioner in apoptosis. One downstream effector that caspase 3 regulates is PGE₂, which links COX-2/PGE₂ axis with this process. Caspase-3 is involved in the production of arachidonic acid (AA), by activation of cytosolic calcium-independent phospholipase A₂ (iPLA₂). Thus, it is implicated, indirectly, in the downstream of eicosanoid derivatives, like PGE₂. Both AA and PGE₂ production participate in stimulating tumour growth and stem cell proliferation (54,55). In this process, the few surviving cells that evade death after

therapies can quickly repopulate the severely damaged tumour by proliferating at a significantly accelerated speed (54,55).

Studies show that after therapy, an increase of PGE₂ that activates the β -catenin–Wnt signalling pathway is known to be implicated in some instances of compensatory proliferation (54). Production of PGE₂ could also lead to abnormal activation of FAK (focal adhesion kinase), a crucial regulator of signals from the extracellular matrix mediated by integrins and growth factors receptors, through phosphorylation. The abnormal activation of FAK has been associated with acceleration of the cell repopulation after conventional therapies (55).

Thus, conventional radiotherapy and chemotherapy induce COX-2/PGE₂ axis in cancer cells and, as an indirect consequence, cause cancer cell repopulation mediated by caspase-3, a therapy resistance mechanism (4,12,54,55). Furthermore, COX-2 is involved in CSC-activity, which can also be associated with therapy resistance due to its molecular adaptations (56,57).

Stemness properties of CSCs contribute to tumour recurrence. COX-2 has been linked to CSCs regulation and was identified as a TGF- β (transforming growth factor- β) downstream target (40,57). TGF- β , a protein crucial in proliferation and differentiation processes, is crucial in stimulating EMT. Cancer cells undergoing EMT in response to this protein showed CSC features, including increased self-renewing capacity and tumourigenicity as well as resistance to chemotherapy. COX-2, as a downstream target, is a relevant element in promoting EMT as also CSC-activity, modulating the TGF- β pathway (57,58).

TGF- β -mediated COX-2 expression, inhibition of telomerase expression and, consequently, cell immortalization are Smad3-dependent (transcript factor) processes. Smad2/3 are crucial mediators of the canonical TGF- β pathway and participate particularly in the regulation of TGF- β responses in a variety of contexts. *Tian et al.* demonstrated that COX-2 is crucial for TGF β /Smad3-mediated regulation (57).

Furthermore, CSC therapy resistance can be induced by ROS at both high and low concentrations. Low ROS levels increase CSC population by control of ERK (extracellular-signal-regulated kinase) and COX-2. Indeed, there is a negative feedback loop between ROS and COX-2 in CSCs. ROS are involved in COX-2 activation. COX-2 from microenvironment, in turn, reduces ROS to possibly increase CSC enhancement. Thus, CSCs are supplied with a useful oxidant/antioxidant molecular pathways obtaining an extremely compatible redox system to habitat immediately with the adjacent milieu and to resist oxidative stress stimulated by radiotherapy and chemotherapy (56).

Because of all these effects, COX-2 overexpression is linked with tumour aggressiveness and poor patient prognosis (4,57). Taking this into account, COX-2 inhibitors offer a therapeutic approach for the reduction of inflammation and related diseases, such as cancer.

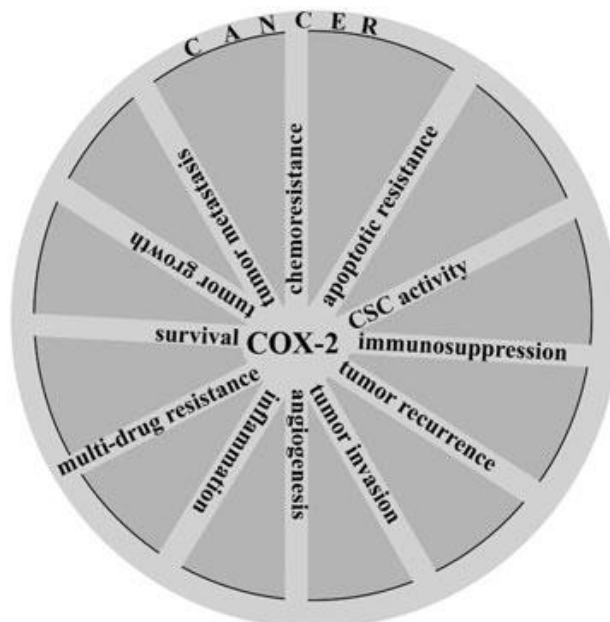


Figure 10 – Multitasking roles of COX-2 in promotion of cancer. From (4).

1.7 COX-2 inhibitors: Pharmaceutical applications

Conventional non-steroidal anti-inflammatory drugs (NSAIDs – Figure 11) are non-selective inhibitors of COX-2, as they inhibit both COX-1 and COX-2. These drugs lead to undesirable side effects, such as gastrointestinal (GI) complications, such as the irritation of the gastric mucosa. By contrast, the rate of injury to GI system applying selective COX-2 inhibitors, such as celecoxib, is low. As described above, COX-2 is mainly expressed in inflammatory tissue, while COX-1 is primarily expressed in the GI tract. For this reason, there is much less gastric aggression associated with selective COX-2 inhibitors (4,10).

Evaluation of the anticancer activity of cinnamic acid derivatives targeting COX-2

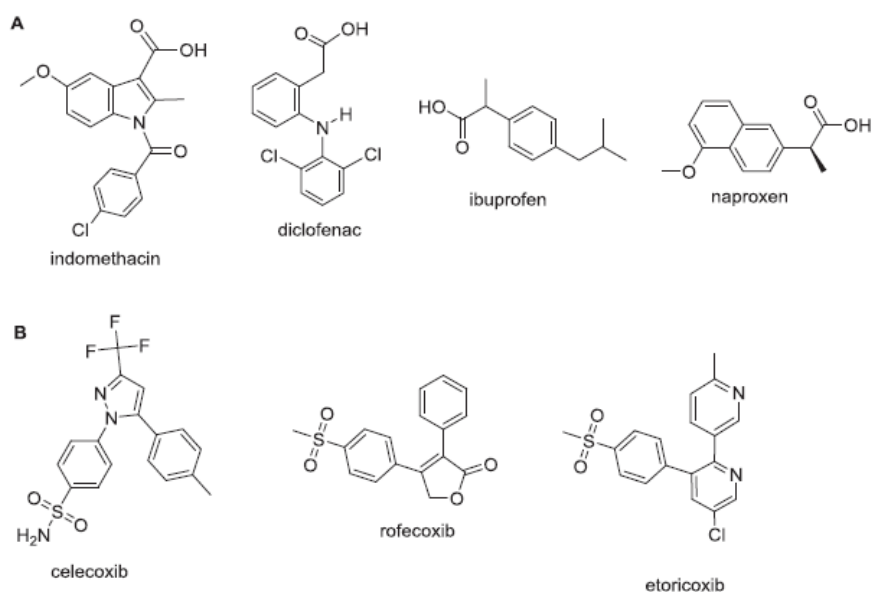


Figure 11 – (A) Some examples of COX-1/COX-2 inhibitors (NSAIDs); (B) Some examples of COX-2 inhibitors (coxibs). From (10).

The anticancer and chemopreventive potential of selective COX-2 inhibitors (coxibs – Figure 11) was already proved at different levels: 1) reduction of cancer risk in various organs, such as breast and lung (4,9); 2) inhibition of growth of cancer cells *in vitro* and in animal models (3); 3) decrease of the risk of metastasis in cancer patients, when administered in a preoperative setting (4,59); 4) sensitization of cancer cells to treatments like radiotherapy and chemotherapy (4,59). Thus, the coxibs have a strong potential as chemopreventive drugs (9). However, nowadays there are no anti-inflammatory drugs that are truly safe and can also be used as a suitable therapy with minimal GI damage and cardiovascular toxicity, including coxibs (10).

To be useful, a chemopreventive agent needs to have an acceptable risk/benefit ratio (1). Because of this, several coxibs were withdrawn from the market, such as rofecoxib (1,9,48,60), lumiracoxib (61) and valdecoxib (62). Up to today, in the United States only one COX-2 selective inhibitor (celecoxib) is available (60). In Portugal, celecoxib and etoricoxib (62–64) are the coxibs available.

Once COX-2 is involved in various molecular processes related to tumours, including inflammation pro-tumour, and coxibs truly safe to prolonged use are still lacking, it is imperative to develop novel anti-tumour and anti-inflammatory drugs to exceed the limitations of coxibs currently used in clinical practice.

1.8 Cinnamic acid derivatives

Cinnamic acid is a natural aromatic carboxylic acid and belongs to a class of phenolics compounds (Figure 12). This compound is widely distributed in Plant Kingdom, and is used as a fragrant, flavourings cosmetics and detergents. However, it is also reported that cinnamic acid exhibits several important biological activities namely, anti-inflammatory (13,65,66), antioxidant (13,65,67), anticancer (13,65,67,68), antimicrobial (65,67), antidiabetic (65) and neuroprotective (65).

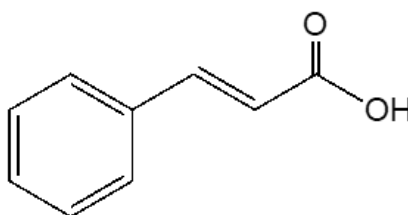


Figure 12 – Cinnamic acid structure.

The presence of an acrylic acid group substituted on the phenyl ring gives cinnamic either a cis or trans configuration with the latter being the most common in nature. Cinnamic acid can be also prepared by enzymatic deamination of phenylalanine (65).

Chemically, in cinnamic acid the 3-phenyl acrylic acid functionality offers three main reactive sites: 1) substitution at the phenyl ring; 2) addition at the α,β -unsaturation and 3) reactions of the carboxylic acid functionality (68). Thus, beyond the cinnamic acid derivatives that exist spontaneously in plants, the presence of a benzene ring and an acrylic acid group makes its alteration possible, resulting in synthetic cinnamic acid derivatives (65). Other important reaction is the introduction of alkyl chains through amidation of cinnamic acids. This reaction enhances the lipophilicity of these compounds allowing them to enter into the cells easily (13).

1.8.1 Biomedical applications

Research investment on the development of new therapeutic compounds is due to drug resistance and lack of therapies with low adverse side effects to control various pathologies such as cancer, microbial growth or neurological disorders (10,65).

Cinnamic acid derivatives have a wide range of pharmacological activities that make them excellent compounds to fight pathologies such as malaria, cancer, *diabetes mellitus* and Alzheimer's disease (65,68). The biological activity of different derivatives has been associated with the position and nature of the substituent groups (65). Some examples of cinnamic acids are caffeic acid, ferulic acid and coumaric acid (11,12,65).

1.9 Cinnamic acid amides: structure and general properties

Widely distributed among groups of plant secondary metabolites, cinnamic acid amides play crucial roles in plant growth, developmental processes, biotic and abiotic stresses responses (69).

In nature, cinnamic acid amides are obtained from aliphatic polyamines or aryl monoamines conjugated with phenolic acids, particularly hydroxycinnamic acids. Amino groups of aliphatic polyamines could be N-acylated with *mono-*, *bis-*, and trisubstituted hydroxycinnamic acids (same or different hydroxycinnamic acids halves). In addition, modifications of hydroxycinnamic acids, such as O-glycosylation, are common in the plants. All these lead to structural diversity of cinnamic acid amides (69).

It is also possible to obtain cinnamic acid amides by a synthetic way (Figure 13). As an example, the carboxylic acids are dissolved in dimethylformamide (DMF) and triethylamine (TEA) and hexylamide or diethylamide is added, following by a solution of (benzotriazole-1-yloxy)tris(dimethylamino)phosphonium hexafluorophosphate (BOP) in dichloromethane (ice-water bath). Posteriorly the dichloromethane is removed under reduced pressure and solution is dissolved with water, at room temperature, followed by extraction (10).

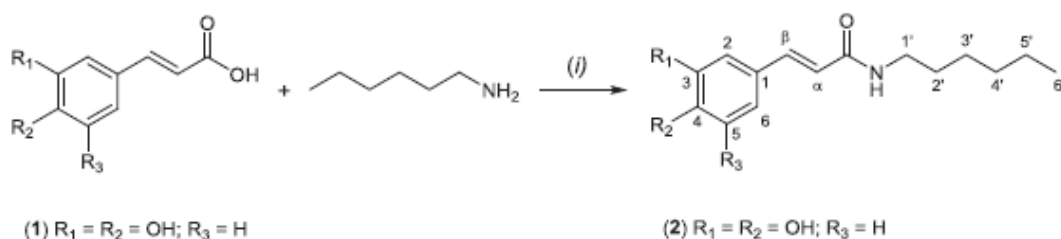


Figure 13 – Example of chemical synthesis of cinnamic acid amide: synthesis of n-hexylamides (secondary amides) of hydroxycinnamic acids. Adapted from (10).

1.9.1 Cinnamic acid amides as COX-2 inhibitors

Some undesirable effects are associated with coxibs use, such as the increased risk of renal failure, heart attack, thrombosis, and stroke, through an increase of thromboxane accumulation (10). Because of these adverse effects, efforts to discover new COX-2 inhibitors have been carried out.

Recently, one cinnamic acid and five cinnamic acid amides have revealed a higher affinity for COX-2, especially for the molecules with a catechol group in aromatic ring and bulky hydrophobic di-*tert*-butyl groups in the phenyl ring (Figure 14). Furthermore, the existence of hexyl or diethylamide side chain is also crucial for COX-2 inhibition, once the compounds, with this type of modification, exhibit higher affinity. Lastly, another important aspect in these molecules is a double bond in the aromatic side chain of hexylamide derivatives allowing a higher selectivity for COX-2 (10).

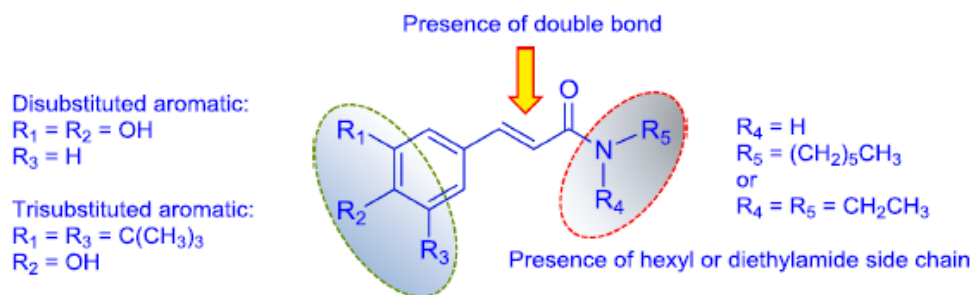


Figure 14 – Principal structural features for COX-2 inhibition. From (10).

Therefore, the principal structural features for COX-2 inhibition by this kind of cinnamic acid amides are: 1) the existence of an amide group; 2) disubstituted aromatic rings with two hydroxyl groups; 3) trisubstituted aromatic rings with 3,5-di-*tert*-butyl-4-hydroxyl substitution pattern; 4) a double bond in the side chain (10).

1.9.2 Antitumour activity of cinnamic acid amides

The efficacy of the majority of the currently used chemotherapeutic agents is brutally limited by drug resistance, since most drugs fail during invasion and metastasis of cancers making patients surrender to the disease (65).

It has been reported that cinnamic derivatives have anticancer effects and are effective against a wide variety of cancers due to their antiproliferative activity (65). It is also known that hydrocinnamic acid derivatives constitute a major group of antioxidant

compounds capable of inducing inhibitory activity of cell proliferation, cell cycle alterations and cell death in several cancer cell lines, being amide derivatives the most active compounds in this biological (11,12). Some phenolcarboxylic acids were shown to be less toxic in isolated mitochondrial fractions as well (11). Furthermore, it has been considered that phenolcarboxylic acids increase the anticancer effect of celecoxib and decrease cardiovascular toxicity in cancer treatment (70).

Taking this into account, the cinnamic acid amides may be a great adjuvant therapy option against cancer, possibly associated with low secondary effects.

1.10 Thesis Objectives

Unfortunately, conventional therapeutic agents can cause cancer cell repopulation through induction of caspase-3-mediated COX-2 activity. Due to the complexity of signalling pathways contributing to the regulation of COX-2 in cancer cells growth and cancer cell resistance to conventional therapies, it would be advisable to use coxibs as an adjuvant treatment along with chemotherapy and/or radiotherapy.

As mentioned above, until now there are no anti-inflammatory drugs that are truly safe and that can also be used as a suitable therapy with minimal GI damage and cardiovascular toxicity, including coxibs. It was established that cinnamic acid amides have important characteristics that allow us to consider these molecules as new therapeutic options such as, selectivity, potent inhibition of COX-2, increase anticancer effect and decrease of cardiovascular toxicity, induction of cell cycle alterations and cell death in cancer cells. Furthermore, some of them were shown to be less toxic in isolated mitochondrial fractions.

Hence, this work aimed to evaluate one cinnamic acid and five cinnamic acid amides biological activity in order to discover new compounds to exceed the limitations of the COX-2 selective inhibitors currently used in clinical practice. The effect of recently synthesized cinnamic acid amides was evaluated in a set of several types of cancer cell lines, which include HCC cells (HepG2, HuH7) and estrogen-dependent BC cells (MCF-7), for their antiproliferative activity. For the most promising compound **E4**, additional studies were performed in the cancer cells along with one normal breast cell line (MCF-12A), to understand its mechanisms of action. The assays performed allowed the analysis of cell cycle, cell viability and cell death profiles, mitochondrial membrane potential, cell morphology, expression of COX-2 and selectivity of the compounds.

Chapter 2. Materials and Methods

In this Chapter, a description of all the chemical and biological materials used in this study is performed, along with crucial explanations required for their preparation. This Chapter is subdivided into eight sections, which refer to the eight steps of this study. The first section presents the compounds and cell lines used and how they were manipulated. The following sections describe the methods used to assess the effects of compounds on several biological processes (COX-2 expression, proliferation, cell cycle, cell viability and death, cell morphology). Finally, last section describes the statistical methods used to process the results obtained.

2.1 Evaluation of compounds *in vitro*

Compounds were provided by Laboratory Pharmaceutical Chemistry of Faculty of Pharmacy of University of Coimbra. Their anticancer activity was evaluated in several cancer cell lines as described below. Their structures and respective names are presented in Figure 15.

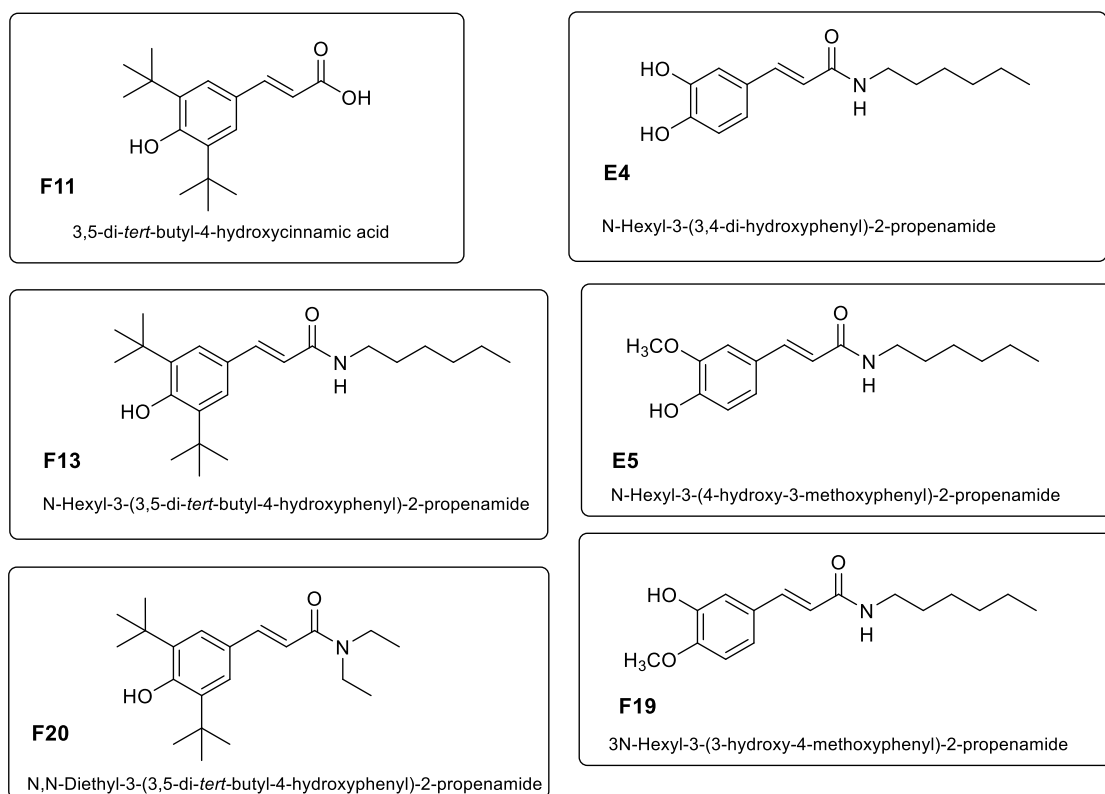


Figure 15 - One cinnamic acid (F11) and five cinnamic acid amides used in this research.

2.1.1 Cell culture

In this study, four human cell lines were used namely, two HCC cell lines (**HepG2**, ATCC® HB-8065™ and **HuH7**, JCRB0403), one BC cell line (**MCF-7**, ATCC® HTB-22™) and one non-tumour human breast epithelial cell line (**MCF-12A**, ATCC® CRL-10782™). These cell lines were selected based on their differences in COX-2 expression and inherent difficulties of nowadays clinical practise – inefficient therapies in HCC advance disease and therapy resistance in BC. HuH7 and HepG2 cell lines presented contradictory results about COX-2 expression in literature (71–74). However, in majority of the published studies, HepG2 presented more COX-2 expression than HuH7. HuH7 is an HCC cell line, characterized to being well differentiated originally taken from a liver tumour in a 57-years-old Japanese male (75). In contrast, HepG2 cell line that is an HCC

cell line derived from a liver hepatocellular carcinoma of a 15-year-old Caucasian male, being also referred as hepatoblastoma cell line (76). MCF-7 is a BC cell line of luminal type (express ER) and have lower COX-2 expression (77,78). MCF-12A is a normal breast epithelial cell line that do not express COX-2, being used in this research to evaluation of selectivity of compounds (79).

All cell lines were acquired from American Type Collection Culture (ATCC), except HuH7 acquired from Japanese Collection of Research Bioresources Cell Bank (JCRB). All cell lines were maintained in optimal conditions at 37°C in 5% CO₂ atmosphere following the repository instructions.

The cell lines HepG2, HuH7 and MCF-7 were cultured in *Dulbecco's Modified Eagle Medium*, DMEM (Sigma, D5648), while MCF-12A cell line was cultured in *Roswell Park Memorial Institute Medium*, RPMI-1640 (Sigma, R4130). Both mediums were supplemented with 5% heat-inactivated fetal bovine serum, FBS (Sigma, F7524), antibiotics (100 U/mL de penicillin e 10 µg/mL streptomycin; Sigma, A5955) and 0.25 mM sodium pyruvate (Sigma, S8636) for DMEM and 1 mM for RPMI. For MCF-12A cell line, the RPMI was also supplemented with 0.5 µg/mL hydrocortisone (Sigma, H0888) and 20 ng/mL human Epidermal Growth Factor (hEGF) (Sigma, 11376454001).

Given that all cell lines grow in adherent monolayer, it was necessary to detach the cells from the flasks prior to each experiment. For that, a solution of Trypsin-EDTA 0.25% (Sigma, T4049) was used.

First, the culture medium was removed and then the cells were washed with phosphate buffered saline (1X), (PBS, 137 mM NaCl [S7653, Sigma], 2.7 mM KCl [P9333, Sigma], 10 mM Na₂HPO₄.2H₂O [S5011, Sigma]) and 2 mM KH₂PO₄ [P0662, Sigma], pH=7.4). PBS was then discarded, and it was added 2 mL of Trypsin-EDTA 0.25%. After 5 minutes in the incubator at 37 °C in 5% CO₂. The effect of the Trypsin-EDTA was then inhibited by using 5 mL of fresh medium. Later, after obtaining the cell suspension, the cell concentration was determined using the trypan blue exclusion method. This method is based on the principle that viable cells maintain their cell membrane intact (brilliant on the microscope), whereas dead cells are permeable to the trypan blue, acquiring then a blue colour. Thus, 20 µL of cell suspension was mixed with 20 µL of trypan blue 0.02% (Sigma, 302643), and the cell concentration was determined by counting the alive cells of the 4 quadrants in a Neubauer chamber, using an inverted optic microscope, with a 100x amplification.

The formula used to calculate cell concentration was the following:

$$[Cell] \text{ (cells/mL)} = \text{Alive cells (average of 4 quadrants)} \times 2 \times 10\,000 \text{ [Equation 1]}$$

2.1.2 Treatment with the compounds

Initially, solutions of 60 mM of each compound dissolved in dimethylsulfoxide (DMSO, Sigma, D4540) were prepared. Before treatment, solutions of each compound were prepared by diluting the original solution so that the volume added was lower than 1% of the culture medium volume in each well or flask.

The treatment description for each experiment is detailed below. The remaining detailed description of each methodology will be made forward in the respective section.

First, to evaluate the basal COX-2 expression in all cancer cell lines used in this research western blot technique was executed. Western blotting allows to detect specific proteins of one cell extract.

Second, the cytotoxic effect of each compound was evaluated in the three cancer cell lines previously described (HepG2, HuH7 and MCF-7) using MTT assay. The cells were seeded in 48 well-plates (Sarstedt) at a density of 100 000 cells/mL in a volume of 500 µL per well. After incubation overnight, cells were treated with cinnamic acids derivatives **E4**, **E5**, **F11**, **F13**, **F19** and **F20** at different concentrations ranging from 0.004 to 300 µM for 48 hours, which are presented in Table 1. Two negative controls were used: one with untreated cells and one with DMSO, corresponding to the solvent of compounds.

Table 1 – Different concentrations of compounds used in MCF-7, HuH7 and HepG2 cell lines to MTT assay.

COMPOUNDS	CONCENTRATIONS
E4	1 to 100 µM
E5	1 to 300 µM
F11	0.004 to 300 µM
F13	1 to 300 µM
F19	1 to 100 µM
F20	1 to 200 µM

For evaluation of selectivity, the compounds **E4**, **F13** and **F19** were selected since they were the ones with better results.

To assess the selectivity of the cytotoxic effect of **E4**, **F13** and **F19**, MCF-12A non-tumour cell line was seeded in 48-well-plates (Sarstedt) at a density of 80 000 cells/mL in a volume of 500 μ L per well. After incubation overnight, cells were treated with compounds at different concentrations ranging from 10 μ M to 200 μ M for 48 hours (Table 2). Cells were treated with compounds at a concentration corresponding to the IC₅₀ (half maximal inhibitory concentration) and a concentration higher than the IC₅₀ (>IC₅₀), except celecoxib (only IC₅₀). The selection of the concentrations used relies on the results of MTT assays in cancer cell lines. Three controls were used: two negative control (untreated cells and DMSO) and one positive control, celecoxib, drug used in clinical practice as COX-2 inhibitor.

Table 2 – Different concentrations of E4, F13, F19 and celecoxib used in MCF-12A cell line to MTT assay.

COMPOUNDS	CONCENTRATIONS
E4	16.05 and 25 μ M
F13	94.9 and 200 μ M
F19	48.8 and 75 μ M
CELECOXIB	10 μ M

For subsequent assays, the compound **E4** was selected since it presented minor IC₅₀ values.

For *May-Grünwald-Giemsa* technique, all cell lines were seeded in 25 cm² flasks (SPL Life Sciences) at a density of 1×10⁶ cells/flask. After overnight incubation, cells were treated with compound **E4** at a concentration corresponding to the IC₅₀ and a concentration higher than the IC₅₀, as represented in Table 3.

For the subsequent assays, all cell lines were seeded in 75 cm² flasks (SPL Life Sciences) in following densities: 3×10⁶ cells/flask (MCF-7), 1.5×10⁶ cells/flask (HepG2) and 1.2×10⁶ cells/flask (HuH7). After overnight incubation, cells were treated with compound **E4** at a concentration corresponding to the IC₅₀ and a concentration higher than the IC₅₀, as represented in Table 3.

Table 3 - Concentrations of E4 compound tested in MCF-7, HuH7 and HepG2 for Flow Cytometry and *May-Grünwald-Giemsa* technique.

CELL LINE	ASSAY	IC ₅₀ (μM)	>IC ₅₀ (μM)	
MCF-7	Flow Cytometry	JC-1	16.05	25
HUH7		AV/PI	29.38	75
HEPG2		PI/RNase	34.74	75

The following assays were then performed by flow cytometry: analysis of cell cycle, detection of cell viability and different types of cell death and evaluation of the mitochondrial membrane potential.

To evaluate the effects of compound treatment (**E4**) in COX-2 expression western blot technique was executed. Thus, the cells were seeded and treated, for 48 hours, with concentrations present in Table 4.

Table 4 - Concentrations of E4 and celecoxib tested in MCF-7, HuH7 and HepG2 cell lines for Protein Extract.

CELL LINE	ASSAY	IC ₅₀ (μM)		>IC ₅₀ (μM)
		E4	Celecoxib	E4
MCF-7	Protein Extract	16.05		25
HUH7		29.38	10	75
HEPG2		34.74		75

The selection of the concentrations used in all the studies relies on the results of the MTT assay in cancer cell lines.

2.2 Analysis of basal COX-2 expression

Western blotting is an important method used to detect specific proteins in a dense mixture of proteins extracted from cells (80).

Protein extractions were obtained by adding 400 μL of RIPA (radioimmunoprecipitation assay buffer) lysis solution to the culture flasks, after washing

it three times with PBS. RIPA lysis solution consists of 150 mM NaCl, 50 mM Tris base (Sigma, T1503), 5 mM EGTA (ethylene glycol-bis(2-aminoethylether)-N,N,N',N'-tetraacetic acid; Sigma, E4378), 1% Triton® X-100 (Merck, K34979403), 0.5% sodium deoxycholate and 0.1% SDS (sodium dodecyl sulphate; Sigma, 436143). Immediately before used, it is supplemented with a cocktail of proteases inhibitors (cOmplete-Mini; Roche, 11836153001), according to supplier's instructions, and 1 mM DTT (DL-dithiothreitol; Sigma, D9779).

After adding RIPA solution to the culture flasks, the cells were scraped from the flask's surface using a "scraper", and the contents were placed in an Eppendorf® microtube. Following vortexing, the samples were sonicated for 20 seconds with a 35% amplitude using a VibraCell sonicator (model VC50, Sonic and Materials Inc.). The samples were then centrifuged at 14000×G for 15 minutes, and the supernatants were transferred to a new and properly labelled Eppendorf® microtubes and kept at -80 °C.

In the first step, gel electrophoresis is used to separate the proteins in a sample based on their isoelectric point, molecular weight, electrical charge, or a combination of these characteristics. Protein separation based on the size of the polypeptide, when denatured, is the most common method of electrophoresis. This process involves polyacrylamide gels and denaturing solutions containing SDS, a detergent that add negative charge to proteins, allowing their separation by their molecular weight using a positive electrode in a polyacrylamide gel. Lower molecular weight proteins migrate faster through the gel and can be found at the bottom, whereas higher molecular weight proteins move slowly and are thus found at the top.

After proteins separation, they were transferred to a nitrocellulose or PVDF (polyvinylidene difluoride) membrane, where the target proteins are analysed and detected using antibodies. At this point, a primary antibody was added to the sample to mark the proteins with antigens. Proteins can be clearly recognized using a secondary analogue antibody by tagging, specifically, the primary antibody.

Western blotting was used to detect basal expression of COX-2 in all cell lines used in this research.

The BCA method (Bicinchoninic acid, BCATM protein assay kit, Pierce) was used to determine the total amount of protein in our protein extract. After solubilization in a denaturing solution composed by 60 mM Tris base, 10% glycerol (Sigma, G2025), 2% SDS, 2-mercaptoethanol 5% (Merck, 444203), and 0.01% bromophenol blue (May&Baker Dagenham England, 14764), the samples were denatured at 95 °C for 5 minutes.

Electrophoresis was performed using acrylamide gels polymerized at a concentration of 10% to separate proteins to identify COX-2. The acrylamide gels were set in the electrophoresis tank with a suitable buffer with pH adjusted to 8.3 (Bio-Rad161-0772). Also, the samples and molecular standard weight (Precision PlusStandards, Dual Colour, Bio-Rad or NZYColour Protein Marker II, Nzytech, MB09002) were prepared. In electrophoresis, a constant electric potential difference of 80 V was applied, for 10 minutes, and secondly a constant electric potential difference of 150 V was used.

The gels were placed in direct contact with PVDF membranes (Polyvinylidene Fluoride Membrane, Millipore) which had already been activated in methanol or ethanol to perform the electrotransfer. The transfer system was prepared, and the reaction happened at a potential difference of 25 V with a duration of 7 minutes, in CAPS buffer (3-(Cyclohexylamino)-1-propanesulfonic acid, Sigma, C2632) at a concentration of 100 mM, with a pH of 11. Next, the membranes were immediately blocked with a solution of BSA (bovine serum albumin) with a concentration of 5% prepared in TBS-T (Tris-Buffered Saline Tween-20), at room temperature. After 30 minutes, the membranes were incubated overnight at 4°C with constant agitation with the primary antibody. To detection of COX-2 was used anti-COX-2 rabbit antibody [(Cox2 (D5H5) XP® Rabbit mAb, Cell Signalling Technology)]. The anti-COX2 antibody was prepared in 2.5:1000 ratio.

On the next day, washes were carried out with TBS-T 1X and for the primary antibody, the membranes were incubated with the corresponding secondary antibody, namely anti-rabbit (goat anti-rabbit IgG-AP, Santa Cruz Biotechnology, sc-2007), under constant agitation and at room temperature for about 1 hour and 30 minutes. The anti-rabbit antibody was prepared in 1:12 000 ratio in 4% of TBST-BSA solution. The membranes were then washed again and incubated for 5 minutes with an enzymatic substrate (ECF Western Blotting Reagent, GE Healthcare, RPN5785) before being revealed on a fluorescence reader (Typhoon FLA 9000).

Posteriorly, the membranes were incubated for β -actin labelling (antibody produced in mouse, Sigma, A5441) about 1h, washed again with TBS-T 1X and incubated with an anti-mouse antibody (goat anti-mouse, GE Healthcare, RPN5781). Both anti-actin and anti-mouse antibodies were prepared in a ratio of 1:12 000 ratio in 4% of TBST-BSA solution. Actin is a protein found in all cells and is frequently used as control for the total amount of protein detected in each lane.

The quantification of COX-2 expression was performed using Fiji software. The results are expressed as arbitrary units (without normalization).

2.3 Antiproliferative effect

To understand the antiproliferative effects of the cinnamic acids derivatives, the MTT and SRB assays were used to evaluate cell metabolic activity and protein content, respectively.

2.3.1 Evaluation of metabolic activity by the MTT assay

Evaluation of metabolic activity was performed by the colorimetric assay MTT, 3-(4,5-dimethylthiazol-2-yl)-2,5-diphenyltetrazolium bromide. MTT, a yellow tetrazole reagent, is reduced forming purple formazan crystals in the presence of dehydrogenase enzymes located mainly in the viable mitochondria, *i.e.*, in metabolically active cells (81). Metabolic activity was evaluated as a measure of cell proliferation.

After an incubation time of 48 hours, the medium was removed, and the cells were washed with PBS (1X). Then, 200 μ L of an MTT solution (Sigma) at 0.5 mg/mL and pH=7.4 was added to each well and cells were incubated for about 2 hours in the dark at 37°C in 5% CO₂. Then, 200 μ L of isopropanol (Sigma) at 0.04 M was added and the plates were agitated to dissolve the purple formazan crystals. Absorbance values were measured at 570 and 620 nm in an ELISA spectrophotometer (EnSpire® Multimode Plate Reader, PerkinElmer®).

The percentual data obtained allowed to establish dose-response curves and to determine the half maximal inhibitory concentration of the compounds, used in this study (IC₅₀), using the GraphPad software 8.0 (*GraphPad Software*, La Jolla California, USA).

2.3.2 Evaluation of cell proliferation by the SRB assay

The SRB assay has been used to evaluate cell proliferation and cytotoxicity of **E4** and **F19** compounds. This method uses a dye called sulforhodamine B (SRB), which binds to proteins under acidic conditions and can be posteriorly extracted under basic environment, so the amount of dye can be extrapolated to measure protein content and indirectly cell proliferation (82,83).

After an incubation time of 48 hours, the medium was removed, and the cells were washed with PBS (1X). Then, 200 μ L of 1% acetic acid in methanol solution was added to fix the cells, leaving it to act for 1 hour. Posteriorly, acetic acid in methanol solution was discarded, and 200 μ L of 0.4 % SRB was added to each well and incubated for 2 hours away from the light and at room temperature. Afterwards, the SRB was taken

out and the plate was kept drying at room temperature for 10 minutes. Once it was completely dry, 200 μ L of Tris-NAOH 10mM (pH=10) was added and the plate was left agitating for 15 minutes until the dye was totally dissolved. Next, the absorbance was measured at 540 nm, with a reference filter of 690 nm, in an ELISA spectrophotometer (EnSpire® Multimode Plate Reader, PerkinElmer®).

The results of SRB assay will be presented below as a percentage of protein content normalized to DMSO control. The data obtained were compared with the results obtained by the MTT assay through a bar graph prepared in GraphPad software 8.0.

2.4 Cell cycle analysis

The effect of the compounds in cell cycle progression (G_0/G_1 phase, G_2/M phase, and S phase) was evaluated through flow cytometry by staining with a solution of propidium iodide (PI) with RNase, 48 hours after treatment with **E4**.

PI intercalates with DNA and RNA bases. This is the reason why this experiment requires incubation of RNase to obtain a specific staining only for DNA. The dye binds stoichiometrically to the cells' DNA allowing to get a histogram of the distribution of the different cell populations in each phase of the cell cycle (84).

Cells in S phase exhibit more DNA content than the cells in G_0/G_1 phase and the cells in G_2/M phase have twice the amount of DNA than cells in G_0/G_1 phase. It is also possible to identify an apoptotic peak, with less DNA amount.

For each assay, 1×10^6 cells were detached from the flasks and centrifuged at $1300 \times G$ for 5 min. To fix the cells, 200 μ L of ethanol at 70% was added to the deposits in agitation and then the samples were incubated for 30 min in the dark at 4°C. After incubation time, the samples were again centrifuged at $1300 \times G$ for 5 min, washed with 2 mL of PBS and 200 μ L of PI/RNase solution (Immunostep, PI/RNase) was added to the resulting pellet, and incubated for 15 min in the dark, at room temperature.

The analysis was performed in a FACSCalibur (Becton Dickinson) flow cytometer with excitation and emission wavelengths of 488 and 640 nm, respectively. Results were expressed as a percentage of the cell in each subpopulation: pre- G_0/G_1 , G_0/G_1 , S and G_2/M .

Results are expressed as a percentage.

2.5 Analysis of cell viability and cell death mechanisms

To assess if the cytotoxic effect of **E4** compound is mediated by cell death pathways, cell viability and cellular death pathways mechanisms were evaluated. Posteriorly, to characterize cell death pathways induced by compounds, changes in mitochondrial membrane potential ($\Delta\Psi_m$) were evaluated.

2.5.1 Analysis of cell viability and death by flow cytometry

Cell viability and the different induced types of cell death were assessed by flow cytometry, 48 hours after treatment with **E4** by double staining the cells with annexin V (AV) labelled with the fluorescein isothiocyanate fluorochrome (FITC), and with PI.

Plasmatic membranes' architecture can be altered by a redistribution of several phospholipids' species, which is one of the modifications associated with apoptosis. One of these species is phosphatidylserine that suffers a translocation from the inner to the outer layer of the plasmatic membrane at the beginning of apoptosis process (85). Consequently, the high affinity of AV to phosphatidylserine allows discriminating between viable and apoptotic cells (86).

The plasmatic membranes' rupture reveals late apoptosis/necrosis, that allows the entrance of PI to the intercellular space where PI binds with DNA and emits fluorescence (87). Thus, the double staining offers a way to discriminate four different populations of cells: the population of live cells, negative for both staining; the population of early apoptotic cells, positive for staining with AV-FITC and negative for staining with PI; the population of late apoptotic/necrotic cells, positive for both AV-FITC and PI and the population of necrotic cells, negative for the AV-FITC staining and positive for PI staining (86).

Thus, 1×10^6 cells were detached from the flasks, per assay. Each cell suspension was centrifuged at 1300 X G for 5 minutes and the obtained pellets were resuspended in 1 mL of PBS and centrifuged again in the same conditions. Cells were incubated with 100 μ L of binding buffer (0.01 M Hepes [H7523, Sigma], 0.14 M NaCl and 0.25 mM of CaCl_2 [C4901, Sigma]), 2.5 μ L of AV-FITC (ANXVKF, Immunostep) and 1 μ L of PI (ANXVKF, Immunostep) during 15 minutes at room temperature and in the dark. After incubation time, 400 μ L of binding buffer was added.

The analysis was performed in a FACSCalibur cytometer (Becton Dickinson) applying excitation wavelength of 488 nm and emission wave lengths of 533 nm for AV-FITC and 640 nm for PI. Results are expressed as the percentage of detected cells in each subpopulation.

2.5.2 Evaluation of the mitochondrial membrane potential

The $\Delta\Psi_m$ is a crucial event in terms of apoptosis. It can be measured using the fluorescence dye JC-1 (5,5',6,6'-tetrachloro-1,1',3,3'-tetraethyl-imidacarbocyanine iodide).

JC-1 is a lipophilic and cationic dye that enters in the mitochondria in the form of monomers (M), which under mitochondria polarization conditions forms aggregates (A) that emit fluorescence in the red zone. With the decrease of the $\Delta\Psi_m$, JC-1 is excluded from the mitochondria and is dispersed in the cytoplasm in the form of monomers that emit fluorescence in the green zone. The ratio between red fluorescence and green fluorescence (A/M) gives us an estimation of the $\Delta\Psi_m$, regardless of mitochondrial mass (88). The analysis was performed 48 hours after treatment.

For each assay, 1×10^6 cells were detached from the flasks, centrifuged at $1300 \times G$ for 5 minutes and then 1 mL of PBS was added. The samples were centrifuged again at the same conditions and incubated with JC-1 (Sigma, T4069) at a concentration of 5 mg/mL for 15 min at $37^\circ C$ in 5% CO_2 . Then, 2 mL of PBS was added to each sample and centrifuged once again at $1300 \times G$ for 5 minutes. Finally, 400 μL of PBS was added and the detection was performed in a FACSCalibur cytometer with excitation wavelengths of 530 nm for the monomers and 590 nm for the aggregates.

Results are expressed as the ratio variation of the fluorescence intensities of monomers/aggregates (M/A), normalized to the control.

2.6 Analysis of cell morphology

To complement flow cytometry results, cells' morphologic characteristics were evaluated, after treatment with (E4). For this, *May-Grünwald-Giemsa* technique was realized by making cells smears, which were analysed through optic microscopy (89).

After 48 hours of treatment with **E4**, the cells were detached, and 200 000 cells of each condition were centrifuged at 1300×G for 5 minutes and supernatant was discarded. The cells were washed with PBS and again centrifuged in same conditions. After discard the supernatant, the cells were resuspended in 50 µL of FBS, to improve the adhesion to slide.

Then, smears were performed in proper slides (Normax), which were allowed to dry for, at least, 30 minutes. The slides were fixed for 5 minutes in methanol. Posteriorly, staining was proceeded with a *May-Grünwald* solution (Merck Millipore, 101424) for 4 minutes and, later, with 5% *Giemsa* solution (Merck Millipore, 109204) in water, for 15 minutes. Finally, the slides were washed with water and allowed to air dry.

Later, the slides were observed and imaged using an optic microscope (Nikon Eclipse Ni optic microscopic equipped with Nikon Digital Camera DS-Fi2). To each cell line, the results were presented qualitatively, with three representative images for each condition (untreated cells, IC₅₀ and >IC₅₀).

2.7 Analysis of COX-2 expression

Western blotting was used to evaluate the effects of compound treatment (**E4**) in COX-2 expression, as described in section 2.2.

Results are expressed as an arbitrary units normalized to the untreated cells control and representative images of membranes COX-2 and actin expression on all conditions (untreated cells, IC₅₀, >IC₅₀, and 10 µM of celecoxib).

2.8 Statistical analysis

The statistical analysis was performed using the GraphPad software 8.0.

In the cell proliferation analysis through MTT assay in cancer cell lines, the experimental values obtained were adjusted to a dose-response sigmoidal model represented through the following equation:

$$Proliferation (\%) = A1 + \frac{A2-A1}{1+10^{(\log x_0 - x)p}} \quad \text{[Equation 2]}$$

where A1 and A2 correspond to the plateaus, x_0 corresponds to the half maximal inhibitory concentration (IC₅₀) and p corresponds to slope factor. After mathematical

adjustment, statistical parameters were obtained, namely, R squared (R^2) and confidence intervals (with 95% of confidence level). Significant differences were accounted when the 95% confidence intervals of the compounds did not intersect.

A significance level of 5% was considering and normal distribution was assessed using *Shapiro-Wilk* test for all other experiments. Outliers' detection was realized using the ROUT method with $Q=10\%$. By default, parametric tests were used in case of normal distribution and non-parametric tests were used otherwise.

For MTT and SRB data, the parametric two factor analysis of variance (ANOVA) with *Sidak* test for multiple comparisons was used, to compare the two assays within each cell line, per compound.

For MTT data in MCF-12A and MCF-7 cell lines, the parametric two factor ANOVA with *Sidak* test for multiple comparisons was used, for comparisons between cell lines and between conditions.

For western blot data, different tests were used. The parametric two factor ANOVA with *Tukey* test for multiple comparisons was used to compare COX-2 expression for different treatments within each cell line. To compare basal expression of COX-2 in three used cell lines it was used the parametric one factor ANOVA with *Tukey* test for multiple comparisons.

For flow cytometry data, different tests were used. The parametric two factor ANOVA with *Tukey* test for multiple comparisons was used to compare the different treatments within each cell line, in viability and cell cycle analysis. For JC-1 data, it was used one factor ANOVA to compare the different treatments within each cell line. In cases of non-normality, the non-parametric *Kruskal-Wallis* with *Dunn's* test for multiple comparisons was used to compare different treatments within each cell line.

Chapter 3. Results and Discussion

In this Chapter, all the results are presented, analysed, and discussed. The data analysis will be backed up by bibliography. The organization of this chapter is identical to the one presented in Chapter 2, and it is divided in five subchapters: basal COX-2 expression, antiproliferative effect assessment, cell cycle, cell viability and death mechanisms and COX-2 expression.

3.1 Basal COX-2 expression

Western blot was performed to clarify the contradictory results found in bibliography (71–74) about basal COX-2 expression in three of the cell lines used. Results are presented as arbitrary units without normalization, by mean \pm standard error of mean (SEM) of, at least, three independent experiments, in triplicate.

Figure 16 represents the different basal COX-2 expression for each cell line. HuH7 cell line has 0.22-fold and 0.54-fold higher COX-2 expression than HepG2 and MCF-7 cell lines, respectively. COX-2 expression in MCF-7 cells was significantly lower ($p=0.02$) from HuH7 COX-2 expression. Antagonistically, MCF-7 and HepG2 COX-2 expressions did not present statistically significant differences, as well as HuH7 and HepG2 COX-2 expression. However, these results showed that HepG2 cell line presented less COX-2 expression than HuH7 cell line.

Despite *Kern*, et al. (2002) and *Baek*, et al. presented western blot (WB) results that demonstrate a great difference between the COX-2 expression in HepG2 and HuH7 cell lines (heavy COX-2 expression in HepG2 cells when compared with HuH7 COX-2 expression) (72,74), not all articles are in agreement (71,73).

Kern, et al. (2006) got one western blot result with less difference between COX-2 expression in HepG2 cells and HuH7 cells (73). *Murata*, et al. showed that in HepG2 cells, COX-2 promoter has a small amount of CpG islands methylated, leading to a partial silencing of COX-2 expression. On the other hand, HuH7 cells have all CpG unmethylated, maintaining total COX-2 expression (71).

Therefore, although there are no significant differences, these results are in agreement with *Murata* et al., which demonstrated that HepG2 COX-2 promoter has a small amount of CpG islands methylated than HuH7 COX-2 promoter, leading to a partial silencing of COX-2 expression in HepG2 cell line (71).

The contradictions described above can be explained by inherent limitations of the technique used to assess protein expression, as western blot, such as the use of different types of antibody or antibodies of different specificities and the use of different methods of transferring the proteins to the membrane. However, considering that HuH7 and HepG2 cell lines did not present significant differences and there are contradictions in bibliography (71–74) about COX-2 expression in these cell lines, it is important to repeat this method with a larger number of samples and complement it with the evaluation of PG levels by ELISA in order to corroborate the results.

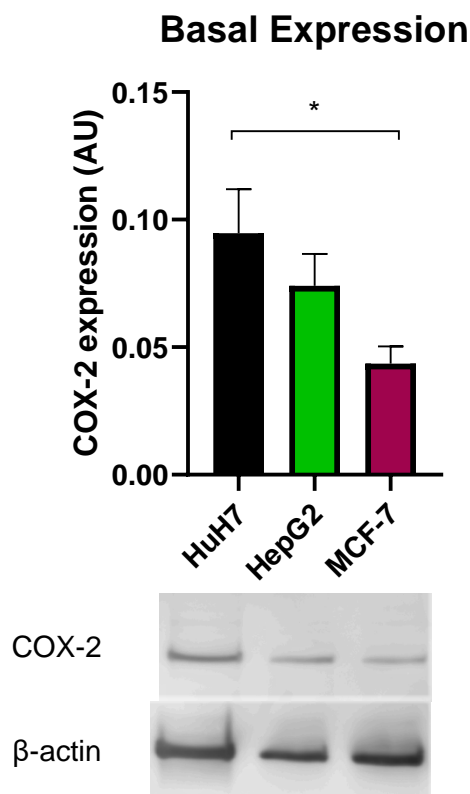


Figure 16 - COX-2 basal expression in three cell lines (HuH7, HepG2 and MCF-7). Results are presented as arbitrary units (AU) (without normalization) of COX-2 expression as a function of different cell lines and express the mean \pm SEM of, at least, three independent experiments, in triplicate. Significant differences are denoted by * p <0.05. Below the bar graph there are western blot diagrams of COX-2 and β -actin expression.

3.2 Antiproliferative effect assessment

The first cytotoxicity study (MTT assay) in this research was performed in order to evaluate the effect of increasing concentrations of the compounds on the metabolic activity of three tumour cell lines previously described. To evaluate the selectivity of the compounds, the metabolic activity of one normal cell line, previously described (MCF-12A), was also assessed.

3.2.1 Metabolic activity

Metabolic activity was assessed 48 hours after the treatment with compounds **E4**, **E5**, **F11**, **F13**, **F19** and **F20** at concentrations ranging from 1 to 300 μ M (depending on the cell response). The metabolic activity was determined relatively to cell cultures treated with DMSO, to which a metabolic activity of 100% was assigned.

The results obtained for **F11** compound will not be presented given that this compound exhibited colour change and unexpected instability. On doing the **F11**

treatment at room temperature, it was observed that its colouration changed over time. At first, the compound was colourless, but after two weeks it showed a yellowish colour, which gradually changed to a dark orange colour from week to week. Although an increase in its antiproliferative capacity was observed, it was not clear whether this antiproliferative activity was due to the compound itself or the by-products of its interaction with the solvent (DMSO). In order to clarify this, the experiment was repeated with a new solution made and stored at 4°C. This time, it was observed that the antiproliferative activity decreased drastically, consequently, a wider band of concentrations was used (0.004 to 300 µM) as presented in Table 3, Materials and Methods section. Considering the contradictory results, it was concluded that this alteration could indicate possible modifications in the chemical structure of the compound, maybe due to the by-products of the interaction between the compound and solvent. Indeed, the research group responsible for the synthesis of the compounds concluded that there is another by-product of the interaction between **F11** and DMSO, however, this study is still in the phase of separation and characterization of the degradation compound. In addition, it was observed that a long period is required for this reaction to occur, so to exceed this gap in future, it would be important to make a new solution each time the compound is tested. To avoid a possible bias on the study conclusions, it was decided not to present those results.

In the analysis of the results, the best-fit sigmoid curves for each cell line were established and represented in Figures 17, 18 and 19. IC₅₀ values were determined using the dose-response curves, shown in Table 5. All results are expressed by mean±SEM of, at least, three independent experiments, in triplicate.

Figure 17 presents the dose-response curves of MCF-7 cell line treated with the synthesized compounds. In general, there was a dose-dependent decrease in cell proliferation for all compounds. However, it was not possible to obtain the IC₅₀ value of the **F20** compound, being **F20** the compound with less antiproliferative activity. **E4** and **F19** showed a more pronounced decrease and minor IC₅₀ values (**E4**: IC₅₀=16.05 µM; **F19**: IC₅₀=48.75 µM).

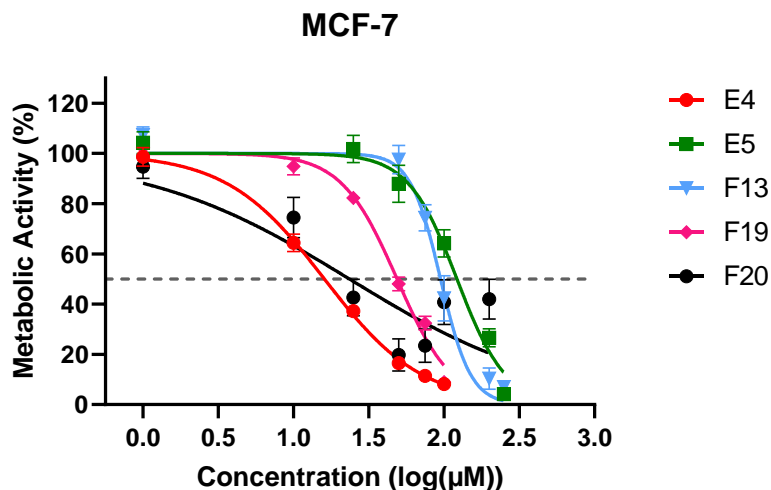


Figure 17 - Dose response curves of MCF-7 cell line after treatment with compounds E4, E5, F13, F19 and F20 for 48h. Results are presented as the percentage (%) of metabolic activity as a function of compounds' concentration $\{\log_{10}[\text{concentration } (\mu\text{M})]\}$ and express the mean \pm SEM of, at least, four independent experiments, in triplicate.

The effect of compounds in HuH7 cells proliferation is shown in Figure 18. All compounds induced a dose-dependent decrease in cell proliferation. Once again, it was not possible to get the IC_{50} value for **F20** compound. **E4** and **F19** showed, again, a more pronounced decrease and minor IC_{50} values (**E4**: $IC_{50}=29.38 \mu\text{M}$; **F19**: $IC_{50}=48.45 \mu\text{M}$).

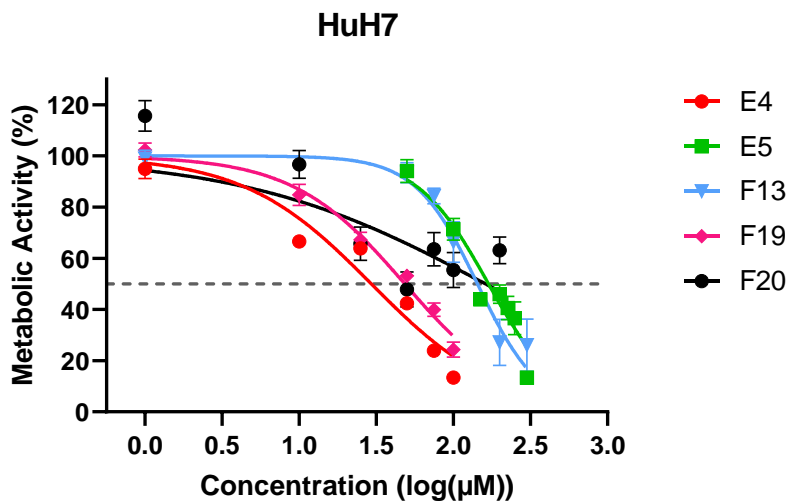


Figure 18 - Dose response curves of HuH7 cell line after treatment with compounds E4, E5, F13, F19 and F20 for 48h. Results are presented as the percentage (%) of metabolic activity as a function of compounds' concentration $\{\log_{10}[\text{concentration } (\mu\text{M})]\}$ and express the mean \pm SEM of, at least, three independent experiments, in triplicate.

Figure 19 represents the dose-response curves of HepG2 cell line treated with all compounds. Generally, all compounds caused a dose-dependent decrease in HepG2 cells proliferation. Once more, it was not possible to obtain the IC_{50} value of the **F20**

compound. **E4** and **F19** showed, again, a more pronounced decrease and minor IC_{50} values (**E4**: IC_{50} =34.74 μ M; **F19**: IC_{50} =58.17 μ M).

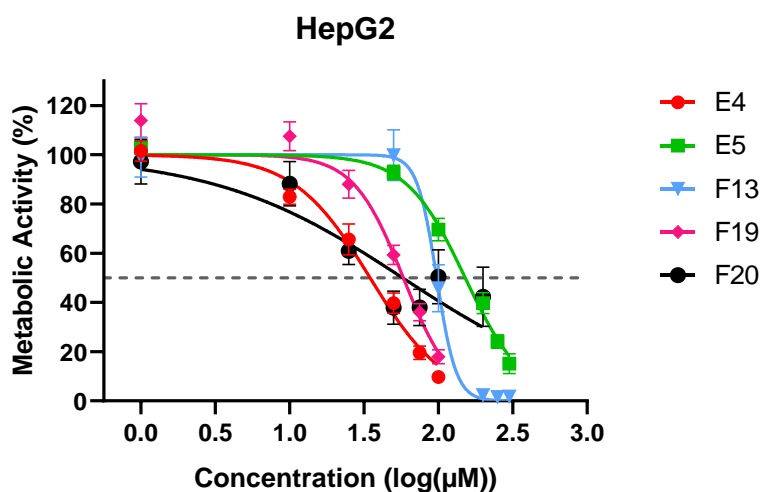


Figure 19 - Dose response curves of HepG2 cell line after treatment with compounds E4, E5, F13, F19 and F20 for 48h. Results are presented as the percentage (%) of metabolic activity as a function of compounds' concentration $\{\log_{10}[\text{concentration } (\mu\text{M})]\}$ and express the mean and standard error of, at least, three independent experiments, in triplicate.

Table 5 - IC_{50} values obtained after incubation of MCF-7, HuH7 and HepG2 cell lines compounds E4, E5, F13, F19 and F20 for 48h. R^2 values and the 95% confidence intervals (95%) are also presented.

Compound	Cell Line	COX-2 Expression	IC_{50} (μ M)	R^2	Confidence Interval (95%)
E4	MCF-7	+	16.05	0.99	15.61 - 16.48
	HepG2	+	34.74	0.95	32.66 - 36.86
	HuH7	++	29.38	0.93	27.08 - 31.74
E5	MCF-7	+	121.90	0.96	117.0 - 127.0
	HepG2	+	151.50	0.98	146.60 - 156.50
	HuH7	++	169.10	0.93	162.10-176.60
F13	MCF-7	+	94.90	0.97	92.32 - 97.86
	HepG2	+	97.50	0.98	93.93 - 100.40
	HuH7	++	143.40	0.93	136.10-151.30
F19	MCF-7	+	48.75	0.98	47.43 - 50.09
	HepG2	+	58.17	0.95	55.57 - 60.80
	HuH7	++	48.45	0.97	46.65 - 50.31
F20	MCF-7	+	> 200	0.56	--
	HepG2	+	> 200	0.66	--
	HuH7	++	> 200	0.53	--

IC_{50} values, presented in Table 5, show that **E4** and **F19** compounds have higher antiproliferative activity, considering the lower IC_{50} values obtained for all cell lines.

The compounds used have already shown to be selective COX-2 inhibitors (10) in blood samples. Thus, linking the basal COX-2 expression of each cell line with IC_{50} values, it can be observed a greater correlation between compounds **E4** and **F19** with the basal expression of HCC cell lines. Considering western blot results presented above, COX-2 expression in HuH7 cells is higher than COX-2 expression in HepG2 cells. Thus, COX-2 is more exposed to the compound's action in HuH7 cells. Therefore, a lower concentration of compounds is required to obtain the same antiproliferative activity, as observed in compounds with minor IC_{50} values, **E4** and **F19**.

Contrarily, compounds **F13** and **E5** presented antiproliferative activity without correlation with COX-2 expression, being the compound **E5** the one demonstrating the lowest antiproliferative activity, with the highest IC_{50} values. Therefore, it may be extrapolated that the **E5** and **F13** antiproliferative action is COX-2-independent. In the future, to confirm if its mechanism of action is really COX-2-independent, one option could be to silence COX-2 gene and evaluate **E5** and **F13** antiproliferative activity again. Identical results would confirm that its action is really COX-2-independent. Besides, it would be interesting to evaluate other proteins related to cancerous processes, such as VEGF (angiogenesis).

With emphasis on **E4** results, it can be observed, with 95% of confidence level, that all IC_{50} values (IC_{50} (MCF-7) = 16.05 μ M, IC_{50} (HuH7) = 29.38 μ M and IC_{50} (HepG2) = 34.74 μ M) were statistically different since there is no intersection between confidence intervals. The same observations can be done regarding **E5** results (IC_{50} (MCF-7) = 121.90 μ M, IC_{50} (HuH7) = 169.10 μ M and IC_{50} (HepG2) = 151.50 μ M). In HCC cell lines, **F19** and **F13** IC_{50} values are distinct, with 95% of confidence level, being IC_{50} values of **F19** much lower (IC_{50} (HuH7) = 48.45 μ M and IC_{50} (HepG2) = 58.17 μ M) than **F13** (IC_{50} (HuH7) = 143.40 μ M and IC_{50} (HepG2) = 97.50 μ M). In its turn, it can be spotted an interception between the **F19** confidence intervals of MCF-7 (47.43 - 50.09 μ M) and HuH7 (46.65 - 50.31 μ M) cells. On the other hand, the **F13** results show an interception among MCF-7 (92.32 - 97.86 μ M) and HepG2 (93.93 - 100.40 μ M) confidence intervals.

Given that the R^2 values of **F20** compound are located between 0.53 and 0.66, there is no reliable confidence interval. Thus, it is not possible to determine the IC_{50} values inferring that, for this compound, IC_{50} values are greater than 200 μ M. All other R^2 values presented are located above 0.93, demonstrating a good fitting of the curves for the experimental results.

Ribeiro et al. showed that COX-2-targeted compounds used in this work present inhibitory capacity to inhibit selectively COX-2, being **F11**, **F13** and **F20** compounds those who presented higher potency (IC_{50} (**F11**) = 3.0 ± 0.3 μ M, IC_{50} (**F13**) = 2.4 ± 0.6 μ M and IC_{50} (**F20**) = 1.09 ± 0.09 μ M) (10). The active site of COX-2 presents an important region: a hydrophobic pocket (49,90), which explains the high potency of compounds **F11**, **F13** and **F20** for inhibit COX-2, as demonstrated in previous study, since these compounds present a very lipophilic nature (10). For the compounds **F11** and **F20** it was not possible to obtain an IC_{50} value for their antiproliferative activity, since the compound **F11** presented molecular instability as previously described, and the compound **F20** presented crystallization after the 48 hours treatment. However, due to the high ability of this compound to inhibit COX-2 (10) one cannot rule out the possibility of using this compound in the future work, so, to exceed this gap, it would be interesting to study again the activity of this compound using a different solvent such as polyethylene glycol. Compound **F13** did not show a good correlation with COX-2 expression, and it was necessary a great increase in its concentration in order to occur antiproliferative activity. This increase went against expectations since it previously showed to be one of the most potent compounds in COX-2 inhibition.

Furthermore, according to *Ribeiro* et al. the compounds **E5** and **F19** showed the lowest potency to inhibit COX-2 (IC_{50} (**E5**) = 20 ± 1 μ M and IC_{50} (**F19**) = 21 ± 2 μ M), which agrees with the MTT results of compound **E5** but not with the results of **F19** (10). Interestingly, compound **F19**, which showed lower potency to inhibit COX-2 of all compounds used in this work (10), was one of the compounds that showed lower IC_{50} values and higher antiproliferative activity, in a COX-2-dependent manner. However, a possible anticancer COX-2-independent mechanism can be involved and must be further studied.

Finally, compound **E4**, which showed the lowest IC_{50} values and greater antiproliferative activity, according to *Ribeiro* et al., was one of the compounds that showed an intermediate potency in COX-2 inhibition (IC_{50} (**E4**) = 12.7 ± 0.5 μ M) (10). It can be observed that, according to COX-2 expression in HCC cell lines, the antiproliferative activity of **E4** was COX-2-dependent, which agrees with its higher capacity to inhibit this protein ($99.0 \pm 0.7\%$) and also with MTT results (10). However, it is important to consider that the results presented by *Ribeiro* et al. relate to tests performed in blood samples (10). Thus, it would be interesting to study this inhibitory capacity also in cancer cells through the assessment of PGs levels by ELISA.

In view of a structure activity relationship, it can be observed that the presence of a catechol group in **E4** compound can confer a higher anticancer activity, as already described previously in the literature by the research group (12). It can also be observed that, comparing the structures of compounds **E5** and **F19**, the compound presenting the hydroxyl group in position 3 has a greater antiproliferative capacity (**F19**) than the compound presenting the same group in position 4 (**E5**). Furthermore, one can connect the low antiproliferative activity presented by compound **F13** with its lipophilic nature, since the hydroxyl group is in a position of difficult access.

The results presented are in agreement with previous observations that denote that some cinnamic acid derivatives have antiproliferative activity against cancer cell lines (11,12,91). Two of these studies have already been performed with the compounds **E4** and **E5** (11,12). *Tavares-da-Silva* et al. proved that these two compounds have antiproliferative activity in colon cancer cell lines and inhibit human neutrophils' oxidative burst (12). It is known from the literature that COX-2 expression in WiDr cells is lower than in C2BBE1 cells, since the latter are a clone of Caco-2 cells that also overexpress the protein (92,93). This fact allows to hypothesize that the antiproliferative activity of compound **E4** also showed a correlation with COX-2 expression in colon cancer lines (IC_{50} (WiDr) = 34.6 μ M and IC_{50} (C2BBE1) = 22.0 μ M). The parallel with colon cancer cells was also observed in the activity of compound **E5**, which did not show any correlation between anticancer activity and COX-2 expression (IC_{50} (WiDr) = 122.6 μ M and IC_{50} (C2BBE1) = 91.0 μ M). Furthermore, it can be observed that the IC_{50} values presented in the study with colon cancer cells are very similar to those presented in this master's Thesis. Thus, it can be concluded that both compounds have similar antiproliferative activity in colon cancer cells and liver cancer cells.

Serafim et al. also showed the antiproliferative activity of **E4** and **E5** in MCF-7 and MDA-MB-231 (oestrogen-independent breast cancer cell line) cell lines, being **E4** the most efficient (11), in accordance with results of this dissertation. According to the results of antiproliferative activity of compound **E4** in MCF-7 and MDA-MB-231 cell lines presented by *Serafim* et al., it can be observed that the compound presented a greater antiproliferative activity in the MCF-7 cell line than in the MDA-MB-231 cell line (11). Considering the higher COX-2 expression of MDA-MB-231 cells compared to MCF-7 cells, it can be observed that, according to the results presented by *Serafim* et al., the action of this compound could be COX-2-independent (11,77). However, further studies are needed to confirm this hypothesis. This hypothesis can be complemented by evaluating the levels of COX-2 expression by western blot and PGs through ELISA or

silencing the expression of COX-2, in order to confirm whether the mechanism of action of **E4** against BC is COX-2-independent or not.

Inflammation is associated with cancer, being the pro-tumour inflammation one *hallmark of cancer* (16). COX-2 and PGE₂ (major product of COX-2 activity) are crucial to the inflammation process and have been associated with various hallmarks of cancer (4,58). Coxibs are selective COX-2 inhibitors, their activity is associated with less adverse effects than non-selective COX-2 inhibitors. However, coxibs have been associated with cardiotoxicity. Because of this, the majority of coxibs were withdrawn from the market (1,9,10,48,60–64). Thus, efforts have been done to overcome these difficulties. Cinnamic acid derivatives have been recognized to display relevant biological activities against several tumour cells and the compounds used in this master's Thesis already revealed capacity to inhibit COX-2 with selectivity (10,11).

Comparing the compound that presented the lowest IC₅₀ values, **E4**, to the conventional chemotherapeutic drugs used in the clinical practice for the treatment of BC, it can be observed that the IC₅₀ value of **E4** for MCF-7 cell line (16.05 µM) is much higher than the IC₅₀ of epirubicin (0.32 µM) but lower than cisplatin (32.5 µM), for the same time of treatment (94). In HCC cell lines, it can be noted that the IC₅₀ value of **E4** (29.38 µM) for HuH7 cell line was much lower than 5-FU (166.6 µM), but higher than the IC₅₀ of cisplatin (1.5 µM), doxorubicin (DOX) (0.1 µM) and sorafenib (9.5 µM) (95). For HepG2 cell line, the IC₅₀ value of **E4** (34.74 µM) was much higher than the IC₅₀ of 5-FU (19.0 µM), cisplatin (2.0 µM), DOX (0.3 µM) and sorafenib (4.6 µM) (95). All other compounds showed higher IC₅₀ values than all conventional therapies, except for 5-FU, in all cell lines. In all cell lines, all compounds showed lower IC₅₀ values than 5-FU, except **E5** in HuH7 cells.

However, despite presenting lower IC₅₀ values than the cinnamic acid amides studied in this master's Thesis, both cisplatin, epirubicin, doxorubicin and sorafenib treatment present several adverse effects such as ototoxicity, cardiotoxicity, myelosuppression and therapeutic resistance (34,40,96–100). As described previously, COX-2 is associated with several chemoresistance-related signalling pathways (4,54,55). Since the cinnamic acid amides used in this work are selective COX-2 inhibitors, they could be used in the future as adjuvant therapy, as COX-2 inhibition allows cells to be sensitised to conventional chemotherapy and also decreases this adverse effect (4,10).

Furthermore, other studies have demonstrated that cinnamic acid derivatives are cardioprotective agents against oxidative and structural damage induced by DOX, a

widely used anticancer drug that presents greater cardiotoxicity (101,102). This evidence reinforces the use of cinnamic acid derivatives as anticancer agents.

Thus, these results are in the same line of reasoning as previous studies, demonstrating that some of these compounds are also promising antiproliferative mediators against BC and HCC cells, being the **E4** compound the most effective.

3.2.2 Protein content

In order to complement the MTT results, SRB assay was used with **E4** and **F19** compounds. This complement is important since MTT assay depends on redox reactions that can be altered in presence of ROS. The SRB assay was performed to suppress any possible interference of production of ROS in results.

In Figures 20, 21 and 22 it is observed that with both the MTT assay and the SRB assay, compounds E4 and F19 demonstrated a dose-dependent antiproliferative activity. These complementary results once again reinforce the antiproliferative capacity of the compounds being promising to be used for anticancer purposes.

In Figure 20, the bar graph presents MTT and SRB assays results, in MCF-7 cell line, after treatment with **E4** and **F19** for 48 hours. In general, there was no significant differences between MTT and SRB assays for all concentrations, excluding 1 μ M and 25 μ M for **E4** compound and 25 μ M for **F19** compound.

The same tendency is observed in Figure 21. Figure 21 represents cell proliferation obtained by both MTT and SRB assays results in HuH7 cell line, after the same treatments. No significant differences were found between these assays for all concentrations with exception of 25 μ M of **E4** compound.

Finally, for HepG2 cell line MTT and SRB results, **E4** treatment did not demonstrate significant differences as opposed to **F19** treatment, which showed significant differences in most of the concentrations (excluding 100 μ M). These results are presented in Figure 22.

These results prove that, in general, there was no significant difference between the two assays. Thus, it was shown that it was possible to evaluate the antiproliferative activity of the compounds using the MTT assay, without any ROS interference in the redox reactions inherent to this method, allowing confidence in the results.

Furthermore, these results are in agreement with a previous study (103), where the author found that both assays had similar linearity in the evaluation of antiproliferative activity of Thai plant extracts in a rat fibroblast cell line (L929). In addition to this study, there is another that proves the same linearity between the two assays in the evaluation of antiproliferative activity of *Artocarpus heterophyllus* methanolic extract in a lung adenocarcinoma cell line (A549) (104).

Because of confidence in the previous results with MTT assay, this method was performed for **E4**, **F13** and **F19** compounds to evaluate whether their cytotoxic activity was selective for cancer cells.

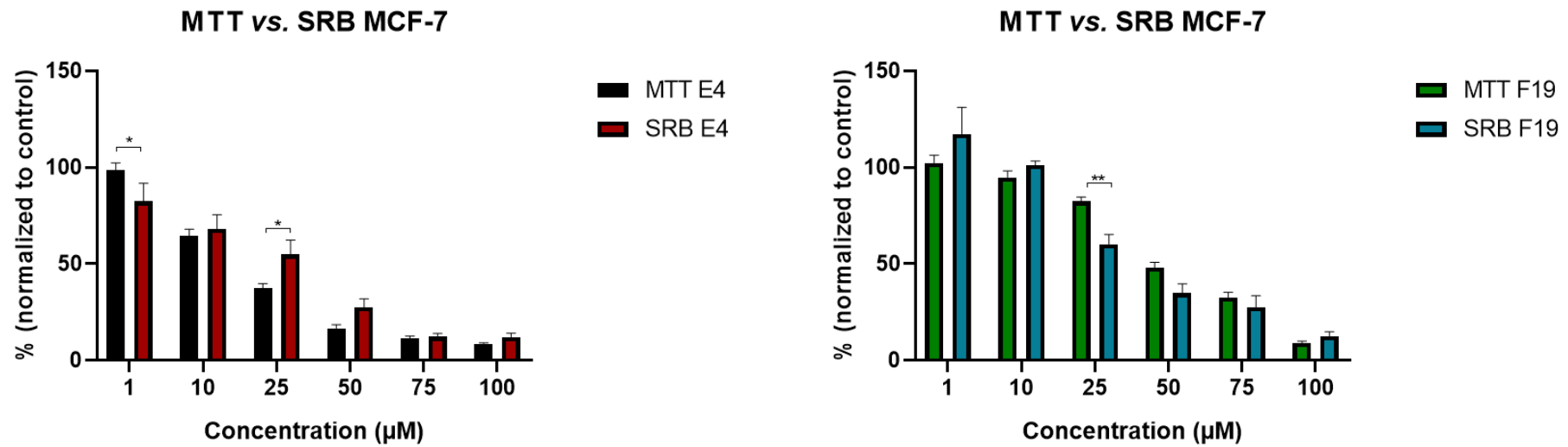


Figure 20 – Results of MTT and SRB assays (MCF-7 cell line) 48 hours after treatment with **E4** and **F19** compounds. Results are presented as the percentage (%) of metabolic activity (MTT) and protein content (SRB) as a function of compounds' concentration (µM) and express the mean±SEM of, at least, three independent experiments, in triplicate. Significant differences are denoted by *p<0.05, **p<0.01.

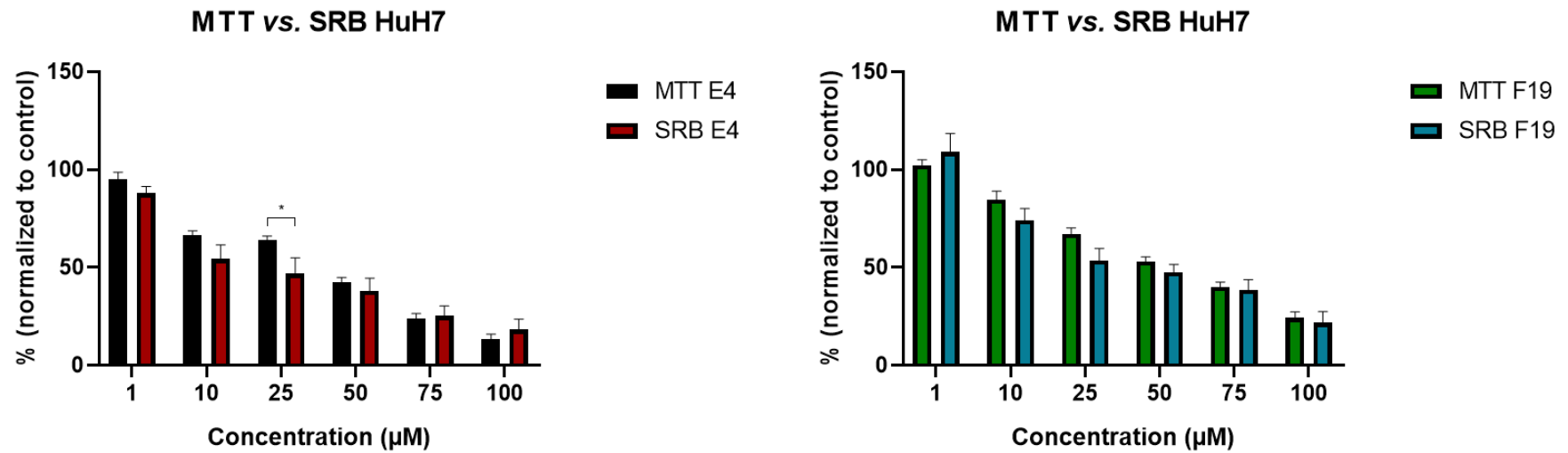


Figure 21 - Results of MTT and SRB assays (HuH7 cell line) 48 hours after treatment with **E4** and **F19** compounds. Results are presented as the percentage (%) of metabolic activity (MTT) and protein content (SRB) as a function of compounds' concentration (μM) and express the mean±SEM of, at least, three independent experiments, in triplicate. Significant differences are denoted by *p<0.05.

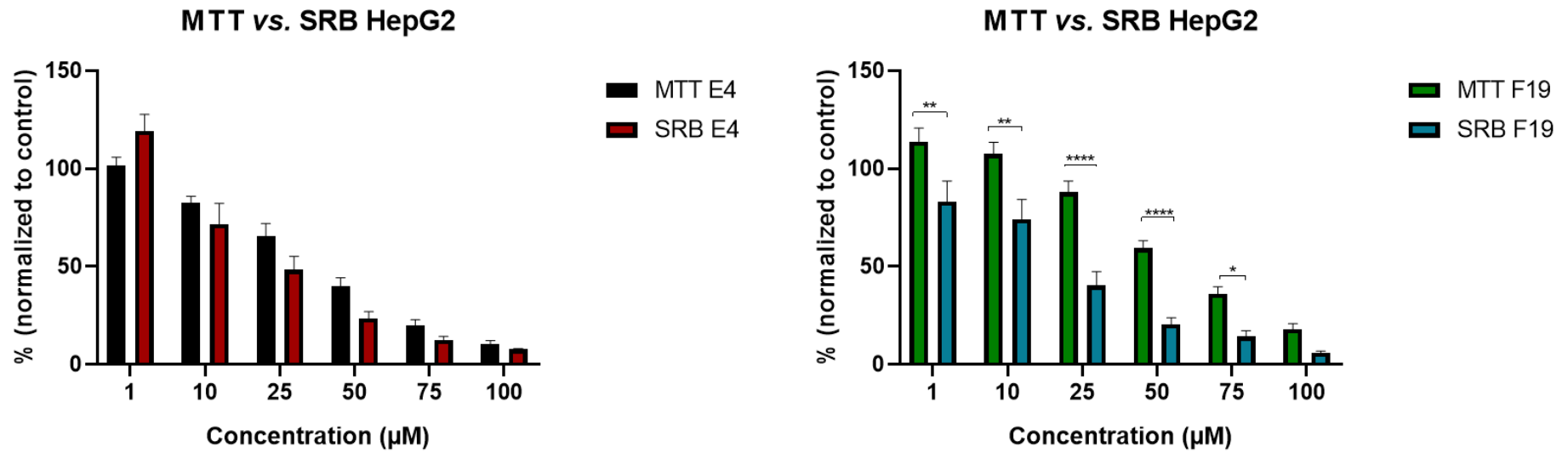


Figure 22 – Results of MTT and SRB assays (HepG2 cell line) 48 hours after treatment with **E4** and **F19** compounds. Results are presented as the percentage (%) of metabolic activity (MTT) and protein content (SRB) as a function of compounds' concentration (µM) and express the mean±SEM of, at least, three independent experiments, in triplicate. Significant differences are denoted by *p<0.05, **p<0.01, ****p<0.0001.

3.2.3 Selectivity

MTT assay with MCF-12A was used as control to assess whether the cytotoxic activity of the compounds is selective for tumour cells or not. A positive control was added to this experiment: celecoxib, a selective COX-2 inhibitor used in clinical practice. This addition is of greater importance because it allows comparison between treatment with cinnamic acid amides and treatment with a well-studied COX-2 selective inhibitor, allowing confidence in the results.

As contradictions were found in the literature about the IC₅₀ values of celecoxib (105–110), MTT assay was performed, with a range between 10 to 100 µM, in MCF-7 cell line. Thus, the concentration used in treatment with celecoxib (10 µM) was selected from the results obtained by MTT assay in cancer cells (Appendix 1 - Figure 39). Furthermore, the two treatments with compounds were used, the concentrations of compounds were selected based on IC₅₀ values obtained previously by MTT assay in MCF-7 cell line: one treatment with the concentration corresponding to the IC₅₀ value for each of the compounds in the MCF-7 line and another treatment with a higher concentration, in order to assess whether there are significant changes in the selectivity of the antiproliferative activity with increasing concentration.

In Figure 23, the bar graph represents the MTT results for MCF-12A and MCF-7 cell lines after treatment with **E4** for 48 hours. In general, there are significant differences between MCF-12A and MCF-7 cell lines for all concentrations. Within each cell line, in MCF-7 it can be observed that there are no significant differences between celecoxib treatment and **E4** treatment, although, there are significant differences between **E4** treatments ($p=0.0002$). In MCF-12A cell line, it can be noted that there are no significant differences between **E4** treatments but there are between these treatments and celecoxib ($p<0.0001$, for both concentrations). With these results, it can be seen that celecoxib treatment has higher cytotoxicity ($p<0.0001$) in normal breast cells (21.2% of metabolic activity) than cancer cells (45.6%). Furthermore, it can be noted that **E4** treatment induced low cytotoxicity in normal breast cells (78.9% for 16.05 µM and 71.9% for 25 µM), in contrast with the higher antiproliferative activity induced in cancer cells (50 and 37.2%, respectively). Thus, it can be assumed that **E4** is a promising compound to be used against breast cancer disease because, in addition to being the compound that demonstrated the greatest antiproliferative activity in tumour cell lines (showing the lowest IC₅₀ values), its antiproliferative activity was also shown to be selective for breast tumour cells.

Figure 24 represents metabolic activity results for MCF-12A and MCF-7 cell lines, after treatment with **F19** for 48 hours. It can be noted that treatment with 48.8 μM in these two cell lines do not present significant differences between them. Contrarily, celecoxib (10 μM) and **F19** treatment with highest concentration (75 μM) presented statistically significant differences between the two cell lines [$p=0.0012$ for celecoxib treatment and $p=0.0124$ for **F19** treatment (75 μM)], being these treatments more cytotoxic for normal cells [21.2% for celecoxib treatment and 16.6% for **F19** treatment (75 μM)] than cancer cells [45.6% for celecoxib treatment and 32.4% for **F19** treatment (75 μM)]. Within MCF-7 cell line, significant differences ($p=0.0004$) can be observed between **F19** treatments, with treatment with 75 μM (32.2%) more cytotoxic than treatment with 48.8 μM (50%). In MCF-12A cell line, there are significant differences between celecoxib and 48.8 μM treatments ($p=0.0011$) and between two **F19** treatments ($p<0.0001$). The celecoxib and 75 μM treatments presented high cytotoxicity (21.2% for celecoxib and 16.6% for 75 μM of **F19**) than 48.8 μM of **F19** (44.1%). These results showed that **F19** treatment demonstrated identical cytotoxicity to that caused by celecoxib treatment, for normal breast cells. Thus, **F19** is not a promising compound to be used against BC, since it showed a high toxicity for normal breast cells compared to tumour cells, demonstrating that its antiproliferative activity is selective for normal cells, contrary to what is required.

In Figure 25, metabolic activity results obtained for MCF-12A and MCF-7 cell lines after treatment with **F13** for 48 hours are presented. Herein, all treatments showed significant differences between the two tested cell lines. Within MCF-7 cell line, significant differences were observed between celecoxib and **F13** (200 μM) treatment ($p<0.0001$) and between two **F13** treatments ($p<0.0001$). Celecoxib treatment provoked lower cytotoxicity (45.6%) than **F13** (200 μM) treatment (10.3%), although, incited highest cytotoxicity than **F13** (94.9 μM) treatment (50%). Moreover, in MCF-12A cell line, all treatments also presented significant differences between them ($p<0.0001$ for all comparisons). These results show that **F13** treatments presented low cytotoxicity for normal breast cells, with 94.9 μM treatment increasing the metabolic activity of these cells (119.1%) and 200 μM with low decrease of metabolic activity (73.7%), contrarily of celecoxib treatment (21.2%). Thus, it can be assumed that **F13** is a promising compound to be used against cancer disease since its antiproliferative activity was also shown to be selective for breast tumour cells.

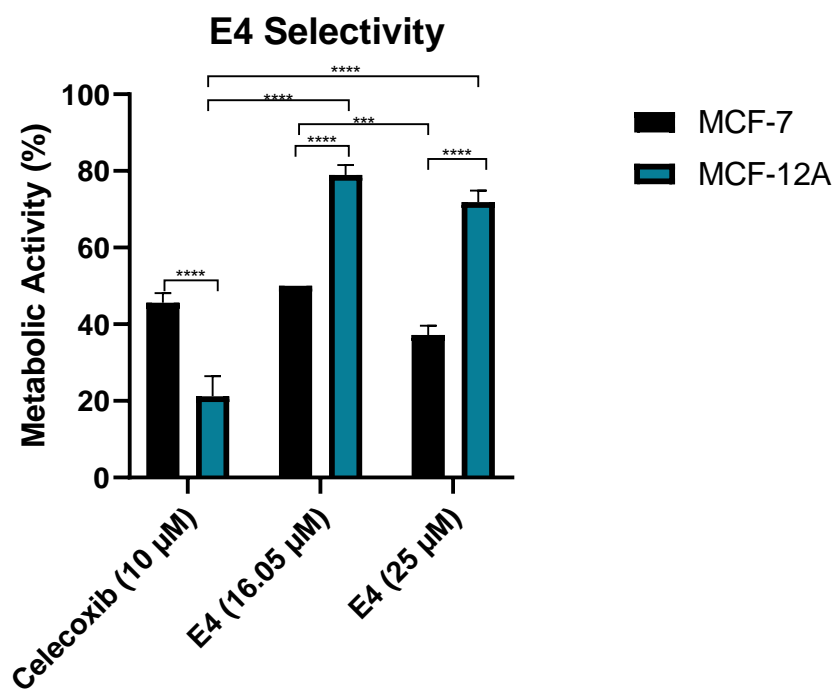


Figure 23 – Results of MTT assay (MCF-12A and MCF-7 cell line) 48 hours after treatment with celecoxib and E4 compound. Results are presented as the percentage of metabolic activity (%) as a function of compounds' concentration (μM) and express the mean \pm SEM of, at least, three independent experiments, in triplicate. Significant differences are denoted by *** $p < 0.001$, **** $p < 0.0001$.

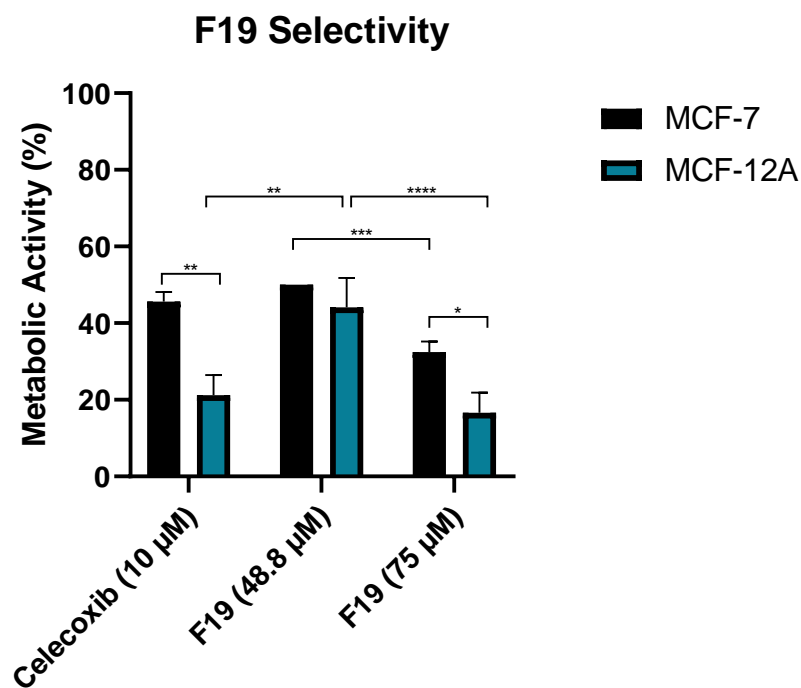


Figure 24 - Results of MTT assay (MCF-12A and MCF-7 cell line) 48 hours after treatment with celecoxib and F19 compound. Results are presented as the percentage of metabolic activity (%) as a function of compounds' concentration (μM) and express the mean \pm SEM of, at least, three independent experiments, in triplicate. Significant differences are denoted by * $p < 0.05$, ** $p < 0.01$, *** $p < 0.001$, **** $p < 0.0001$.

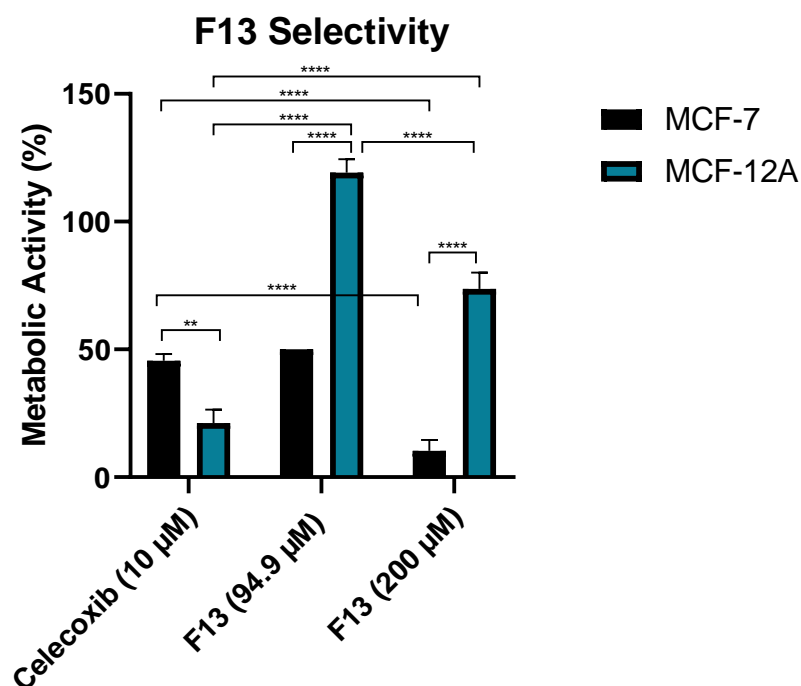


Figure 25 - Results of MTT assay (MCF-12A and MCF-7 cell line) 48 hours after treatment with celecoxib and F13 compound. Results are presented as the percentage of metabolic activity (%) as a function of compounds' concentration (μM) and express the mean \pm SEM of, at least, three independent experiments, in triplicate. Significant differences are denoted by ** $p < 0.01$, **** $p < 0.0001$.

According to Figures 23, 24 and 25, it is concluded that celecoxib and **F19** compound showed high cytotoxicity to normal breast cells than **F13** and **E4** compounds. The **F13** compound presented low cytotoxicity for normal breast cells, with **F13** (94.9 μM) treatment increasing the proliferative activity in these cells. Even with higher concentrations, the cytotoxic activity of this compound is low, even though there are significant differences between the two treatments (94.9 and 200 μM). Nevertheless, for tumour cells, high concentrations were needed in order to obtain an antiproliferative activity, making this compound less promising than **E4**. The **E4** compound demonstrated to be the most promising of all other compounds tested, due to its higher cytotoxic activity in cancer cells, and lower cytotoxic activity in normal breast cells.

A previous study using the **E4** compound in colon cancer cells showed that treatment with this compound incited an increase in the intracellular production of superoxide anion (O_2^-), a by-product of the mitochondrial respiratory chain, which can produce oxidative damage at that very site, but also diffuse away from its origin and cause damage to many different macromolecules such as DNA, phospholipids, and proteins (12). This increase may lead to the induction of apoptosis since the antioxidant

defence machinery is diminished in cancer cells and may also be one of the reasons for the selectivity of the antiproliferative activity of this compound (111). However, further studies are needed to infer whether the selectivity of this compound is due to the production of ROS or to the failure of their antioxidative defences. Therefore, in the future it would be interesting to evaluate the levels of production of ROS such as $O_2^{\cdot-}$ and peroxides, and reduced glutathione (acts in the detoxification of hydrogen peroxides) by flow cytometry.

Cytotoxic assays, such as SRB and MTT assays, have different linearities depending on cell lines used (112), thus, it is important to repeat these types of assays in other cell lines. Other important evidence is the fact that NSAIDs reveal different actions depending on cancer type (113), which can also be extrapolated to cinnamic acid derivatives on cancer and normal cell lines.

It is known that coxibs, including celecoxib, are associated with cardiotoxicity. One study revealed that celecoxib cytotoxicity for cardiac myocytes involves COX-2-independent mechanisms (100). Moreover, *El-Awady* et al. demonstrated that celecoxib cannot be used with DOX, once its cardiotoxicity is identical to cardiotoxicity of DOX, and that celecoxib interaction with different anti-cancer drugs is antagonistic in breast cancer. Thus, celecoxib is not a suitable chemosensitizer for breast cancer (106). On the other hand, as mentioned above, cinnamic acid derivatives revealed a cardioprotective activity against DOX action in myocardial cells, reinforcing, again, the use of these molecules against cancer (102). Since cinnamic acid derivatives have a cardioprotective activity and celecoxib is not suitable chemosensitizer for breast cancer, these results are in accordance with previous studies (101,106,113), demonstrating the importance of cinnamic acid derivatives for clinical practice. Although, it is important to repeat evaluation of selectivity of cytotoxic activity of the compounds in other normal cell lines, such as normal liver cells.

Since compound **E4** proved to be the most promising, exhibiting a higher antiproliferative activity (lower IC_{50} values) and a higher selectivity for breast cancer cells than for normal cells, subsequent experiments were performed only with this compound.

3.3 Cell cycle

To analyse if **E4** treatment induces or not modifications in cell cycle of the three used cell lines, flow cytometry was performed by staining cells with a solution of PI with RNase, 48 hours after treatment.

Figure 26 represents cell cycle analysis of MCF-7 cell line. It can be noted that there are no significant differences between the three conditions. However, the results of cytotoxic assays (MTT and SRB) performed in this master's Thesis demonstrate a high decrease in cell proliferation. These results can be explained since cell proliferation decrease can also be associated to cell death or quiescence (114). Considering that the number of cells in each cell cycle phase is identical between conditions, there are no significant differences that support the presence of quiescence.

In this case, as no alterations in the cell cycle are observed it can be hypothesized that, for the concentrations used (16.05 and 25 μM), the antiproliferative activity of the compound **E4** could act especially by necrosis. Observing the results obtained in the flow cytometry it can be inferred that there are no cells in sub G_0/G_1 phase population (apoptotic peak).

Furthermore, previous results in the same cell line revealed that 75 μM of **E4** treatment, a 3-fold higher concentration than the maximum used in MCF-7 studies, induced an increase of apoptotic peaks and a strong decrease of cells arrested in S phase (11). Also, another previous studies with celecoxib treatment in MCF-7 cells presented a dose-dependent cell cycle arrest in G_0/G_1 phase with concentrations between 10 and 40 μM and a consequent decrease of cells in S phase, being in accordance with *Serafim et al.* study (106,109).

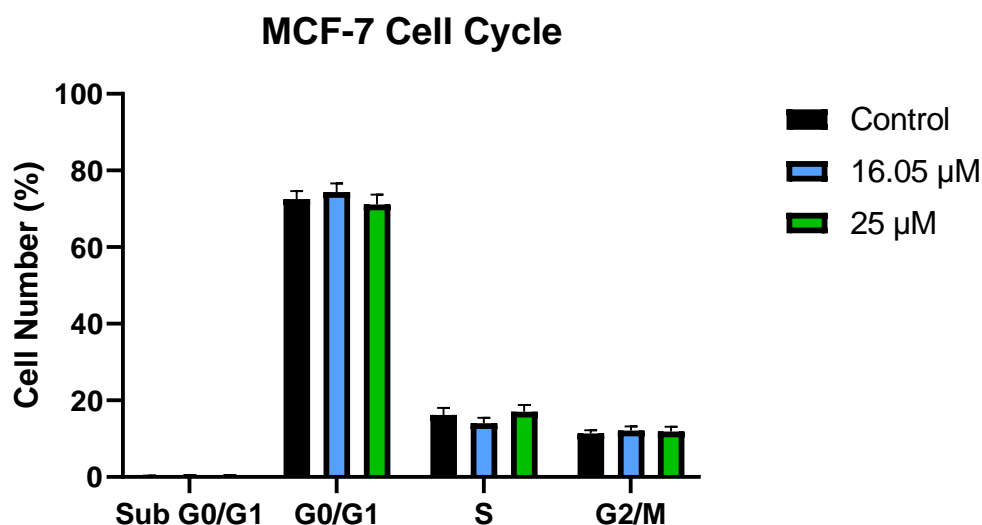


Figure 26 – Cell cycle analysis of MCF-7 cell line, 48 hours after treatment with **E4**. Results are presented as the percentage of cells in phases G₀/G₁, S or G₂/M and express the mean \pm SEM of, at least, three independent experiments, in duplicate.

Figure 27 represents cell cycle analysis of HuH7 cell line. In overall, there are statistically significant differences, contrarily to other used cell lines. In this cell line, significant differences can be observed between control and **E4** treatments. **E4** treatments induced cell cycle arrest in S phase, which was more pronounced in the treatment with 29.38 μ M compared to 75 μ M. The treatment with 29.38 μ M induced a significant increase from 26.6 \pm 1.83% to 51.5 \pm 0.5% ($p < 0.0001$) comparatively to the control, and 75 μ M treatment induced a significant increase of 26.6 \pm 1.8% to 41.5 \pm 2.2% ($p < 0.0001$) comparatively to the control. As a consequence of cycle arrest in S phase, in **E4** 29.38 μ M treatment, a decrease of the number of cells in G₀/G₁ phase occurred, which resulted in a significant decrease from 59.8 \pm 1.6% to 45.5 \pm 0.5% ($p = 0.0003$) comparatively to the control.

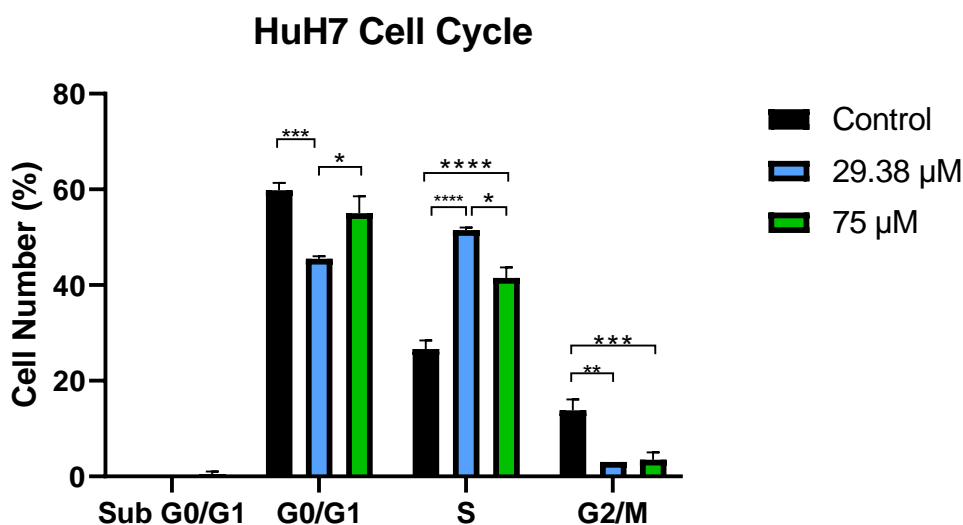


Figure 27 - Cell cycle analysis of HuH7 cell line, 48 hours after treatment with **E4**. Results are presented as the percentage of cells in phases G₀/G₁, S or G₂/M and express the mean \pm SEM of, at least, three independent experiments, in duplicate. Significant differences are denoted by *p<0.05, **p<0.01, ***p<0.001, ****p<0.0001.

In HuH7, **E4** treatment induced cell cycle arrest in S phase, which is in agreement with previous results with **E4** treatment in WiDr cells (colon cancer cells) (12). Similar to the WiDr cell line, the HuH7 cell line also has the *TP53* gene mutated (115), which makes it transcriptionally inactive form of P53 (116). *TP53* gene in WiDr cell line is presented mutated, according to ATCC, to prevent *TP53* of regulating P21 protein following DNA damage. P21 is a cyclin-dependent kinase inhibitor with the function of regulating cell cycle arrest in G₁ phase. Commonly, DNA damages provoke an increase in P53 levels and, consequently, P21 transcription in order to activate G₁ checkpoint and permit cells to repair damages or proceed to apoptosis. Therefore, in HuH7 cells, mutated *TP53* gene may lead to cell cycle arrest in S phase, since G₁ checkpoint is not activated (12).

In Figure 28 cell cycle analysis of HepG2 cell line is represented. In this cell line, significant differences can be observed between control and **E4** 75 μ M treatment. This treatment induced a cycle arrest in phase S, which resulted in a statistically significant increase of the number of cells from 29.0 \pm 3.24% to 45.0 \pm 9.0% (p=0.04), comparatively to the control. With the cycle arrest in S phase, a decrease of the number of cells in G₀/G₁ phase occurred, which resulted in a significant decrease from 57.0 \pm 2.1% to 39.7 \pm 5.1% (p=0.03), comparatively to the control.

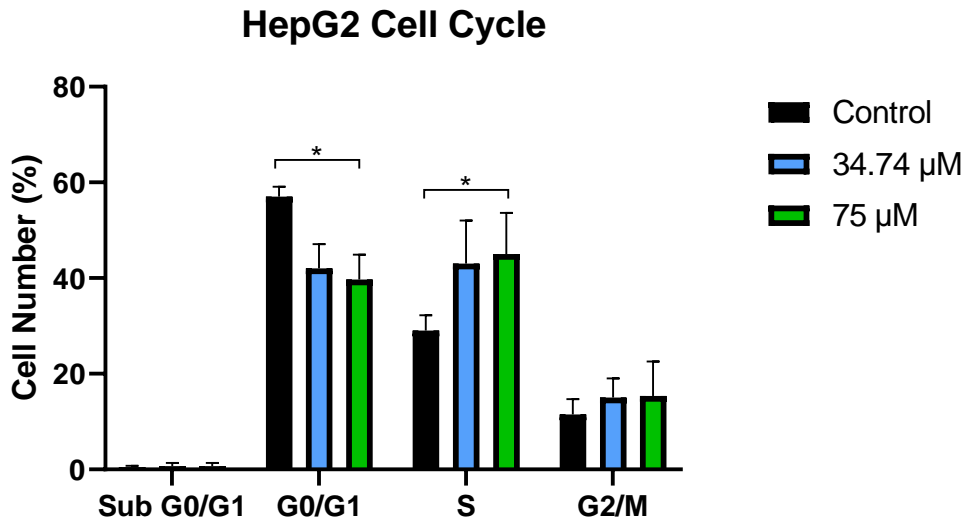


Figure 28 - Cell cycle analysis of HepG2 cell line, 48 hours after treatment with **E4**. Results are presented as the percentage of cells in phases G₀/G₁, S or G₂/M and express the mean±SEM of, at least, three independent experiments, in duplicate. Significant differences are denoted by *p<0.05.

In HepG2 cells, **E4** treatment induced cell cycle arrest in S phase, which is in agreement with previous results obtained with **E4** treatment in WiDr cells (12). If on the one hand *TP53* gene in WiDr cell line is presented mutated, according to ATCC, to prevent *TP53* of regulating P21 protein following DNA damage, on the other hand HepG2 cell line presents wild-type *TP53* gene (117). In addition to the *Tavares-da-Silva et al.* study, another study with phenolic compounds treatments (with range of concentrations of 16 to 75 µM, for 72 hours) in HepG2 cells also demonstrated cell cycle arrest in S phase (118). One hypothesis for these results is that **E4** treatment, somehow is capable to affect *TP53* wild-type, presented in these cells, action allows prevent P21 regulation. Therefore, in future, it would be interesting to study P21 levels by ELISA with and without **E4** treatment in order to infer if there is or not interference in its regulation. Additionally, one treatment with silencing of COX-2 expression would be added to evaluate if that cell cycle arrest induced by **E4** is dependent or independent of COX-2 activity.

Overall, **E4** treatment provoked cell cycle arrest in S phase in HCC cell lines.

3.4 Cell viability and cell death mechanisms

To assess if the decrease of cell proliferation after the treatment with **E4** was accompanied by an increase of cell death, cell viability and death profile induced were

analysed by flow cytometry, using the double staining with AV and IP. This experiment is important to identify how **E4** compound induce its activity since antiproliferative activity can occur due to cell death or quiescence. Further, to complement the results of flow cytometry, it was performed *May-Grünwald-Giemsa* staining in order to visualize morphological changes induced by **E4** treatment and help to identify the type of cell death induced by it.

To study the active cell death pathways, the alterations of the mitochondrial membrane potential ($\Delta\Psi_m$) were evaluated by flow cytometry. All these experiments were performed 48 hours after treatment with **E4** and the concentrations used correspond to the IC_{50} for each cell line (16.05 μM for MCF-7, 29.38 μM for HuH7 and 34.74 μM for HepG2) and to a concentration higher than the IC_{50} value ($>IC_{50}$), which corresponded to 25 μM for MCF-7 cell line and 75 μM for HepG2 and HuH7 cell lines, according to the Materials and Methods section (Table 3).

3.4.1 Viability and cell death

Figures 29 and 30 show bar graphs with the analysis of cell viability and types of cell death induced in MCF-7 cell line and representative images of morphologic changes induced by **E4** treatment, respectively.

In Figure 29, it can be observed that the highest concentration of **E4** induced a statistically significant decrease of cell viability from $73.1 \pm 1.8\%$ to $59.8 \pm 4.8\%$ ($p=0.0002$). In focus to cell death types, overall, there is a tendency to **E4** treatment induce necrosis (increase from $17.2 \pm 1.6\%$ to $24.3 \pm 2.5\%$ in treatment with 25 μM) and apoptosis (increase from $5.9 \pm 1.2\%$ to $9.5 \pm 1.6\%$ in treatment with 25 μM), despite there are no significant differences comparatively to control. These results are in agreement with *Serafim* et al. results once they proved that **E4** treatment induces apoptosis in this cell line. Nevertheless, as mentioned above, they used a concentration (75 μM) higher than the one used in this master's Thesis. Also, apoptosis markers (caspase-8 and caspase-9) were only expressed 96 hours after treatment (11).

In Figure 30, it is noted that the **E4** treatment induced death especially by apoptosis, in contrast to what is observed in the flow cytometry results. This discrepancy in results can be explained by the fact that since the reduction in viability is low, the ability of flow cytometry to distinguish between different types of cell death was limited. It can be noted that in control most of the cells are viable, with some necrotic and apoptotic

cells. With increase of **E4** treatment, it can be observed an increase of apoptotic cells and fewer necrotic cells. Thus, the observation of cells under the microscope corroborates the results already revealed in previous studies with **E4** treatment (75 μ M) (11).

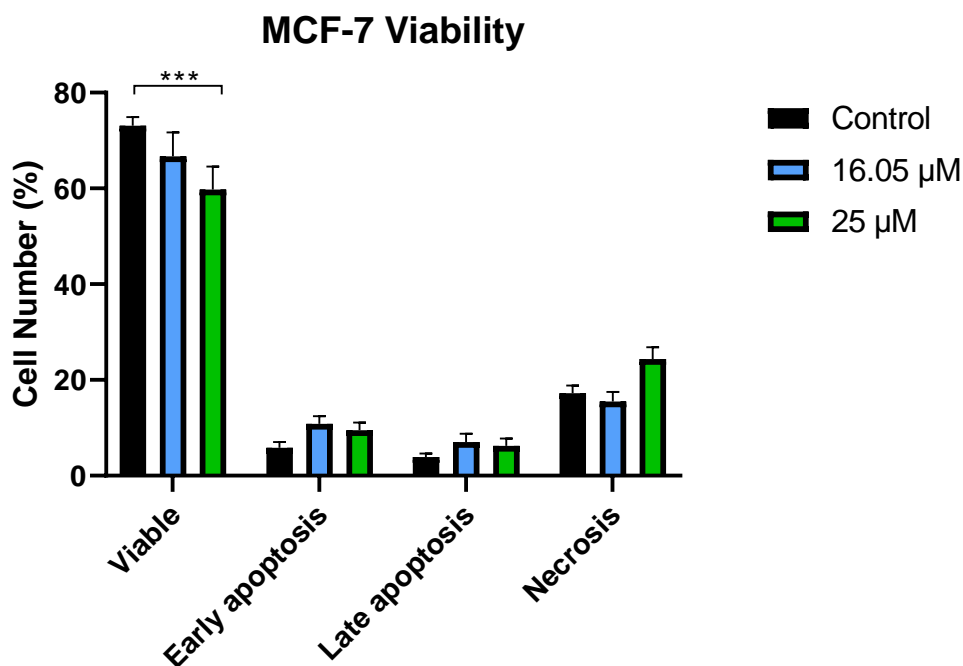


Figure 29 – Cell viability and types of cell death induced in MCF-7 cell line 48 hours after treatment with **E4**. Results are presented as a percentage (%) of viable cells, in early apoptosis, in late apoptosis and necrosis and express the mean \pm SEM of, at least, three independent experiments, in duplicate. Significant differences are denoted by *** p <0.001.

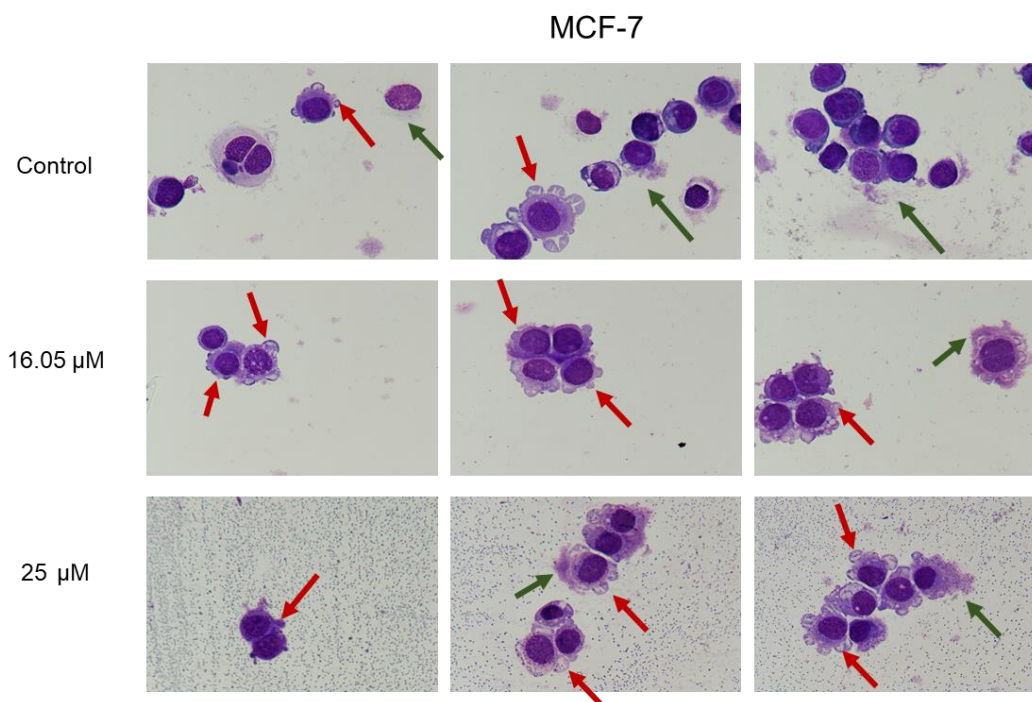


Figure 30 – Representative images (50x) of morphologic features in MCF-7 cell line after treatment with **E4** compound for 48 hours, after cells staining by May-Grünwald-Giemsa staining. Red arrows correspond to blebbings (apoptosis marker), and green arrows to cytoplasm leakage (necrotic marker).

Figures 31 and 32 show the analysis of cell viability and types of cell death induced in HuH7 cell line and representative images of morphologic changes induced by **E4** treatment, respectively.

Overall, in Figure 31, a statistically significant decrease in viable cells is seen between control and the highest concentration of **E4** treatment, from $62.1 \pm 3.9\%$ to $45.1 \pm 4.9\%$ ($p=0.0008$). In focus of cell death types, overall, there is a tendency to **E4** treatment induce apoptosis. Considering early apoptosis, there is an increase from 10.8% to 21.3%, despite there are no statistically significant differences comparatively to control, being much higher than the tendency increase of cells in necrosis (19.1% to 20.4%).

In Figure 32, although several viable cells exist in control, apoptotic cells are also the greatest population in this condition. The increase of **E4** concentration incites a rise of apoptotic and necrotic cells in 29.38 μM treatment, being the amount of both types of cell death very similar. However, the presence of apoptotic cells as a consequence of 75 μM treatment is very clear.

Even though there are no significant differences between **E4** treatment and control, these results are in accordance with previous study, which was used the same

compound (with 35 and 50 μM treatments, for 48 hours) that revealed similar results for WiDr cell line (colon cancer cell line) (12). Thus, overall, it can be concluded that **E4** treatment induced apoptosis in HuH7 cell line, in accordance with previous studies.

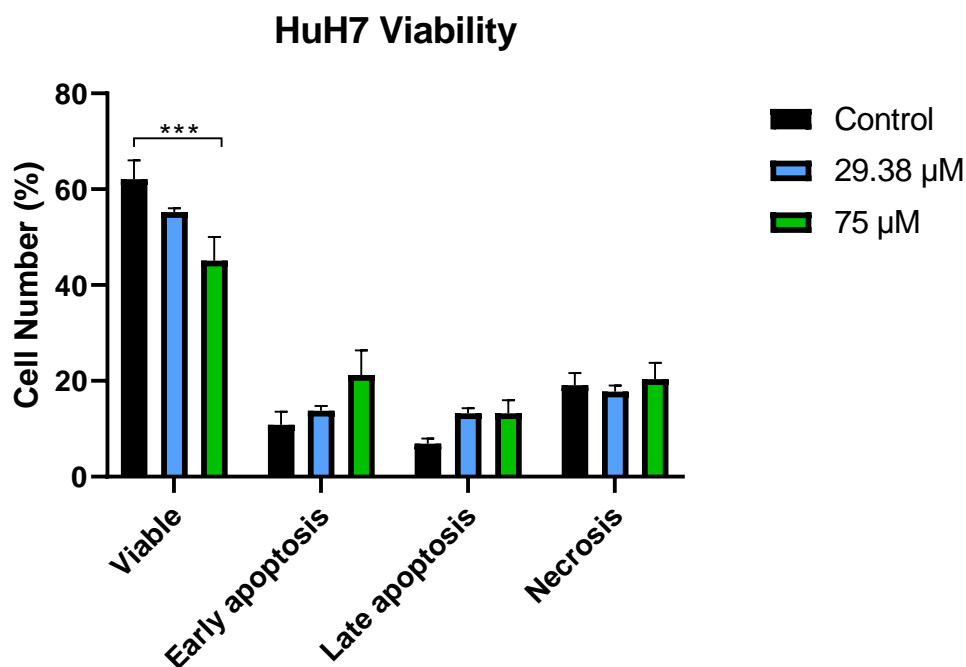


Figure 31 - Cell viability and types of cell death induced in HuH7 cell line 48 hours after treatment with **E4**. Results are presented as a percentage (%) of viable cells, in early apoptosis, in late apoptosis and necrosis and express the mean \pm SEM of, at least, two independent experiments, in duplicate. Significant differences are denoted by *** $p < 0.001$.

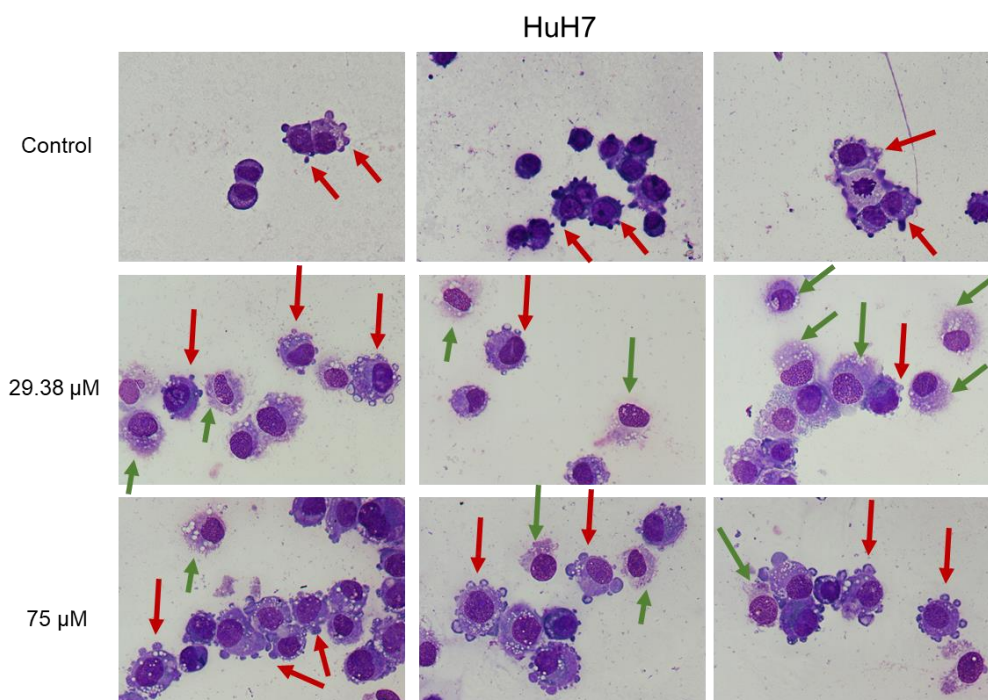


Figure 32 - Representative images (50x) of morphologic features in HuH7 cell line after treatment with **E4** compound for 48 hours, after cells staining by May-Grünwald-Giemsa staining. Red arrows correspond to blebbings (apoptosis marker) and green arrows to cytoplasm leakage (necrotic marker).

Figures 33 and 34 show the results of the analysis of cell viability and types of cell death induced in HepG2 cell line and representative images of morphologic changes induced by **E4** treatment, respectively.

Overall, in Figure 33, no significant differences between the treatments are noted. However, it can be observed a tendency to **E4** 34.74 μM treatment incite a strong decrease in viable cells and increase in necrosis. Although there are no significant differences between treatments, these results are in accordance with a previous study using the same compound, which revealed similar results for WiDr cell line (colon cancer cell line) (12). Furthermore, it can also be related to the decrease of necrosis observed between **E4** treatments with cell cycle results presented above (Figure 28) since **E4** treatment 75 μM induces cell arrest in S phase that could be related to quiescence.

Also, it can be noticed that the level of viable cells in control is low, which is corroborated by the existence of a high number of cells in apoptosis observed in Figure 34. Although some viable cells can be observed in control, necrotic and apoptotic cells are the highest number of cells in control. Increase of treatment with **E4** provokes a rise of apoptotic and necrotic cells, being the amount of both types of cell death very similar.

Moreover, in **E4** 34.74 μM treatment can be noted a binucleated cell, indicating difficulties in mitosis process.

This increase of apoptotic and necrotic cells in the control can be explained by three experimental factors: the long process that the cells go through before entering in the cytometer to be analysed (minimum 4 hours); the use of trypsinization to detach them since the cells take time to recover; and the high passages of the cell cultures.

During trypsinization cell adhesion is disrupted by the presence of EDTA since calcium is crucial for cell adhesion occur, leading to membrane dissolution. Membrane damage is measured through annexin V and the processes inherent to the use of trypsin or tryPLE can be detected as markers of apoptosis (false positive). This marking occurs since cells take some time to recover from the damage caused by detachment through trypsinisation, which depends on cell line to cell line (119,120).

To try to overcome this problem, whenever a longer wait was required, the cells were placed in an incubator with the reference conditions for cell line maintenance (37 °C and 5% CO₂). Since the problem persisted, a test reading of the controls with different brands of dyes was performed, which showed that there were no significant differences. In addition, early in the staining process for flow cytometry, cell numbers started to be counted by the trypan blue exclusion method, giving confidence that the cells were still in good culture conditions.

The highest concentration of **E4** treatment (75 μM) reduced cell viability in 17% in HuH7 cell line and 10% in HepG2 cell line, compared to control. Thus, comparing the two HCC lines, it can be inferred that they have similar sensitivity to **E4** treatment. Comparing both HCC cell lines, it can be observed that **E4** treatment induced cell death mainly by apoptosis in HuH7 cells and that in HepG2 cells, although apoptosis was also observed, the main cell death mechanism was necrosis.

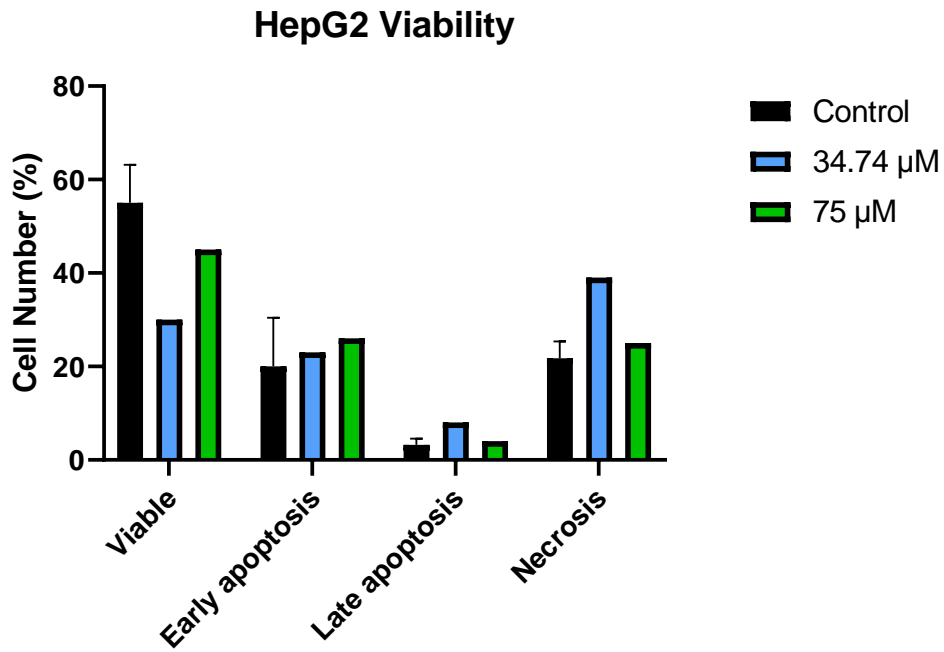


Figure 33 - Cell viability and types of cell death induced in HepG2 cell line 48 hours after treatment with **E4**. Results are presented as a percentage (%) of viable cells, in early apoptosis, in late apoptosis and necrosis and express the mean \pm SEM of, at least, two independent experiments.

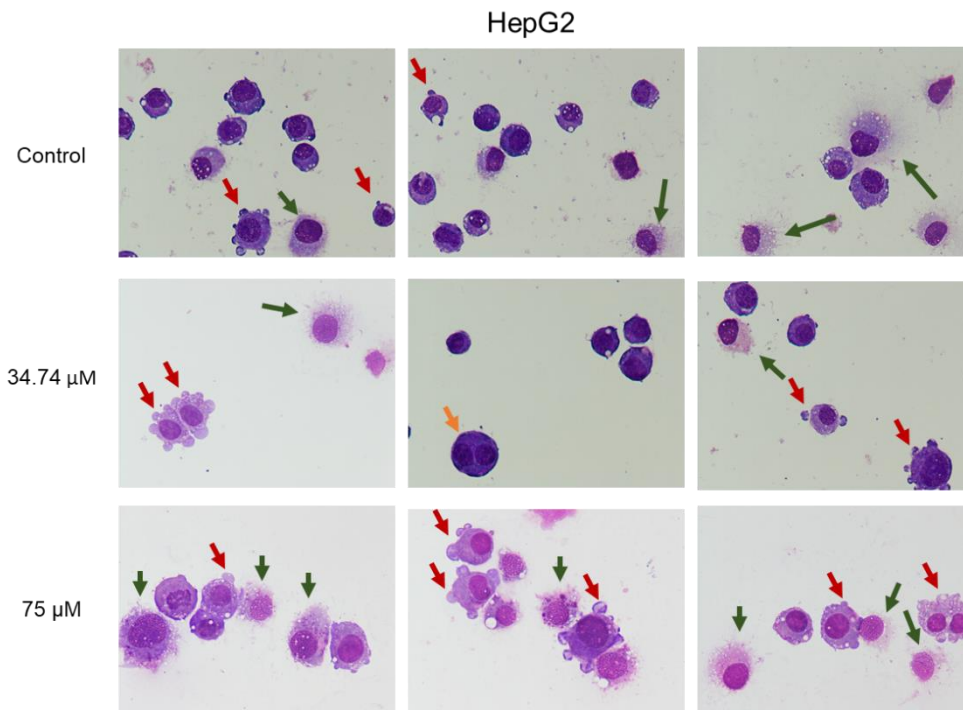


Figure 34 - Representative images (50x) of morphologic features in HepG2 cell line after treatment with **E4** compound for 48 hours, after cells staining by May-Grünwald-Giemsa staining. Red arrows correspond to blebbings (apoptosis marker), green arrows to cytoplasm leakage (necrotic marker) and orange arrow to binucleated cells (failure in mitosis).

3.4.2 Mitochondrial membrane potential ($\Delta\Psi_m$)

To assess the role of mitochondria in cell death mechanism induced by **E4**, the changes in the $\Delta\Psi_m$ on MCF-7, HepG2 and HuH7 cell lines, 48 hours after treatment, were evaluated through flow cytometry and using JC-1 staining. It is important to point out that the higher M/A ratio, the lower the mitochondrial membrane potential, indicating mitochondrial dysfunction.

Figure 35, Figure 36 and Figure 37 represent M/A ratios for the three conditions in MCF-7, HuH7 and HepG2 cell lines, respectively. In general, there are no statistically significant differences between the treatments, in all cell lines. Nonetheless, it can be observed a tendency for an increase in all M/A ratios, agreeing with a previous study with same treatment (**E4** for 48 hours) in colon cancer cell lines (12). *Tavares-da-Silva* et al. showed that treatments with 22 and 50 μM of **E4** in C2BBE1 cell line and treatments with 35 and 50 μM of **E4** in WiDr cell line induced a dependent-dose increase in M/A ratios, indicating a mitochondrial dysfunction with increase of **E4** concentration used (12).

Thus, the increase of M/A ratios suggests a reduction of mitochondrial membrane potential, revealing mitochondrial dysfunction, which is an important event in the activation of the intrinsic pathway of apoptosis (12). However, repetition of the experiment is required to ensure the assay reproducibility, and then to confirm whether this tendency is associated with mitochondrial dysfunction.

Intrinsic apoptosis is a mitochondrial-centred cell death triggered by intracellular stress, which is mediated by mitochondrial outer membrane permeabilization, resulting in apoptosome formation and activation of caspase-9. Initiation and execution of these mechanisms are regulated by BCL-2 and caspase families of proteins. Activation of BCL-2 family member BAX results in permeabilization of mitochondrial outer membrane and in the release of pro-apoptotic proteins, such as cytochrome c from the intermembrane space into the cytosol. The exit of cytochrome c for cytosol triggers the apoptosome formation and activation of caspase-9, which can directly cleave and activate caspase-3, an effector caspase. Effector caspases are responsible for initiating the hallmarks of the degradation phase of apoptosis, including DNA fragmentation, mitochondrial remodelling, ROS production and membrane blebbing. Nevertheless, other BCL-2 family members have an anti-apoptotic activity, regulating these processes, such as BCL-2, which can be responsible for cancer cells resistance to standard chemotherapy and radiotherapy (121,122).

Therefore, other important measurement that can complement these results is the study of caspase-9, caspase-3, BAX, and BCL-2 expression by western blot (121,122).

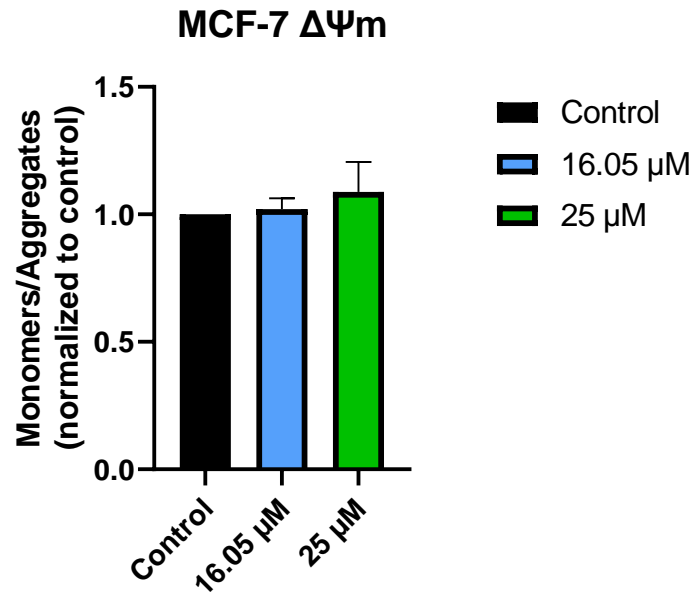


Figure 35 – Mitochondrial membrane potential ($\Delta\Psi_m$) of MCF-7 cell line 48 hours after treatment with **E4**. Results are presented as ratio of M/A for each condition relatively to control expressed by mean \pm SEM of, at least, three independent experiments, in duplicate. The increase of ratio is directly correlated with mitochondrial dysfunction.

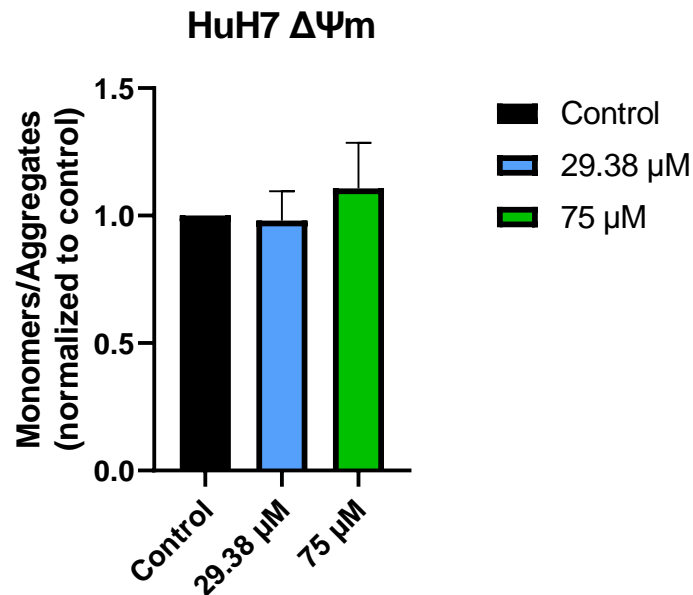


Figure 36 - Mitochondrial membrane potential ($\Delta\Psi_m$) of HuH7 cell line 48 hours after treatment with **E4**. Results are presented as ratio of M/A for each condition relatively to control expressed by mean \pm SEM of, at least, three independent experiments, in duplicate. The increase of ratio is directly correlated with mitochondrial dysfunction.

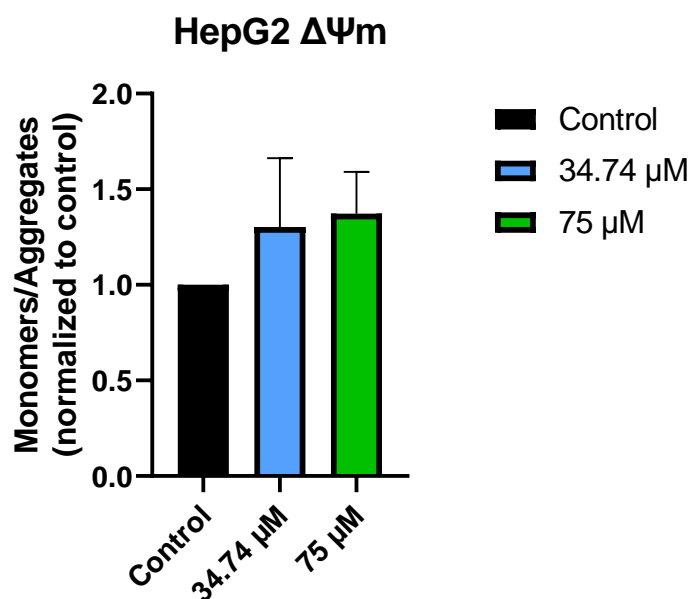


Figure 37 - Mitochondrial membrane potential ($\Delta\Psi_m$) of HepG2 cell line 48 hours after treatment with **E4**. Results are presented as ratio of M/A for each condition relatively to control expressed by mean \pm SEM of, at least, three independent experiments, in duplicate. The increase of ratio is directly correlated with mitochondrial dysfunction.

3.5 COX-2 expression

Western blot was performed to evaluate if the treatment with **E4** compound modifies COX-2 expression. In this experiment, one positive control was added: celecoxib, a COX-2 selective inhibitor used in clinical practice. This addition is of greater importance because it allows comparison between treatment with cinnamic acid amides and treatment with a well-studied COX-2 selective inhibitor, allowing confidence in the results. This method was performed to evaluate if the treatment with **E4** alters COX-2 expression, inferring whether there is or not a possible association between its antiproliferative activity COX-2 expression. Comparison with positive control allows to infer some differences in anticancer activity between **E4** and celecoxib.

The results are presented as arbitrary units with normalization to negative control (untreated cells).

Figure 38 represents the COX-2 expression in three cell lines and respective conditions. In all cell lines, **E4** treatment provokes a decrease in COX-2 expression, being the highest concentrations the most efficient – 25 μM for MCF-7 cell line and 75 μM for HuH7 and HepG2 cell lines. However, these results do not present statistically significant differences between control and treatments (including with celecoxib).

In MCF-7 cell line, IC₅₀ **E4** treatment (16.05 μ M) induced a 0.27-fold decrease of COX-2 expression, in contrast, >IC₅₀ **E4** treatment (25 μ M) caused a decrease of 0.76-fold. Celecoxib induced an increase of 0.63-fold in COX-2 expression, in agreement to what is described in the bibliography (123). *Niederberger et al.* refer that treatment with 50 μ M of celecoxib incites an increase in COX-2 expression since it activates NF- κ B, an upstream regulator of COX-2 expression (123).

In HuH7 cell line, although there are no significant differences between treatments and control, western blot results show a 0.3-fold decrease of COX-2 expression relative to control, when cells are treated with 29.38 μ M of **E4**. The highest concentration was more efficient in decreasing COX-2 expression by 0.55-fold. In terms of COX-2 inhibition, no difference was observed between **E4** treatment and celecoxib (decrease of 0.5-fold) in this cell line. The same conclusions can be reported regarding HepG2 cell line. However, in this case, celecoxib (decrease of 0.37-fold) treatment is comparable to IC₅₀ (34.74 μ M) **E4** treatment (decrease of 0.41-fold), being >IC₅₀ (75 μ M) **E4** treatment more efficient in decreasing COX-2 expression by 0.51-fold.

The action of celecoxib in COX-2 expression in MCF-7 cell line is significantly different to **E4** treatments [$p=0.0447$ for IC₅₀ treatment (16.05 μ M) and $p=0.0024$ for >IC₅₀ treatment (25 μ M)] in this cell line and action of celecoxib in HCC cell lines [$p=0.0082$ for HuH7 cell line and $p=0.0198$ for HepG2 cell line].

According to *Ribeiro et al.*, **E4** was one of the compounds with intermediate potency to inhibit COX-2 (12.7 \pm 0.5 μ M) in blood samples (10). These western blot results are in agreement with the inhibitory capacity of this compound and its antiproliferative activity, since they demonstrated a tendency for a decrease in COX-2 expression, after treatment with **E4**, in all cancer cell lines.

Notwithstanding these are preliminary results, other studies with phenolic compounds treatments revealed a dose-dependent COX-2 expression decrease (70,124). *Yun et al.* demonstrated that treatment with sinapic acid (40, 80 and 160 μ M) in RAW 264.7 mice macrophages induced dose-dependent decrease of COX-2 expression (124) and *Tao et al.* proved that treatment with dahshensu (200 μ M) for 24 hours also provoked one reduce of COX-2 expression in lung cancer cell line (A549 cell line) (70). Furthermore, another study also revealed that treatment with various doses of celecoxib for 48 hours significantly reduced proliferation in HuH7 cells with association with decreased COX-2 expression (105). Thus, although the repetition of this method is needed, **E4** compound seems to decrease COX-2 expression in the used cell lines.

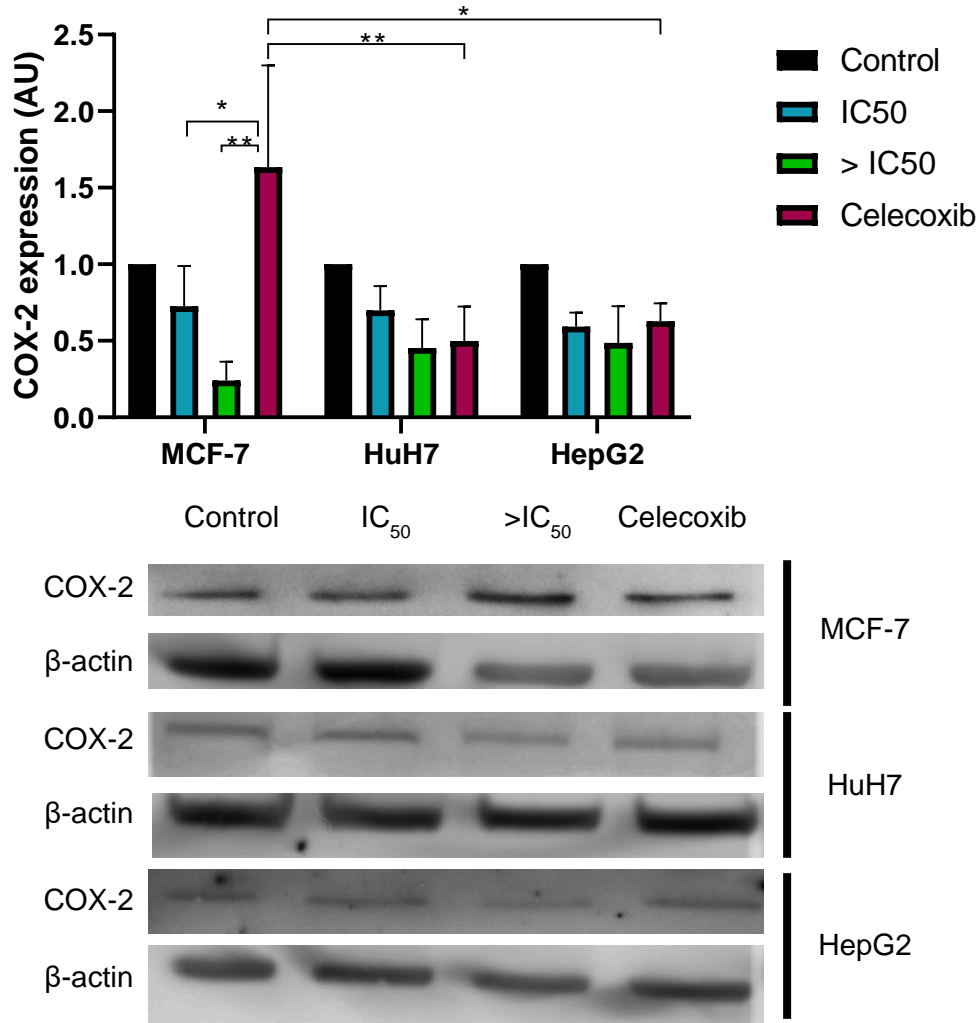


Figure 38 - COX-2 expression in three used cell lines (HuH7, HepG2 and MCF-7) 48 hours after following treatments: untreated cells (control), IC₅₀, >IC₅₀ and celecoxib. Results are presented as arbitrary units (AU) with normalization to control (untreated cells) of COX-2 expression as a function of different treatments and express the mean±SEM of, at least, three independent experiments, in triplicate. Significant differences are denoted by *p<0.05, **p<0.01. Below the bar graph there are western blot diagram of COX-2 and β-actin expression.

Several reports refer that many of the anticancer effects of NSAIDs are independent of COX-2 inhibition, including celecoxib. These COX-2-independent mechanisms can be explained by the fact that these molecules possess antiproliferative and apoptotic effects on cell lines regardless of their level of COX-2 expression and that growth-suppressing effect in cancer cells are not reversible with prostaglandin supplementation (113).

Celecoxib anticancer activity involves both COX-2-dependent and COX-2-independent mechanisms, including induction of endoplasmic reticulum stress, induction of apoptosis, cell cycle arrest and regulation of angiogenesis (105,125). In COX-2-independent mechanisms, the major COX-2-independent target is PI3K/PDK-1/Akt signalling. *Kulp* et al. demonstrated that a deficient in COX-2-inhibitory activity compound (DMC), analogue to celecoxib, inhibits PC3 cell proliferation through attenuation of Akt activity as a result of partial inhibition of PDK-1 (3-phosphoinositide-dependent protein kinase-1) (126). Other study also demonstrated that inhibition of this signalling pathway is correlated with celecoxib-induced apoptosis and that celecoxib also inhibits sarcoplasmic/endoplasmic reticulum ATPase leading to rapid leakage of calcium into the cytosol and, consequently, triggering endoplasmic reticulum stress and ultimately leading to apoptosis (125). Celecoxib also can inhibit G1-S progression, suppressing tumor growth and arresting cell cycle through inhibiting formation of CD1/CDK4 (cyclin D1/ cyclin-dependent kinase 4) complex in a COX-2-independent way. Furthermore, celecoxib promotes apoptosis of HCC cells by modulating activation of caspase-3 and caspase-9 in a COX-2 expression-independent manner (105). This latter evidence can be extrapolated for **E4** treatment in HCC cell lines, since a slight difference in COX-2 expression is observed, nevertheless, it will be necessary to study this hypothesis in the future through, e.g., evaluating caspase-9 and caspase-3 expression by western blot after silencing COX-2 expression. If **E4** treatment will be capable to inhibit caspase-9 and caspase-3 without COX-2 expression, it concluded that it antiproliferative activity is COX-2 independent.

In future, these results can be complemented by measuring the production of PGs by ELISA (105,109) and evaluating caspase-3 expression by western blot. It is known that most COX-2 functions in tumour-related processes are mediated through overproduction of PGE₂. Once COX-2 expression decreases in a dose-dependent way with **E4** treatment in these cell lines, it is expected the consequent decrease of PGE₂ production. However, caspase-3 is an upstream regulator of PGE₂, involved in the production of AA, by activation of iPLA₂, therefore, it is important to evaluate whether caspase-3 expression also decreases with **E4** treatment. Caspase-3/COX-2/PGE₂ pathway is associated with stimulating tumour growth and stem cell proliferation after chemo- and radiotherapy and, consequently, therapy resistance (54,55). Therapy resistance is the major challenge when treating cancer patients, including BC and HCC patients, reinforcing the importance of evaluating caspase-3 expression, in order to discover new strategies to exceed this challenge.

Mutations in *TP53* gene are similarly frequent in tumours, e.g. HCC, and in chronic inflammatory diseases, such as rheumatoid arthritis. Obesity, which is a well-known risk factor of BC, is a condition of low-level chronic inflammation that has been associated with accelerated tumour progression and decreased response to treatment. It is known that a hallmark of inflammation is increased vascular permeability, which incites extravasation of inflammatory and immune cells as well as the escape of protein-rich fluid into the extravascular tissue. This vascular permeability in the inflammation process is similar to that seen in tumours, giving a link between inflammation and cancer. Vascular permeability in both, inflammation and cancer, leads to leaky blood vessels, which compromises the delivery of chemotherapy in cancer (127). Some molecules with natural origin, such as curcumin and resveratrol, showed anti-angiogenesis effects by regulating multiple signalling pathways as NF- κ B and PI3/Akt that are involved in COX-2 expression and activity (51,128). Thus, as **E4** treatment decreases COX-2 expression, it can be a promising mediator to increase drug delivery to the tumour. Therefore, testing the ability of **E4** treatment as an alternative way to increase drug delivery to the tumour can be also a future work to do.

Several studies demonstrate that the bioavailability of compounds of this nature in blood plasma is low. Furthermore, previous studies use doses far above those used in this work.

Jung et al. used for studies with animal models doses of 200 and 500 mg/kg of ethyl acetate fraction and ferulic acid, respectively, by oral administration (129). However, the authors do not refer to bioavailability of compounds in plasma, being difficult to extrapolate for the concentrations used in this work. Nonetheless, *Liang et al.* performed *in vivo* studies with administration of bergenin/cinnamic acid hybrids via intraperitoneal, which permits comparing two ranges of doses employed. *Liang et al.* used doses of 15 and 30 mg/kg, daily, for 14 days. For conversion, the highest concentration used in this master's work is 7.1 mg/kg (200 μ M), that is very lower than the one used in *Liang et al.* study (130). In a study with spheroids was used a range of concentrations of 0-4 mM of cinnamic acids (131).

Furthermore, other evidence reveals low plasma concentrations of cinnamic acid derivatives after oral administration due to limited absorption, intensive metabolism and/or fast elimination from circulation. Thus, efforts have been made to enhance bioavailability and its biological effects with new formulations when cinnamic acid derivatives are entrapped into particles (132).

Thus, it can be concluded that the concentrations employed in this research are much lower than the ones used in animal models, allowing for a dose increase if necessary and that cinnamic acid amides are promising compounds to exceed the limitations of the COX-2 selective inhibitors currently used in the clinical practice and used as anti-inflammatory and anticancer agents.

Chapter 4. Conclusions and Future perspectives

In this Chapter, the major conclusions obtained with this work are emphasized and summarized. Some main obstacles and challenges that were raised during this Thesis are described. Perspectives and proposals for further research are also identified and presented.

4.1 Conclusions

Female BC is one of the most frequent and deadliest cancers and HCC is also one of the deadliest cancers worldwide, being therapy resistance the major challenges when treating these cancer patients.

One of the hallmarks of cancer is tumour-promoting inflammation that can be linked to COX-2 protein. COX-2 is a protein involved in inflammation processes through production of PGs and is overexpressed in various types of cancer, such as BC and HCC. Its overexpression is related to diverse hallmarks of cancer including inflammation, angiogenesis, apoptosis and therapy resistance. Therefore, COX-2 inhibitors have been studied for anticancer purposes. However, nowadays there are no anti-inflammatory drugs which are truly safe and can also be used as a suitable therapy. For this reason, efforts have been made to discover new compounds to exceed the limitations of COX-2 inhibitors currently used in clinical practice. Cinnamic acid derivatives have been revealed to be potent and selective COX-2 inhibitors and considerable antiproliferative agents against various cancers.

In this master's Thesis, antiproliferative activity of one cinnamic acid and five cinnamic acid amides was assessed, with the objective of discovering promising compounds to exceed the limitations of COX-2 inhibitors currently used in clinical practice and discover, thus, a compound with both anticancer and anti-inflammatory activities.

All compounds demonstrated antiproliferative activity, being **E4** the most promising compound. Further, antiproliferative activities of **E4** and **F13** compounds demonstrated selectivity for breast cancer cells in comparison to normal breast cells. Although selectivity evaluation was not done in normal liver cells, inhibition of cell proliferation was much more pronounced in breast cancer cells than in non-tumor breast cells.

Cell cycle alterations, cell viability and cell death mechanisms data showed slight but biologically relevant differences between treatments. To support this data, cell morphology was assessed by *May-Grünwald-Giemsa* staining. **E4** treatment in MCF-7 and HuH7 cells induced apoptosis, while induced necrosis and apoptosis in HepG2 cells. This treatment also provoked cell cycle arrest in S phase in HepG2 and HuH7 cells. HCC cell cycle results can be associated with mutation of *TP53* gene (HuH7), or interference in *TP53*-related P21 regulation, which is involved in G1 checkpoint activation. **E4**

treatment also revealed the ability to stimulate reduction of mitochondrial membrane potential, implicated in apoptosis intrinsic pathway activation.

COX-2 expression data are preliminary. In general, slight differences were apparent between conditions and cell lines. However, **E4** treatment tend to diminish COX-2 expression in MCF-7, HepG2 and HuH7 cell lines, whereas celecoxib increased COX-2 expression in MCF-7 cell lines. These preliminary results are in accordance with previous studies on phenolic compounds.

4.2 Future perspectives

Throughout the development of this project, it was noticed that additional data coming from complementary tests could enrich the results obtained in this Thesis. However, due to time and pandemic constraints some tests were not possible to perform. Namely, it would be important to expand the timings of treatment and the screening against other cancer cell lines, *e.g.*, lung (A549 and H1299) and cholangiocarcinoma (HuCCT1 and TFK-1) cell lines, since within each type of cancer cell lines present pronounced differences in COX-2 expression (133–135). Moreover, it is necessary to evaluate the effects of the compounds in other normal cell lines to explore the selectivity of studied compounds. Moreover, the evaluation of ROS production and GSH by flow cytometry is also important to evaluate if the selectivity of compounds to cancer cells can be explained by the increase of ROS production and failure of antioxidant defences. Expanding the timings of treatment might allow to decrease concentrations used, as well as, to explore if the treatment may last longer. It would be also interesting to continue the studies using more complex preclinical models, namely spheroids (tridimensional cell cultures) and animal models.

Because of instability of compounds **F11** and **F20** demonstrated in this work, it would be interesting to repeat the experiments with these compounds with some alterations in protocol. For **F20**, an approach could be to alter the solvent used, polyethylene glycol instead of DMSO, since **F20** compound demonstrated to be promising due to its huge capacity for inhibit COX-2. For **F11** it could be an option to repeat the experiment making a new solution each time the compound is tested, avoiding the production of by-products. Due to the drastic difference observed between the antiproliferative actions of compounds **E5** and **F19**, it would be interesting to perform

future molecular modelling and docking studies, in order to understand why one isomer has more activity than the other.

Furthermore, the repetition of western blot and flow cytometry assays is also important due to the few statistical differences found between treatments with reduced experiments and technical problems faced. As a complement to western blot results, it would be interesting to evaluate the production of PGs by ELISA, as well as to assess the expression of caspase-3 and other proteins associated with signalling cascades that bind COX-2 to tumorigenic processes by western blot and evaluate the effect of these compounds on lines with COX-2 silencing, in order to assess whether their antiproliferative activity is dependent or independent of COX-2. Additionally, as a complement to flow cytometry results, the silencing of COX-2 expression and the assessment of caspase-9, BCL-2 and BAX expression by western blot would allow to verify whether apoptosis is caused through the intrinsic pathway, and if these processes is COX-2-dependent or COX-2-independent. In addition, to complement cell cycle results would be interesting study P21 levels by ELISA with and without **E4** treatment in order to infer if there is or not interference in *TP53*-related P21 regulation.

Due to the differences in linearity between the MTT and SRB assays in the HepG2 line with the **F19** treatment, the repetition of the SRB assay with this compound, including the selectivity assessment, would be important. Also, to confirm if the mechanism of action of cinnamic acid amides is COX-2-dependent or COX-2-independent one could silence COX-2 expression and evaluate its antiproliferative activity again. In case of identical results, it would be confirmed that its action is really COX-2-independent. Besides, it would be interesting to evaluate expression of other proteins related to cancerous processes, such as VEGF (angiogenesis), caspase-8, caspase-9, BCL-2, and BAX (resistance to apoptosis), and PI3K/PDK-1/Akt pathway, the major COX-2-independent target of celecoxib. In addition, due to evidence showing low plasma concentrations of cinnamic acid derivatives after oral administration, further formulation of these cinnamic acid amides in a particle-bound form would also be of interest.

Finally, the evaluation of **E4**, the most promising compound, in combination with radiotherapy or standard of care drugs, might pave the way to overcome resistance and cardiotoxicity.

References

1. Dannenberg AJ, Lippman SM, Mann JR, Subbaramaiah K, DuBois RN. Cyclooxygenase-2 and epidermal growth factor receptor: pharmacologic targets for chemoprevention. *Journal of clinical oncology : official journal of the American Society of Clinical Oncology* [Internet]. 2005;23:254–66. Available from: <http://www.ncbi.nlm.nih.gov/pubmed/15637389>
2. Ribeiro D, Freitas M, Tomé SM, Silva AMS, Laufer S, Lima JLFC, et al. Flavonoids inhibit COX-1 and COX-2 enzymes and cytokine/chemokine production in human whole blood. *Inflammation* [Internet]. 2015;38:858–70. Available from: <http://www.ncbi.nlm.nih.gov/pubmed/25139581>
3. Wu T. Cyclooxygenase-2 and prostaglandin signaling in cholangiocarcinoma. *Biochimica et biophysica acta* [Internet]. 2005;1755:135–50. Available from: <http://www.ncbi.nlm.nih.gov/pubmed/15921858>
4. Hashemi Goradel N, Najafi M, Salehi E, Farhood B, Mortezaee K. Cyclooxygenase-2 in cancer: A review. *Journal of cellular physiology* [Internet]. 2019;234:5683–99. Available from: <http://www.ncbi.nlm.nih.gov/pubmed/30341914>
5. Sheng J, Sun H, Yu F-B, Li B, Zhang Y, Zhu Y-T. The Role of Cyclooxygenase-2 in Colorectal Cancer. *International journal of medical sciences* [Internet]. 2020;17:1095–101. Available from: <http://www.ncbi.nlm.nih.gov/pubmed/32410839>
6. Wu T, Leng J, Han C, Demetris AJ. The cyclooxygenase-2 inhibitor celecoxib blocks phosphorylation of Akt and induces apoptosis in human cholangiocarcinoma cells. *Molecular cancer therapeutics* [Internet]. 2004;3:299–307. Available from: <http://www.ncbi.nlm.nih.gov/pubmed/15026550>
7. Petkova DK, Clelland C, Ronan J, Pang L, Coulson JM, Lewis S, et al. Overexpression of cyclooxygenase-2 in non-small cell lung cancer. *Respiratory medicine* [Internet]. 2004;98:164–72. Available from: <http://www.ncbi.nlm.nih.gov/pubmed/14971881>
8. Chen H, Cai W, Chu ESH, Tang J, Wong C-C, Wong SH, et al. Hepatic cyclooxygenase-2 overexpression induced spontaneous hepatocellular

carcinoma formation in mice. *Oncogene* [Internet]. 2017;36:4415–26. Available from: <http://www.ncbi.nlm.nih.gov/pubmed/28346420>

9. Harris RE, Casto BC, Harris ZM. Cyclooxygenase-2 and the inflammogenesis of breast cancer. *World journal of clinical oncology* [Internet]. 2014;5:677–92. Available from: <http://www.ncbi.nlm.nih.gov/pubmed/25302170>

10. Ribeiro D, Proença C, Varela C, Janela J, Tavares da Silva EJ, Fernandes E, et al. New phenolic cinnamic acid derivatives as selective COX-2 inhibitors. Design, synthesis, biological activity and structure-activity relationships. *Bioorganic chemistry* [Internet]. Elsevier; 2019;91:103179. Available from: <https://doi.org/10.1016/j.bioorg.2019.103179>

11. Serafim TL, Carvalho FS, Marques MPM, Calheiros R, Silva T, Garrido J, et al. Lipophilic caffeic and ferulic acid derivatives presenting cytotoxicity against human breast cancer cells. *Chemical research in toxicology* [Internet]. 2011;24:763–74. Available from: <http://www.ncbi.nlm.nih.gov/pubmed/21504213>

12. Tavares-da-Silva EJ, Varela CL, Pires AS, Encarnação JC, Abrantes AM, Botelho MF, et al. Combined dual effect of modulation of human neutrophils' oxidative burst and inhibition of colon cancer cells proliferation by hydroxycinnamic acid derivatives. *Bioorganic & medicinal chemistry* [Internet]. 2016;24:3556–64. Available from: <http://www.ncbi.nlm.nih.gov/pubmed/27290693>

13. Roleira FMF, Varela CL, Costa SC, Tavares-da-Silva EJ. Phenolic Derivatives From Medicinal Herbs and Plant Extracts: Anticancer Effects and Synthetic Approaches to Modulate Biological Activity. *Studies in Natural Products Chemistry*. Elsevier B.V.; 2018. page 115–56.

14. Sung H, Ferlay J, Siegel RL, Laversanne M, Soerjomataram I, Jemal A, et al. Global Cancer Statistics 2020: GLOBOCAN Estimates of Incidence and Mortality Worldwide for 36 Cancers in 185 Countries. *CA: a cancer journal for clinicians* [Internet]. Wiley; 2021;71:209–49. Available from: <http://www.ncbi.nlm.nih.gov/pubmed/33538338>

15. Hanahan D, Weinberg RA. The hallmarks of cancer. *Cell* [Internet]. 2000 [cited 2020 Dec 11];100:57–70. Available from: <https://linkinghub.elsevier.com/retrieve/pii/S0092867400816839>

16. Hanahan D, Weinberg RA. Hallmarks of cancer: the next generation. Cell [Internet]. Elsevier Inc.; 2011;144:646–74. Available from: <http://dx.doi.org/10.1016/j.cell.2011.02.013>
17. GLOBOCAN - Portugal Fact Sheets [Internet]. [cited 2021 Jun 8]. Available from: <https://gco.iarc.fr/today/data/factsheets/populations/620-portugal-fact-sheets.pdf>
18. Ferlay J, Laversanne M, Ervik M, Lam F, Colombet M, Mery L, Piñeros M, Znaor A, Soerjomataram I, Bray F. Global Cancer Observatory: Cancer Tomorrow. [Internet]. International Agency for Research on Cancer. Available, Lyon, France. 2020 [cited 2021 Nov 18]. Available from: <https://gco.iarc.fr/tomorrow>
19. Harbeck N, Penault-Llorca F, Cortes J, Gnant M, Houssami N, Poortmans P, et al. Breast cancer. Nature reviews Disease primers [Internet]. 2019;5:66. Available from: <http://www.ncbi.nlm.nih.gov/pubmed/31548545>
20. Akram M, Iqbal M, Daniyal M, Khan AU. Awareness and current knowledge of breast cancer. Biological research [Internet]. BioMed Central; 2017;50:33. Available from: <http://www.ncbi.nlm.nih.gov/pubmed/28969709>
21. Sun Y, Zhao Z, Yang Z, Xu F, Lu H, Zhu Z, et al. Risk Factors and Preventions of Breast Cancer. International journal of biological sciences [Internet]. 2017;13:1387–97. Available from: <http://www.ncbi.nlm.nih.gov/pubmed/29209143>
22. Ginsburg O, Yip C, Brooks A, Cabanes A, Caleffi M, Dunstan Yataco JA, et al. Breast cancer early detection: A phased approach to implementation. Cancer [Internet]. 2020;126 Suppl:2379–93. Available from: <http://www.ncbi.nlm.nih.gov/pubmed/32348566>
23. Waks AG, Winer EP. Breast Cancer Treatment: A Review. JAMA [Internet]. 2019;321:288–300. Available from: <http://www.ncbi.nlm.nih.gov/pubmed/30667505>
24. Schünemann HJ, Lerda D, Quinn C, Follmann M, Alonso-Coello P, Rossi PG, et al. Breast Cancer Screening and Diagnosis: A Synopsis of the European Breast Guidelines. Annals of internal medicine [Internet]. 2020;172:46–56. Available from: <http://www.ncbi.nlm.nih.gov/pubmed/31766052>

25. Saiki H, Petersen IA, Scott CG, Bailey KR, Dunlay SM, Finley RR, et al. Risk of Heart Failure With Preserved Ejection Fraction in Older Women After Contemporary Radiotherapy for Breast Cancer. *Circulation* [Internet]. 2017;135:1388–96. Available from: <http://www.ncbi.nlm.nih.gov/pubmed/28132957>
26. Lam CSP, Arnott C, Beale AL, Chandramouli C, Hilfiker-Kleiner D, Kaye DM, et al. Sex differences in heart failure. *European heart journal* [Internet]. 2019;40:3859–3868c. Available from: <http://www.ncbi.nlm.nih.gov/pubmed/31800034>
27. Ameri P, Canepa M, Anker MS, Belenkov Y, Bergler-Klein J, Cohen-Solal A, et al. Cancer diagnosis in patients with heart failure: epidemiology, clinical implications and gaps in knowledge. *European journal of heart failure* [Internet]. 2018;20:879–87. Available from: <http://www.ncbi.nlm.nih.gov/pubmed/29464808>
28. Derakhshani A, Rezaei Z, Safarpour H, Sabri M, Mir A, Sanati MA, et al. Overcoming trastuzumab resistance in HER2-positive breast cancer using combination therapy. *Journal of cellular physiology* [Internet]. 2020;235:3142–56. Available from: <http://www.ncbi.nlm.nih.gov/pubmed/31566722>
29. Hanker AB, Sudhan DR, Arteaga CL. Overcoming Endocrine Resistance in Breast Cancer. *Cancer cell* [Internet]. Elsevier Inc.; 2020;37:496–513. Available from: <https://doi.org/10.1016/j.ccell.2020.03.009>
30. Dahn ML, Marcato P. Targeting the Roots of Recurrence: New Strategies for Eliminating Therapy-Resistant Breast Cancer Stem Cells. *Cancers* [Internet]. 2020;13:1–5. Available from: <http://www.ncbi.nlm.nih.gov/pubmed/33379132>
31. Massarweh NN, El-Serag HB. Epidemiology of Hepatocellular Carcinoma and Intrahepatic Cholangiocarcinoma. *Cancer control: journal of the Moffitt Cancer Center* [Internet]. 2017;24:1073274817729245. Available from: <http://www.ncbi.nlm.nih.gov/pubmed/28975830>
32. Yang JD, Hainaut P, Gores GJ, Amadou A, Plymoth A, Roberts LR. A global view of hepatocellular carcinoma: trends, risk, prevention and management. *Nature reviews Gastroenterology & hepatology* [Internet]. Springer US; 2019;16:589–604. Available from: <http://dx.doi.org/10.1038/s41575-019-0186-y>

33. Ogunwobi OO, Harricharran T, Huaman J, Galuza A, Odumuwagon O, Tan Y, et al. Mechanisms of hepatocellular carcinoma progression. *World journal of gastroenterology* [Internet]. 2019;25:2279–93. Available from: <http://www.ncbi.nlm.nih.gov/pubmed/31148900>
34. Marin JJG, Macias RIR, Monte MJ, Romero MR, Asensio M, Sanchez-Martin A, et al. Molecular Bases of Drug Resistance in Hepatocellular Carcinoma. *Cancers* [Internet]. 2020;12:1–26. Available from: <http://www.ncbi.nlm.nih.gov/pubmed/32585893>
35. El-Serag HB. Epidemiology of Hepatocellular Carcinoma. *The Liver: Biology and Pathobiology*, 6th Edition. 2020. page 758–72.
36. Zucman-Rossi J, Nault J. Mutations and Genomic Alterations in Liver Cancer. *The Liver*. 2020;773–81.
37. Craig AJ, von Felden J, Garcia-Lezana T, Sarcognato S, Villanueva A. Tumour evolution in hepatocellular carcinoma. *Nature reviews Gastroenterology & hepatology* [Internet]. Springer US; 2020;17:139–52. Available from: <http://dx.doi.org/10.1038/s41575-019-0229-4>
38. Sayiner M, Golabi P, Younossi ZM. Disease Burden of Hepatocellular Carcinoma: A Global Perspective. *Digestive diseases and sciences* [Internet]. Springer US; 2019;64:910–7. Available from: <https://doi.org/10.1007/s10620-019-05537-2>
39. Fornari F, Giovannini C, Piscaglia F, Gramantieri L. Elucidating the Molecular Basis of Sorafenib Resistance in HCC: Current Findings and Future Directions. *Journal of hepatocellular carcinoma* [Internet]. 2021;8:741–57. Available from: <http://www.ncbi.nlm.nih.gov/pubmed/34239844>
40. Dong X-F, Liu T-Q, Zhi X-T, Zou J, Zhong J-T, Li T, et al. COX-2/PGE2 Axis Regulates HIF2 α Activity to Promote Hepatocellular Carcinoma Hypoxic Response and Reduce the Sensitivity of Sorafenib Treatment. *Clinical cancer research: an official journal of the American Association for Cancer Research* [Internet]. 2018;24:3204–16. Available from: <http://www.ncbi.nlm.nih.gov/pubmed/29514844>
41. Yang H, Xuefeng Y, Shandong W, Jianhua X. COX-2 in liver fibrosis. *Clinica chimica acta; international journal of clinical chemistry* [Internet].

2020;506:196–203. Available from: <http://www.ncbi.nlm.nih.gov/pubmed/32184095>

42. Huang F, Wang B-R, Wang Y. Role of autophagy in tumorigenesis, metastasis, targeted therapy and drug resistance of hepatocellular carcinoma. *World journal of gastroenterology* [Internet]. 2018;24:4643–51. Available from: <http://www.ncbi.nlm.nih.gov/pubmed/30416312>

43. Lohitesh K, Chowdhury R, Mukherjee S. Resistance a major hindrance to chemotherapy in hepatocellular carcinoma: an insight. *Cancer cell international* [Internet]. BioMed Central; 2018;18:44. Available from: <https://doi.org/10.1186/s12935-018-0538-7>

44. Lanza E, Donadon M, Poretti D, Pedicini V, Tramarin M, Roncalli M, et al. Transarterial Therapies for Hepatocellular Carcinoma. *Liver cancer* [Internet]. 2016;6:27–33. Available from: <http://www.ncbi.nlm.nih.gov/pubmed/27995085>

45. Wei X, Zhao L, Ren R, Ji F, Xue S, Zhang J, et al. MiR-125b Loss Activated HIF1 α /pAKT Loop, Leading to Transarterial Chemoembolization Resistance in Hepatocellular Carcinoma. *Hepatology (Baltimore, Md)* [Internet]. 2021;73:1381–98. Available from: <http://www.ncbi.nlm.nih.gov/pubmed/32609900>

46. Huang A, Yang X, Chung W, Dennison AR, Zhou J. Targeted therapy for hepatocellular carcinoma. *Signal transduction and targeted therapy* [Internet]. Springer US; 2020;5:146. Available from: <http://dx.doi.org/10.1038/s41392-020-00264-x>

47. Pinyol R, Sia D, Llovet JM. Immune Exclusion-Wnt/CTNNB1 Class Predicts Resistance to Immunotherapies in HCC. *Clinical cancer research : an official journal of the American Association for Cancer Research* [Internet]. 2019;25:2021–3. Available from: <http://www.ncbi.nlm.nih.gov/pubmed/30617138>

48. Kirkby NS, Chan M v., Zaiss AK, Garcia-Vaz E, Jiao J, Berglund LM, et al. Systematic study of constitutive cyclooxygenase-2 expression: Role of NF- κ B and NFAT transcriptional pathways. *Proceedings of the National Academy of Sciences of the United States of America* [Internet]. 2016;113:434–9. Available from: <http://www.ncbi.nlm.nih.gov/pubmed/26712011>

49. Alexanian A, Sorokin A. Cyclooxygenase 2: protein-protein interactions and posttranslational modifications. *Physiological genomics* [Internet]. 2017;49:667–81. Available from: <http://www.ncbi.nlm.nih.gov/pubmed/28939645>
50. Proença C, Ribeiro D, Soares T, Tomé SM, Silva AMS, Lima JLFC, et al. Chlorinated Flavonoids Modulate the Inflammatory Process in Human Blood. *Inflammation* [Internet]. *Inflammation*; 2017;40:1155–65. Available from: <http://www.ncbi.nlm.nih.gov/pubmed/28405852>
51. Zhou W, Yang L, Nie L, Lin H. Unraveling the molecular mechanisms between inflammation and tumor angiogenesis. *American journal of cancer research* [Internet]. 2021;11:301–17. Available from: <http://www.ncbi.nlm.nih.gov/pubmed/33575073>
52. Wyatt GL, Crump LS, Young CM, Wessells VM, McQueen CM, Wall SW, et al. Cross-talk between SIM2s and NFκB regulates cyclooxygenase 2 expression in breast cancer. *Breast cancer research: BCR* [Internet]. *Breast Cancer Research*; 2019;21:131. Available from: <http://www.ncbi.nlm.nih.gov/pubmed/31783895>
53. Wang Q, Lu D, Fan L, Li Y, Liu Y, Yu H, et al. COX-2 induces apoptosis-resistance in hepatocellular carcinoma cells via the HIF-1α/PKM2 pathway. *International journal of molecular medicine* [Internet]. 2019;43:475–88. Available from: <http://www.ncbi.nlm.nih.gov/pubmed/30365092>
54. Huang Q, Li F, Liu X, Li W, Shi W, Liu F-F, et al. Caspase 3-mediated stimulation of tumor cell repopulation during cancer radiotherapy. *Nature medicine* [Internet]. *Nature Publishing Group*; 2011;17:860–6. Available from: <http://dx.doi.org/10.1038/nm.2385>
55. Cui L, Zhao Y, Pan Y, Zheng X, Shao D, Jia Y, et al. Chemotherapy induces ovarian cancer cell repopulation through the caspase 3-mediated arachidonic acid metabolic pathway. *OncoTargets and therapy* [Internet]. 2017;10:5817–26. Available from: <http://www.ncbi.nlm.nih.gov/pubmed/29263678>
56. Najafi M, Mortezaee K, Majidpoor J. Cancer stem cell (CSC) resistance drivers. *Life sciences* [Internet]. 2019;234:116781. Available from: <http://www.ncbi.nlm.nih.gov/pubmed/31430455>

57. Tian J, Hachim MY, Hachim IY, Dai M, Lo C, Raffa F al, et al. Cyclooxygenase-2 regulates TGF β -induced cancer stemness in triple-negative breast cancer. *Scientific reports* [Internet]. Nature Publishing Group; 2017;7:40258. Available from: <http://dx.doi.org/10.1038/srep40258>
58. Gómez-Valenzuela F, Escobar E, Pérez-Tomás R, Montecinos VP. The Inflammatory Profile of the Tumor Microenvironment, Orchestrated by Cyclooxygenase-2, Promotes Epithelial-Mesenchymal Transition. *Frontiers in oncology* [Internet]. 2021;11:686792. Available from: <http://www.ncbi.nlm.nih.gov/pubmed/34178680>
59. Li S, Jiang M, Wang L, Yu S. Combined chemotherapy with cyclooxygenase-2 (COX-2) inhibitors in treating human cancers: Recent advancement. *Biomedicine & pharmacotherapy = Biomedecine & pharmacotherapie* [Internet]. Elsevier; 2020;129:110389. Available from: <https://doi.org/10.1016/j.biopha.2020.110389>
60. Brænne I, Willenborg C, Tragante V, Kessler T, Zeng L, Reiz B, et al. A genomic exploration identifies mechanisms that may explain adverse cardiovascular effects of COX-2 inhibitors. *Scientific reports* [Internet]. 2017;7:10252. Available from: <http://www.ncbi.nlm.nih.gov/pubmed/28860667>
61. INFARMED. Medicamentos contendo lumiracoxib - Recomendação de revogação da Autorização de Introdução no Mercado na União Europeia [Internet]. 2007 [cited 2021 Aug 22]. Available from: https://www.infarmed.pt/web/infarmed/infarmed?p_p_id=101&p_p_lifecycle=0&p_p_state=maximized&p_p_mode=view&_101_struts_action=%2Fasset_publisher%2Fview_content&_101_assetEntryId=1091660&_101_type=document&inheritRedirect=false&redirect=https%3A%2F%2Fwww.i
62. Tavares IA. Riscos e benefícios dos anti-inflamatórios não esteróides inibidores seletivos da ciclo-oxigenase 2 Universidade Fernando Pessoa. 2012;
63. INFARMED. Etoricoxib [Internet]. 2017 [cited 2021 Aug 22]. Available from: https://www.infarmed.pt/web/infarmed/infarmed?_3_formDate=1629599059188&p_p_id=3&p_p_lifecycle=0&p_p_state=maximized&p_p_mode=view&_3_struts_action=%2Fsearch%2Fsearch&_3_cur=1&_3_format=&_3_keywords=etoricoxib&_3_entryClassName=&_3_assetTagNames=&_3_asset

64. Anti-inflamatórios não esteroides sistémicos em adultos: orientações para a utilização de inibidores da COX-2 [Internet]. Ordem dos Médicos. 2013 [cited 2021 Aug 22]. Available from: https://ordemdosmedicos.pt/wp-content/uploads/2017/09/013___2011_atualizada_a_13_02_2013_Anti_inflamat_órios_COX2.pdf
65. Ruwizhi N, Aderibigbe BA. Cinnamic Acid Derivatives and Their Biological Efficacy. *International journal of molecular sciences* [Internet]. 2020;21:1–36. Available from: <http://www.ncbi.nlm.nih.gov/pubmed/32784935>
66. Peperidou A, Pontiki E, Hadjipavlou-Litina D, Voulgari E, Avgoustakis K. Multifunctional Cinnamic Acid Derivatives. *Molecules (Basel, Switzerland)* [Internet]. 2017;22:1–17. Available from: <http://www.ncbi.nlm.nih.gov/pubmed/28757554>
67. Pontiki E, Hadjipavlou-Litina D, Litinas K, Geromichalos G. Novel cinnamic acid derivatives as antioxidant and anticancer agents: design, synthesis and modeling studies. *Molecules (Basel, Switzerland)* [Internet]. 2014;19:9655–74. Available from: <http://www.ncbi.nlm.nih.gov/pubmed/25004073>
68. De P, Baltas M, Bedos-Belval F. Cinnamic acid derivatives as anticancer agents-a review. *Current medicinal chemistry* [Internet]. 2011;18:1672–703. Available from: <http://www.ncbi.nlm.nih.gov/pubmed/21434850>
69. Li Z, Zhao C, Zhao X, Xia Y, Sun X, Xie W, et al. Deep Annotation of Hydroxycinnamic Acid Amides in Plants Based on Ultra-High-Performance Liquid Chromatography-High-Resolution Mass Spectrometry and Its in Silico Database. *Analytical Chemistry*. 2018;90:14321–30.
70. Tao L, Wang S, Zhao Y, Sheng X, Wang A, Zheng S, et al. Phenolcarboxylic acids from medicinal herbs exert anticancer effects through disruption of COX-2 activity. *Phytomedicine* [Internet]. Elsevier GmbH.; 2014;21:1473–82. Available from: <http://dx.doi.org/10.1016/j.phymed.2014.05.001>
71. Murata H, Tsuji S, Tsujii M, Sakaguchi Y, Fu HY, Kawano S, et al. Promoter hypermethylation silences cyclooxygenase-2 (Cox-2) and regulates growth of human hepatocellular carcinoma cells. *Laboratory investigation; a journal of technical methods and pathology* [Internet]. 2004;84:1050–9. Available from: <http://www.ncbi.nlm.nih.gov/pubmed/15156159>

72. Baek JY. Selective COX-2 inhibitor, NS-398, suppresses cellular proliferation in human hepatocellular carcinoma cell lines via cell cycle arrest. *World Journal of Gastroenterology* [Internet]. 2007;13:1175. Available from: <http://www.wjgnet.com/1007-9327/13/1175.asp>
73. Kern MA, Haugg AM, Koch AF, Schilling T, Breuhahn K, Walczak H, et al. Cyclooxygenase-2 inhibition induces apoptosis signaling via death receptors and mitochondria in hepatocellular carcinoma. *Cancer research* [Internet]. 2006;66:7059–66. Available from: <http://www.ncbi.nlm.nih.gov/pubmed/16849551>
74. Kern MA, Schubert D, Sahi D, Schöneweiss MM, Moll I, Haugg AM, et al. Proapoptotic and antiproliferative potential of selective cyclooxygenase-2 inhibitors in human liver tumor cells. *Hepatology (Baltimore, Md)* [Internet]. 2002;36:885–94. Available from: <http://www.ncbi.nlm.nih.gov/pubmed/12297835>
75. JCRB. HuH7 characteristics [Internet]. [cited 2021 May 8]. Available from: https://cellbank.nibiohn.go.jp/~cellbank/en/search_res_det.cgi?ID=385
76. ATCC. HepG2 characteristics [Internet]. [cited 2021 May 8]. Available from: <https://www.atcc.org/products/hb-8065>
77. Liu XH, Rose DP. Differential expression and regulation of cyclooxygenase-1 and -2 in two human breast cancer cell lines. *Cancer research* [Internet]. 1996;56:5125–7. Available from: <http://www.ncbi.nlm.nih.gov/pubmed/8912844>
78. Dai X, Cheng H, Bai Z, Li J. Breast Cancer Cell Line Classification and Its Relevance with Breast Tumor Subtyping. *Journal of Cancer* [Internet]. 2017;8:3131–41. Available from: <http://www.ncbi.nlm.nih.gov/pubmed/29158785>
79. Natarajan K, Mori N, Artemov D, Bhujwala ZM. Exposure of human breast cancer cells to the anti-inflammatory agent indomethacin alters choline phospholipid metabolites and Nm23 expression. *Neoplasia (New York, NY)* [Internet]. 2012;4:409–16. Available from: <http://www.ncbi.nlm.nih.gov/pubmed/12192599>
80. Mahmood T, Yang P-C. Western blot: technique, theory, and trouble shooting. *North American journal of medical sciences* [Internet]. 2012;4:429–34. Available from: <http://www.ncbi.nlm.nih.gov/pubmed/23050259>

81. Mosmann T. Rapid colorimetric assay for cellular growth and survival: application to proliferation and cytotoxicity assays. *Journal of immunological methods* [Internet]. 1983 [cited 2021 Apr 13];65:55–63. Available from: <https://linkinghub.elsevier.com/retrieve/pii/0022175983903034>
82. Vichai V, Kirtikara K. Sulforhodamine B colorimetric assay for cytotoxicity screening. *Nature protocols* [Internet]. 2006;1:1112–6. Available from: <http://www.ncbi.nlm.nih.gov/pubmed/17406391>
83. Orellana EA, Kasinski AL. Sulforhodamine B (SRB) Assay in Cell Culture to Investigate Cell Proliferation. *Bio-protocol* [Internet]. 2016;6. Available from: <http://www.ncbi.nlm.nih.gov/pubmed/28573164>
84. Deitch AD, Law H, deVere White R. A stable propidium iodide staining procedure for flow cytometry. *The journal of histochemistry and cytochemistry: official journal of the Histochemistry Society* [Internet]. 1982;30:967–72. Available from: <http://www.ncbi.nlm.nih.gov/pubmed/6182188>
85. Vermes I, Haanen C, Steffens-Nakken H, Reutelingsperger C. A novel assay for apoptosis. Flow cytometric detection of phosphatidylserine expression on early apoptotic cells using fluorescein labelled Annexin V. *Journal of immunological methods* [Internet]. 1995;184:39–51. Available from: <http://www.ncbi.nlm.nih.gov/pubmed/7622868>
86. Vermes I, Haanen C, Reutelingsperger C. Flow cytometry of apoptotic cell death. *Journal of immunological methods* [Internet]. 2000;243:167–90. Available from: <http://www.ncbi.nlm.nih.gov/pubmed/10986414>
87. Abrantes AM, Serra MES, Gonçalves AC, Rio J, Oliveiros B, Laranjo M, et al. Hypoxia-induced redox alterations and their correlation with 99mTc-MIBI and 99mTc-HL-91 uptake in colon cancer cells. *Nuclear medicine and biology* [Internet]. Elsevier Inc.; 2010;37:125–32. Available from: <http://dx.doi.org/10.1016/j.nucmedbio.2009.11.001>
88. Cossarizza A, Baccarani-Contri M, Kalashnikova G, Franceschi C. A new method for the cytofluorimetric analysis of mitochondrial membrane potential using the J-aggregate forming lipophilic cation 5,5',6,6'-tetrachloro-1,1',3,3'-tetraethylbenzimidazolcarbocyanine iodide (JC-1). *Biochemical and biophysical research communications* [Internet]. 1993;197:40–5. Available from: <http://www.ncbi.nlm.nih.gov/pubmed/8250945>

89. Nogueira ML, Lima EJSP de, Adrião AAX, Fontes SS, Silva VR, Santos LDS, et al. *Cyperus articulatus* L. (Cyperaceae) Rhizome Essential Oil Causes Cell Cycle Arrest in the G2/M Phase and Cell Death in HepG2 Cells and Inhibits the Development of Tumors in a Xenograft Model. *Molecules* (Basel, Switzerland) [Internet]. 2020;25. Available from: <http://www.ncbi.nlm.nih.gov/pubmed/32527068>
90. D'mello P, Gadhwal MK, Joshi U, Shetgiri P. Modeling of COX-2 inhibitory activity of flavonoids. *International Journal of Pharmacy and Pharmaceutical Sciences*. 2011;3:33–40.
91. Cai H, Huang X, Xu S, Shen H, Zhang P, Huang Y, et al. Discovery of novel hybrids of diaryl-1,2,4-triazoles and caffeic acid as dual inhibitors of cyclooxygenase-2 and 5-lipoxygenase for cancer therapy. *European journal of medicinal chemistry* [Internet]. Elsevier Masson SAS; 2016;108:89–103. Available from: <http://dx.doi.org/10.1016/j.ejmech.2015.11.013>
92. Bijman MNA, Hermelink CA, van Berkel MPA, Laan AC, Janmaat ML, Peters GJ, et al. Interaction between celecoxib and docetaxel or cisplatin in human cell lines of ovarian cancer and colon cancer is independent of COX-2 expression levels. *Biochemical pharmacology* [Internet]. 2008;75:427–37. Available from: <http://www.ncbi.nlm.nih.gov/pubmed/17936723>
93. Grösch S, Tegeder I, Niederberger E, Bräutigam L, Geisslinger G. COX-2 independent induction of cell cycle arrest and apoptosis in colon cancer cells by the selective COX-2 inhibitor celecoxib. *FASEB journal : official publication of the Federation of American Societies for Experimental Biology* [Internet]. 2001;15:2742–4. Available from: <http://www.ncbi.nlm.nih.gov/pubmed/11606477>
94. Pires AS, Batista J, Murtinho D, Nogueira C, Karamysheva A, Luísa Ramos M, et al. Synthesis, Characterization and Evaluation of the Antibacterial and Antitumor Activity of HalogenatedSalen Copper (II) Complexes derived from Camphoric Acid. *Applied Organometallic Chemistry*. 2020;34:1–18.
95. Pires AS, Varela CL, Marques IA, Abrantes AM, Gonçalves C, Rodrigues T, et al. Oxymestane, a cytostatic steroid derivative of exemestane with greater antitumor activity in non-estrogen-dependent cell lines. *The Journal of steroid biochemistry and molecular biology* [Internet]. 2021;212:105950. Available from: <http://www.ncbi.nlm.nih.gov/pubmed/4271024>

96. Galluzzi L, Senovilla L, Vitale I, Michels J, Martins I, Kepp O, et al. Molecular mechanisms of cisplatin resistance. *Oncogene* [Internet]. Nature Publishing Group; 2012;31:1869–83. Available from: <http://www.ncbi.nlm.nih.gov/pubmed/21892204>
97. Cersosimo RJ, Hong WK. Epirubicin: a review of the pharmacology, clinical activity, and adverse effects of an adriamycin analogue. *Journal of clinical oncology : official journal of the American Society of Clinical Oncology* [Internet]. 1986;4:425–39. Available from: <http://www.ncbi.nlm.nih.gov/pubmed/3005521>
98. Najafi M, Tavakol S, Zarrabi A, Ashrafizadeh M. Dual role of quercetin in enhancing the efficacy of cisplatin in chemotherapy and protection against its side effects: a review. *Archives of physiology and biochemistry* [Internet]. Taylor & Francis; 2020;0:1–15. Available from: <https://doi.org/10.1080/13813455.2020.1773864>
99. Khongkow M, Olmos Y, Gong C, Gomes AR, Monteiro LJ, Yagüe E, et al. SIRT6 modulates paclitaxel and epirubicin resistance and survival in breast cancer. *Carcinogenesis* [Internet]. 2013;34:1476–86. Available from: <http://www.ncbi.nlm.nih.gov/pubmed/23514751>
100. Hasinoff BB, Patel D, Wu X. The cytotoxicity of celecoxib towards cardiac myocytes is cyclooxygenase-2 independent. *Cardiovascular toxicology* [Internet]. 2007;7:19–27. Available from: <http://www.ncbi.nlm.nih.gov/pubmed/17646679>
101. Koczurkiewicz-Adamczyk P, Klaś K, Gunia-Krzyżak A, Piska K, Andrysiak K, Stępniewski J, et al. Cinnamic Acid Derivatives as Cardioprotective Agents against Oxidative and Structural Damage Induced by Doxorubicin. *International journal of molecular sciences* [Internet]. 2021;22. Available from: <http://www.ncbi.nlm.nih.gov/pubmed/34207549>
102. Koczurkiewicz-Adamczyk P, Piska K, Gunia-Krzyżak A, Bucki A, Jamrozik M, Lorenc E, et al. Cinnamic acid derivatives as chemosensitising agents against DOX-treated lung cancer cells - Involvement of carbonyl reductase 1. *European journal of pharmaceutical sciences : official journal of the European Federation for Pharmaceutical Sciences* [Internet]. 2020;154:105511. Available from: <http://www.ncbi.nlm.nih.gov/pubmed/32801001>
103. Vajrabhaya L ongthong, Korsuwannawong S. Cytotoxicity evaluation of a Thai herb using tetrazolium (MTT) and sulforhodamine B (SRB) assays. *Journal*

of Analytical Science and Technology. *Journal of Analytical Science and Technology*; 2018;9.

104. Patel RM, Patel SK. Cytotoxic activity of methanolic extract of *artocarpus heterophyllus* against a549, hela and mcf-7 cell lines. *Journal of Applied Pharmaceutical Science*. 2011;1:167–71.

105. Cui W, Yu C-H, Hu K-Q. In vitro and in vivo effects and mechanisms of celecoxib-induced growth inhibition of human hepatocellular carcinoma cells. *Clinical cancer research: an official journal of the American Association for Cancer Research* [Internet]. 2005;11:8213–21. Available from: <http://www.ncbi.nlm.nih.gov/pubmed/16299255>

106. El-Awady RA, Saleh EM, Ezz M, Elsayed AM. Interaction of celecoxib with different anti-cancer drugs is antagonistic in breast but not in other cancer cells. *Toxicology and applied pharmacology* [Internet]. Elsevier Inc.; 2011;255:271–86. Available from: <http://dx.doi.org/10.1016/j.taap.2011.06.019>

107. Cervello M, Bachvarov D, Cusimano A, Sardina F, Azzolina A, Lampiasi N, et al. COX-2-dependent and COX-2-independent mode of action of celecoxib in human liver cancer cells. *Omics: a journal of integrative biology* [Internet]. 2011;15:383–92. Available from: <http://www.ncbi.nlm.nih.gov/pubmed/21410330>

108. Bocca C, Bozzo F, Bassignana A, Miglietta A. Antiproliferative effects of COX-2 inhibitor celecoxib on human breast cancer cell lines. *Molecular and cellular biochemistry* [Internet]. 2011;350:59–70. Available from: <http://www.ncbi.nlm.nih.gov/pubmed/21140284>

109. Dai Z-J, Ma X-B, Kang H-F, Gao J, Min W-L, Guan H-T, et al. Antitumor activity of the selective cyclooxygenase-2 inhibitor, celecoxib, on breast cancer in Vitro and in Vivo. *Cancer cell international* [Internet]. 2012;12:53. Available from: <http://www.ncbi.nlm.nih.gov/pubmed/23249419>

110. Morisaki T, Umebayashi M, Kiyota A, Koya N, Tanaka H, Onishi H, et al. Combining celecoxib with sorafenib synergistically inhibits hepatocellular carcinoma cells in vitro. *Anticancer research* [Internet]. 2013;33:1387–95. Available from: <http://www.ncbi.nlm.nih.gov/pubmed/23564777>

111. Kogure K, Hama S, Manabe S, Tokumura A, Fukuzawa K. High cytotoxicity of alpha-tocopheryl hemisuccinate to cancer cells is due to failure of

their antioxidative defense systems. *Cancer letters* [Internet]. 2002;186:151–6. Available from: <http://www.ncbi.nlm.nih.gov/pubmed/12213284>

112. Papadimitriou M, Hatzidaki E, Papatotiriou I. Linearity Comparison of Three Colorimetric Cytotoxicity Assays. *Journal of Cancer Therapy* [Internet]. 2019;10:580–90. Available from: <http://www.scirp.org/journal/doi.aspx?DOI=10.4236/jct.2019.107047>

113. Wong RSY. Role of Nonsteroidal Anti-Inflammatory Drugs (NSAIDs) in Cancer Prevention and Cancer Promotion. *Advances in pharmacological sciences* [Internet]. 2019;2019:3418975. Available from: <http://www.ncbi.nlm.nih.gov/pubmed/30838040>

114. Blagosklonny M v. Cell cycle arrest is not senescence. *Aging* [Internet]. 2011;3:94–101. Available from: <http://www.ncbi.nlm.nih.gov/pubmed/21297220>

115. HuH7.com [Internet]. [cited 2021 Sep 21]. Available from: <https://huh7.com/>

116. Mitchell JK, Midkiff BR, Israelow B, Evans MJ, Lanford RE, Walker CM, et al. Hepatitis C Virus Indirectly Disrupts DNA Damage-Induced p53 Responses by Activating Protein Kinase R. *mBio* [Internet]. 2017;8. Available from: <http://www.ncbi.nlm.nih.gov/pubmed/28442604>

117. Brito AF, Abrantes AM, Ribeiro M, Oliveira R, Casalta-Lopes J, Gonçalves AC, et al. Fluorine-18 Fluorodeoxyglucose Uptake in Hepatocellular Carcinoma: Correlation with Glucose Transporters and p53 Expression. *Journal of clinical and experimental hepatology* [Internet]. INASL; 2015;5:183–9. Available from: <http://dx.doi.org/10.1016/j.jceh.2015.05.003>

118. Sánchez-Carranza JN, Alvarez L, Marquina-Bahena S, Salas-Vidal E, Cuevas V, Jiménez EW, et al. Phenolic Compounds Isolated from *Caesalpinia coriaria* Induce S and G2/M Phase Cell Cycle Arrest Differentially and Trigger Cell Death by Interfering with Microtubule Dynamics in Cancer Cell Lines. *Molecules* (Basel, Switzerland) [Internet]. 2017;22. Available from: <http://www.ncbi.nlm.nih.gov/pubmed/28441723>

119. Tsuji K, Ojima M, Otabe K, Horie M, Koga H, Sekiya I, et al. Effects of Different Cell-Detaching Methods on the Viability and Cell Surface Antigen Expression of Synovial Mesenchymal Stem Cells. *Cell transplantation* [Internet].

2017;26:1089–102. Available from:
<http://www.ncbi.nlm.nih.gov/pubmed/28139195>

120. Bundscherer A, Malsy M, Lange R, Hofmann P, Metterlein T, Graf BM, et al. Cell harvesting method influences results of apoptosis analysis by annexin V staining. *Anticancer research* [Internet]. 2013;33:3201–4. Available from:
<http://www.ncbi.nlm.nih.gov/pubmed/23898079>

121. Brentnall M, Rodriguez-Menocal L, de Guevara RL, Cepero E, Boise LH. Caspase-9, caspase-3 and caspase-7 have distinct roles during intrinsic apoptosis. *BMC cell biology* [Internet]. 2013;14:32. Available from:
<http://www.ncbi.nlm.nih.gov/pubmed/23834359>

122. Jendrossek V. Targeting apoptosis pathways by Celecoxib in cancer. *Cancer Letters* [Internet]. Elsevier Ireland Ltd; 2013;332:313–24. Available from:
<http://dx.doi.org/10.1016/j.canlet.2011.01.012>

123. Niederberger E, Manderscheid C, Geisslinger G. Different COX-independent effects of the COX-2 inhibitors etoricoxib and lumiracoxib. *Biochemical and biophysical research communications* [Internet]. 2006;342:940–8. Available from: <http://www.ncbi.nlm.nih.gov/pubmed/16598848>

124. Yun K-J, Koh D-J, Kim S-H, Park SJ, Ryu JH, Kim D-G, et al. Anti-inflammatory effects of sinapic acid through the suppression of inducible nitric oxide synthase, cyclooxygenase-2, and proinflammatory cytokines expressions via nuclear factor-kappaB inactivation. *Journal of agricultural and food chemistry* [Internet]. 2008;56:10265–72. Available from:
<http://www.ncbi.nlm.nih.gov/pubmed/18841975>

125. Gong L, Thorn CF, Bertagnolli MM, Grosser T, Altman RB, Klein TE. Celecoxib pathways: pharmacokinetics and pharmacodynamics. *Pharmacogenetics and genomics* [Internet]. 2012;22:310–8. Available from:
<http://www.ncbi.nlm.nih.gov/pubmed/22336956>

126. Kulp SK, Yang Y-T, Hung C-C, Chen K-F, Lai J-P, Tseng P-H, et al. 3-phosphoinositide-dependent protein kinase-1/Akt signaling represents a major cyclooxygenase-2-independent target for celecoxib in prostate cancer cells. *Cancer research* [Internet]. 2004;64:1444–51. Available from:
<http://www.ncbi.nlm.nih.gov/pubmed/14973075>

127. Gkretsi V, Zacharia LC, Stylianopoulos T. Targeting Inflammation to Improve Tumor Drug Delivery. Trends in cancer [Internet]. Elsevier Inc.; 2017;3:621–30. Available from: <http://dx.doi.org/10.1016/j.trecan.2017.07.006>
128. Khuda-Bukhsh AR, Das S, Saha SK. Molecular approaches toward targeted cancer prevention with some food plants and their products: inflammatory and other signal pathways. Nutrition and cancer [Internet]. 2014;66:194–205. Available from: <http://www.ncbi.nlm.nih.gov/pubmed/24377653>
129. Jung EH, Kim SR, Hwang IK, Ha TY. Hypoglycemic effects of a phenolic acid fraction of rice bran and ferulic acid in C57BL/KsJ-db/db mice. Journal of agricultural and food chemistry [Internet]. 2007;55:9800–4. Available from: <http://www.ncbi.nlm.nih.gov/pubmed/17973443>
130. Liang C, Pei S, Ju W, Jia M, Tian D, Tang Y, et al. Synthesis and in vitro and in vivo antitumour activity study of 11-hydroxyl esterified bergenin/cinnamic acid hybrids. European journal of medicinal chemistry [Internet]. 2017;133:319–28. Available from: <http://www.ncbi.nlm.nih.gov/pubmed/28395218>
131. Huang Y, Zeng F, Xu L, Zhou J, Liu X, Le H. Anticancer effects of cinnamic acid in lung adenocarcinoma cell line h1299-derived stem-like cells. Oncology research [Internet]. 2013;20:499–507. Available from: <http://www.ncbi.nlm.nih.gov/pubmed/24063280>
132. Adisakwattana S. Cinnamic Acid and Its Derivatives: Mechanisms for Prevention and Management of Diabetes and Its Complications. Nutrients [Internet]. 2017;9. Available from: <http://www.ncbi.nlm.nih.gov/pubmed/28230764>
133. Pan J, Yang Q, Shao J, Zhang L, Ma J, Wang Y, et al. Cyclooxygenase-2 induced β 1-integrin expression in NSCLC and promoted cell invasion via the EP1/MAPK/E2F-1/FoxC2 signal pathway. Scientific reports [Internet]. Nature Publishing Group; 2016;6:33823. Available from: <http://dx.doi.org/10.1038/srep33823>
134. Eguchi H, Iwaki K, Shibata K, Ogawa T, Ohta M, Kitano S. Protease-activated receptor-2 regulates cyclooxygenase-2 expression in human bile duct cancer via the pathways of mitogen-activated protein kinases and nuclear factor kappa B. Journal of hepato-biliary-pancreatic sciences [Internet]. 2011;18:147–53. Available from: <http://www.ncbi.nlm.nih.gov/pubmed/20740367>

135. Zhu YM, Azahri NSM, Yu DCW, Woll PJ. Effects of COX-2 inhibition on expression of vascular endothelial growth factor and interleukin-8 in lung cancer cells. *BMC cancer* [Internet]. 2008;8:218. Available from: <http://www.ncbi.nlm.nih.gov/pubmed/18671849>

Appendix 1 – MTT assay with Celecoxib treatment

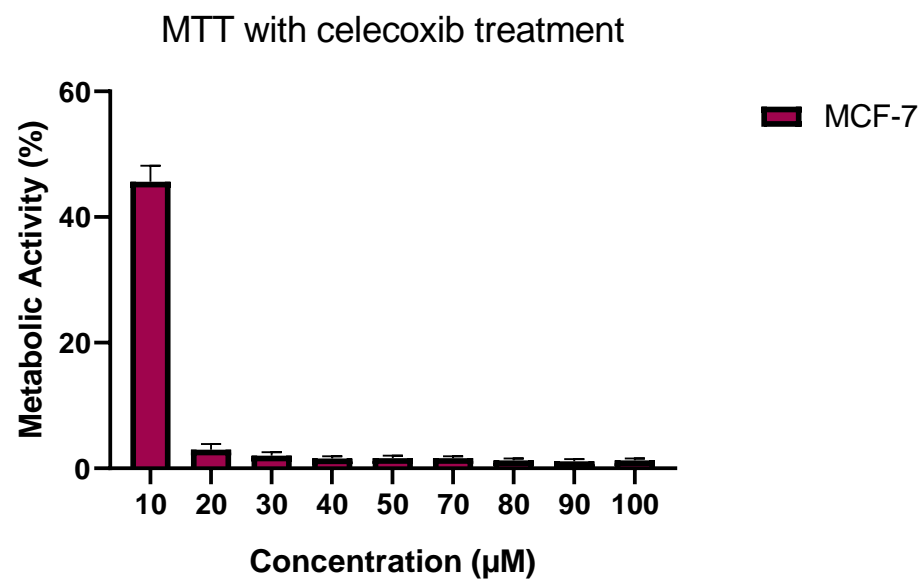


Figure 39 - Results of MTT in MCF-7 cell line 48 hours after treatment with compounds E4 and F19. Results are presented as the percentage of metabolic activity (%) as a function of compounds' concentration (µM) and express the mean±SEM of, at least, three independent experiments, in triplicate.